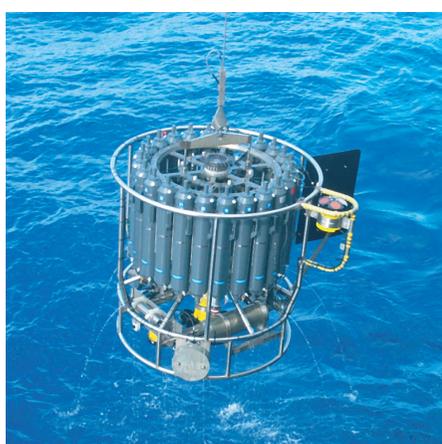# Assessing the Agricultural System and the Carbon Cycle under Climate Change in Europe using a Dynamic Global Vegetation Model

Luca Criscuolo

Hinweis

Die Berichte zur Erdsytemforschung werden vom Max-Planck-Institut für Meteorologie in Hamburg in unregelmäßiger Abfolge herausgegeben.

Sie enthalten wissenschaftliche und technische Beiträge, inklusive Dissertationen.

Die Beiträge geben nicht notwendigerweise die Auffassung des Instituts wieder.

Die "Berichte zur Erdsystemforschung" führen die vorherigen Reihen "Reports" und "Examensarbeiten" weiter.

Notice

The Reports on Earth System Science are published by the Max Planck Institute for Meteorology in Hamburg. They appear in irregular intervals.

They contain scientific and technical contributions, including Ph. D. theses.

The Reports do not necessarily reflect the opinion of the Institute.

The "Reports on Earth System Science" continue the former "Reports" and "Examensarbeiten" of the Max Planck Institute.

Anschrift / Address

Max-Planck-Institut für Meteorologie
Bundesstrasse 53
20146 Hamburg
Deutschland

Tel.: +49-(0)40-4 11 73-0
Fax: +49-(0)40-4 11 73-298
Web: www.mpimet.mpg.de

Layout:

Bettina Diallo, PR & Grafik

Titelfotos:
vorne:
Christian Klepp - Jochem Marotzke - Christian Klepp
hinten:
Clotilde Dubois - Christian Klepp - Katsumasa Tanaka

Assessing the Agricultural System and the Carbon Cycle under Climate Change in Europe using a Dynamic Global Vegetation Model

Luca Criscuolo

aus Rom, Italien

Hamburg 2006

Luca Criscuolo
Max-Planck-Institut für Meteorologie
Bundesstrasse 53
20146 Hamburg
Germany

Assessing the Agricultural System and the Carbon Cycle under Climate Change in Europe using a Dynamic Global Vegetation Model
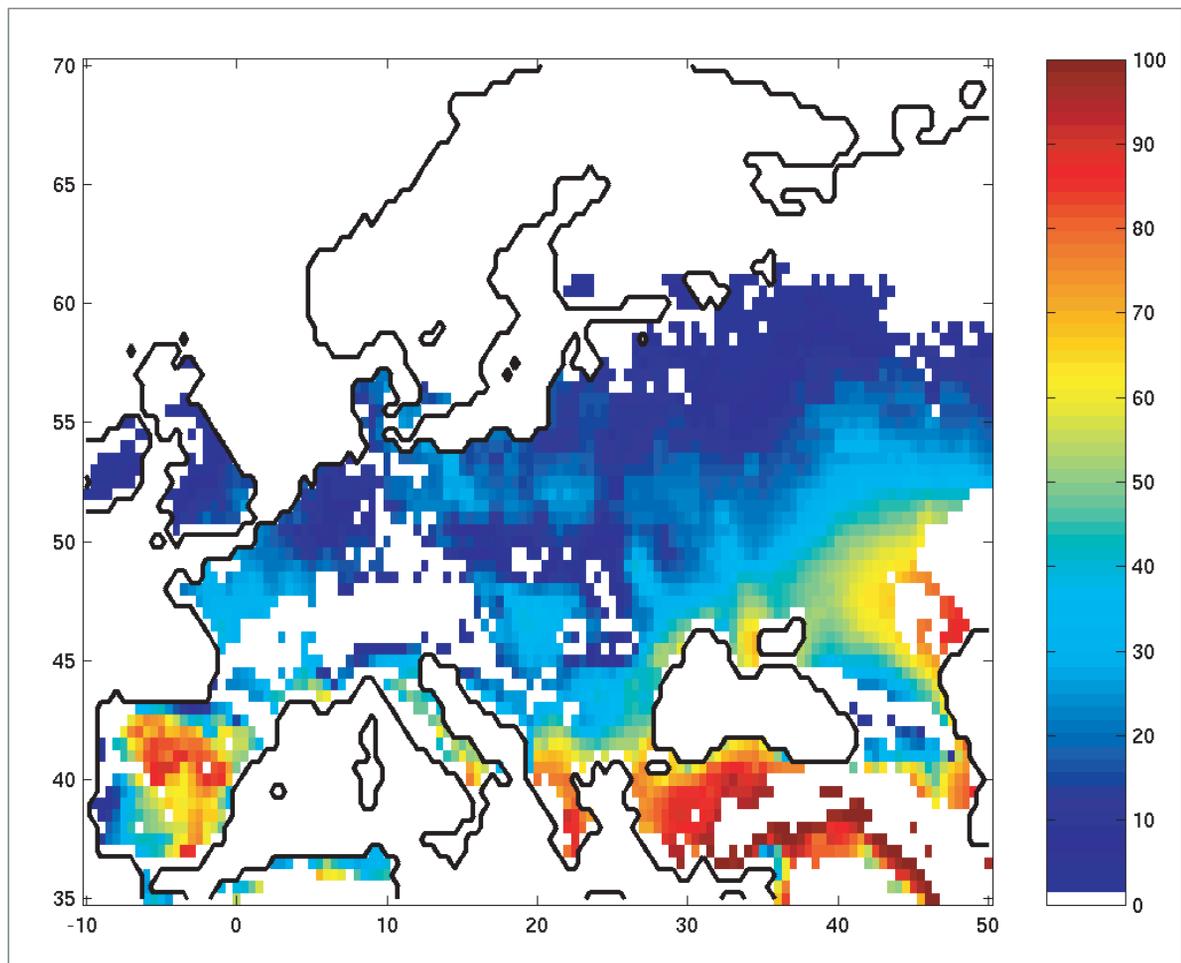
Luca Criscuolo

Hamburg 2006

Contents

Contents

Abstract

Several recent studies predicted changes in the climatic conditions in Europe driven by the increased atmospheric CO2 concentration due anthropogenic activities. The climate change can affect the agriculture through many aspects of crop production over the European continent. Not only plant productivity, but also geographical shifts of cultivation areas, changes in crop phenology, in land use, and in soil carbon stocks have to be taken into account for assessments of the next future. This study provides a potentially powerful baseline to perform integrated assessments on the impacts of the changing climate by assessing crop production with a single integrated framework for large-scale studies. Not only crops and natural vegetation in a single Dynamic Global Vegetation Model, the LPJ-C, but also potential and water-limited crop production are included within the same biosphere scheme.

The LPJ-C is extended to simulate not only natural biomes, but also crops. We perform an optimization procedure, which provides a set of crop parameters used in the regional assessment over Europe. Further, we used the resulting modelling framework to study the changes of potential production of maize and wheat together with the shift in their potential growing area. The results show that wheat yield will suffer from a decline, but fertilization due to the CO_2 enriched atmosphere will compensate this effect. For maize, cultivation will clearly expand towards north and east. Since maize, as a C4 plant, is mostly unaffected by the CO_2 fertilization effect, the shorter growing season will lead to a lower net primary productivity, while the mean over the continent will increase according to the large geographical spread.

Furthermore, LPJ-C is able to reproduce the observed relative increase of water use efficiency under water-limited conditions and a CO_2 fertilization effect. The improved water use efficiency of wheat leads to a relatively smaller transpiration per unit of biomass, so that precipitation will partially satisfy the

transiration demand. On the other hand, wheat will suffer from an increase of yield variability and a higher frequency of extreme crop failures. Even though maize potential distribution will be enlarged, the yield will be affected by strong losses, unless largely improved irrigation will satisfy the increased water demand.

We perform also the coupling of LPJ-C with the land-use model KLUM, as a connection between a profit maximization procedure for land allocation and a process-based description of crop production. The coupled system showed that temperature would play a major role in the soil carbon dynamics over the expected northward shift of crops. However, important changes have to be expected for distribution of "warm" cereals as rice and maize.

1 Introduction

1.1 Overview

The largest part of carbon flux between land and atmosphere belongs to photosynthesis and respiration activities. During daytime, leaves absorb sunlight, take up CO_2 from the atmosphere and produce organic carbon for growth. In parallel, plants, animals and microorganisms respire the organic matter and exchange back CO_2 to the atmosphere. The amounts of carbon moving through photosynthesis and respiration are not constant in time, but have seasonal and interannual natural oscillations. Significant amounts of carbon can be stored or released on land over periods of years to decades, and the human activity influences the dynamic equilibrium of the carbon storages. When land use changes from forests to agriculture the carbon contained in the living material and soil is quickly released into the atmosphere. On the contrary, when agricultural land is abandoned and natural vegetation is allowed to grow again carbon is stored slowly back in the growing biomass (Caspersen *et al.*, 2000). Global estimation for 1990s show an annual carbon flux to the atmosphere of 2240 $TgCy^{-1}$ due to deforestation, and 20 $TgCy^{-1}$ due to soil carbon loss including cultivation of new lands (Houghton, 2003). There is more consistent evidence that this change in land-use, together with the intensified use of fossil fuels, altered the natural equilibrium of the carbon cycle. A consequence seems to be that the atmospheric CO_2 concentration increased in the last 200 years by about 37%, to current levels of more than 370 μmol mol^{-1} (Keeling and Whorf, 2000). One of the responses of the climatic system appears to be an increase of average temperature: during the last 100 years the mean global surface temperature increased by 0.7 ± 0.2 °C, with large regional differences (IPCC, 2001a; CRU, 2003). Focusing on Europe, the surface warming was around 0.95 °C, and 1998 was the warmest year since 1900, followed by 2002 and 2003 (Jones

and Moberg, 2003). Precipitation variability has also shown important changes during the 20th century. Between 1981 and 1994, Northern Europe was experiencing an increase in precipitation, while less occurred in the Mediterranean (Hurrell and van Loon, 1997).

Current climate predictions indicate that the observed trends will probably reinforce within the next 50-100 years. The predicted global mean temperature increase between 1990 and 2100 is within the range of 1.4–5.8 °C (IPCC, 2001a; EAA, 2004). Europe will face an increase likely to be between 2 and 6.3 °C, with more intense warming occurring in Southern and Northeastern Europe (Parry, 2000; EAA, 2004). It is also expected that the observed precipitation trend will intensify, leading to a reduction of 1% per decade in Southern and an increase of 1-4% per decade in Northern Europe with increased seasonal variability. Additionally, the predicted precipitation reduction in some Mediterranean areas will be even higher during the summer, with more frequent droughts (IPCC, 2001a ; Ragab and Proudhomme, 2002; Chartzoulakis and Psarras, 2005).

The predicted changes in the climatic conditions in Europe will impact the biosphere in all its components, agro-ecosystems included. Agro-ecosystems exist as, and depend on, the result of the interaction of natural resources, human activity and climate. From the biophysical perspective, they regulate the water and carbon fluxes at the land-atmosphere interface, and influences the heat fluxes and micro dynamics of weather and climate; on the other hand, they also play an important economic role. The European agriculture is one of the world's largest food and fiber producers. Even though the agricultural sector covers only 2.6% of the total GDP, its share is 10% of global cereal and 16% of global meat production (Olesen and Bindi, 2002). Furthermore, 5 % of the European workforce is employed in this sector and 44% of the land is dedicated to agricultural use (European Commission, 2002; EAA, 2004). The potential impacts of the predicted changing climate on this complex system involve many components as, for example, the productivity and phenology of crop plants, the geographical distribution of cultivated land, the flux at the land surface, and the carbon content in the soil.

1.2   The modelling perspective

The impacts of the changing climate on such an important production system have been already investigated. The modelling tools used in these studies were usually crop models adapted to regional level with extensions to explicitly include policy and agronomic adaptation (Wolf and van Diepen, 1995; Rosenzweig and Tubiello, 1997; Tubiello et al., 2000; Tubiello and Ewert 2002; Olesen and Bindi, 2002; Rosenzweig et al., 2004). Even though these studies give an important picture of the potential responses, they lack an integrated biosphere modelling perspective, as well as the necessary generalization for studies at the global scale. The use of crop models dramatically improves the understanding of possible changes in yields, but it excludes often the description of the soil carbon dynamics and natural vegetation growth (Kucharick and Brye 2003). The amount and detail of the required data limits their use to assessment of specific crops in well-defined areas (Scholze et al, 2005). A broader biospheric view is available today in a new generation of models designed for regional and global scale assessments. The Dynamic Global Vegetation Models (DGVMs) give an integrated representation of natural vegetation taking into account carbon and water within a single grid-based modelling framework (Smith et al., 2001; McGuire et al., 2001; Cramer et al., 2001; Sitch et al., 2003). Moreover, these models have been recently developed to include crops and pastures as parts of the terrestrial vegetation. The Integrated Biosphere Simulator (IBIS) has been extended to include crops and validated on the U.S. Corn Belt (Kucharick and Brye 2003; Kucharick, 2003). IBIS was lately used to study the influence of land cover and land use changes on nitrate transport through the Mississippi Basin (Donner et al., 2004). Another example, with different modelling approach, is the Organizing Carbon and Hydrology in Dynamic Ecosystems model (ORCHIDEE) (Gervois et al., 2004; de Noblet-Ducoudré et al., 2005). This DGVM includes a separate crop model to specifically simulate crop variables. Three crops are implemented (wheat, maize, and soybeans) and the model was used to assess the water and carbon budget of Europe. A similar strategy is implemented in the General Large Area Model (GLAM) (Challinor et al., 2004), which operates on large spatial scales using a traditional crop modelling approach. GLAM is incorporated into the land

surface scheme of the general circulation model (GCM) of the U.K. Met Office to investigate large-scale interactions between crops and climate. Even though still in development, this new frontier of the integrated biosphere modelling represents already a powerful baseline to study long-term changes in a changing climate, including agro-ecosystems. However, the existing hybrids DGVMs currently lack the description of some important processes, such as land-use allocation and soil carbon dynamics. Moreover, none of the above-mentioned tools has been used in ecosystem service assessments to investigate the impacts on agricultural production of the changing climate in Europe.

This work represents a step further in the integrated representation of the biosphere. We incorporate crops within a single modelling framework of a state-of-the-art DGVM, the Lund-Potsdam-Jena (LPJ) model (Sitch et al., 2003) by introducing a crop carbon allocation scheme adapted from a crop growth model. The new version of the LPJ model is, therefore, able to simulate the growth and development of crops and natural vegetation, soil carbon dynamics and fire disturbances within the carbon and water cycle. A particular feature of this model is that only the allocation scheme has been modified, while photosynthesis, carbon and water balance equations remain the same as for natural vegetation. We also introduce a land-use scheme to set crops dynamically according to their demand and yield. Such a new system was originally designed to be included within an integrated assessment modelling framework; in this context, however, it has been used independently to investigate several aspects of the impacts of the climate change on crop production, water requirements and soil carbon in Europe.

1.3   Structure

In Chapter 2, we describe the model development and the optimization procedure used for validation. Additionally, we illustrate and discuss the results of a climate change modelling experiment focussed on assessing the changes in potential production and geographical patterns of maize and wheat. Potential crop production is the production under ideal, well

watered and fertilized, conditions. This chapter corresponds to the following paper:

Criscuolo L., Knorr W., Ceotto E., Smith B. (2005). An assessment of climate change impacts on maize and wheat productivity in Europe using a Dynamic Global Vegetation Model. Part I: Model evaluation and potential production. Submitted to *Earth Interactions*.

Further, in Chapter 3, we analyse the water-limited production and, in this context, we give a description of the potential changes in the water use. The change in the frequency of drought events is often considered even more important for future agriculture impacts. Therefore, a study of the changing statistics of extreme crop yield failures due to water stress is also performed in this chapter, which corresponds to the following paper:

Criscuolo L., Knorr W. (2005). An assessment of climate change impacts on maize and wheat productivity in Europe using a Dynamic Global Vegetation Model. Part II: Irrigation demand and drought risk. Submitted to *Earth Interactions*.

In Chapter 4 we perform the coupled study with a land-use model, the Kleines Land Use Model (KLUM). The soil carbon in agricultural land is highly influenced by the land-use. Depending on the characteristics of the plant structure, higher quantities of carbon can be moved to the soil at the harvest. The soil carbon decomposition, on the other hand, depends mainly on temperature. We further assess, in this chapter, how the climate change may potentially lead to new land allocation patterns and how the soil carbon can consequently change. The following work corresponds to this chapter:

Criscuolo L., Ronneberger K., Knorr W., Tol R.S.J. (2005). Changes in agricultural land use and soil carbon storage in Europe under climate change: results of an integrated modelling study. To be submitted to: *Global Change Biology*.

Chapter 5 provides a summary, an outlook and the concluding remarks.

1.4 References

Alcamo J., Kreileman G.J.J., Bollen J.C., van den Born G.J., Gerlagh R., Krol M.S., Toet A.M.C., de Vries H.J.M. (1996). Baseline scenarios of global environmental change. Global Environmental Change, 6, 261–303.

Caspersen J. P., S. W. Pacala, J.C. Jenkins, G.C. Hurtt, P.R. Moorcroft, R.A. Birdsey (2000). Contributions of Land-Use History to Carbon Accumulation in U.S. Forests. Science 290: 1148-1151.

Challinor A.J., Wheeler T.R., Craufurd P.Q., Slingo J.M. and Grimes D.I.F. (2004). Design and optimisation of a large area process-based model for annual crops. Agricultural and Forest Meteorology, 124, 1-2, 99-120.

Chartzoulakis K., Psarras G. (2005). Global change effects on crop photosynthesis and production in Mediterranean: the case of Crete, Greece. Agriculture, Ecosystems and Environment, 106, 147–157.

Cramer W., Bondeau A., Woodward F.I., Prentice I.C., Betts R.A., Bronvik V., Cox P.M., Fisher V., Foley J.A., Friend A.D., Kucharik C., Lomas M.R., Ramankutty N., Sitch S., Smith B., White A., Young-Molling C. (2001). Global response of terrestrial ecosystem structure and function to CO_2 and climate change: results from six dynamic global vegetation models. Global Change Biology, 7, 357-373.

Criscuolo L., Knorr W., Ceotto E., Smith B. (2005). An assessment of climate change impacts on potential maize and wheat productivity in Europe using a Dynamic Global Vegetation Model. Submitted to:

CRU (2003). Global average temperature change 1856–2003. h.p//www.cru.uea. ac.uk/cru/data/temperature.

Donner S.D., Kucharik C.J., Foley J.A. (2004). Impact of changing land use practices on nitrate export by the Mississippi River. *Global Biogechemical Cycles*, 17, 1085-2004.

European Commission (2002). European agriculture entering the 21st century, European Commission, Directorate General for Agriculture.

EAA (2004). Impacts of Europe's changing climate an indicator-based assessment, EAA Report No 2/2004, European Environment Agency, Copenhagen, Denmark, 67-70.

FAO (2004). Compendium of Food and Agriculture Indicators 2004. FAO statistic Division, http://www.fao.org/es/ess/compendium_2004/list.asp.

Gervois S., de Noblet-Ducoudré N., Viovy N., Ciais P., Brisson N., Seguin B. and Perrier A. (2004). Including Croplands in a Global Biosphere Model: Methodology and Evaluation at Specific Sites. Earth Interactions, 8, 16, 1–25.

Houghton R. A. (2003). Revised estimates of the annual net flux of carbon to the atmosphere from changes in land use and land management 1850–2000. Tellus 55B: 378–390.

Hurrell J.W., van Loon H. (1997). Decadal variations in climate associated with the North Atlantic oscillation. Climate Change, 36, 301-326.

IPCC (2001a). Climate Change 2001: Working Group I: The Scientific Basis. Contribution of the Working Group I to the Third Assessment Report of the Intergovernmental Panel on Climate Change (eds. Houghton J.T. et al.), Cambridge University Press, Cambridge, UK.

Jones P.D., Moberg D. (2003). Hemispheric and large-scale surface air temperature variations: An extensive revision and an update to 2001, Journal of Climate, 16, 206–223.

Keeling C.D., Whorf T.P. (2000). Atmospheric CO2 records from sites in the SIO air sampling network. In Trends: A compendium enriched aerial environment, Agronomy Journal, 81, 692–695.

Kucharik C.J., Brye K.R. (2003). Integrated BIosphere Simulator (IBIS) yield and nitrate loss predictions for Wisconsin maize receiving Varied Amounts of nitrogen fertilizer. Journal Environmental Quality, 32, 247-268.

Kucharik C. J. (2003). Evaluation of a process-based agro-ecosystem model (Agro-IBIS) across the U.S. cornbelt: Simulations of the inter-annual variability in maize yield. *Earth Interactions*, 7, 14, 1–33.

McGuire A.D., Stich S., Clein J.S., Dargaville R., Esser G., Foley J., Heimann M., Joos M., Kaplan J., Kicklighter D.W., Meier R.A., Melillo J. M., Moore III B., Prentice I.C., Ramankutty N., Reichenau T., Tian H., Williams L.J., Wittenberg U. (2001). Carbon balance of the terrestrial biossphere in the tweniteh century: analyses of CO2, climate and land use effects with four processes-based ecosystem models. Global Biogeochemical Cycles, 15, 183-206.

de Noblet-Ducoudré N., Gervois S., Ciais P., Viovy N., Brisson N., Seguin B. and Perrier A. (2005). Coupling the Soil–Vegetation Atmosphere Transfer Scheme ORCHIDEE to the agronomy model STICS to study the influence of croplands on the European carbon and water budgets. *Agronomie.,* in press.

Olesen J., Bindi M. (2002). Consequences of climate change for European agricultural productivity, land use and policy. *European journal of Agronomy*, 16, 239-262.

Parry M.L. (2000). Assessment of potential effects and adaptation for climate change in Europe: The Europe Acacia Project, Jackson Environmental Institute, University of East Anglia, Norwich, UK.

Ragab R., Prudhomme C. (2002). Climate change and water resources management in arid and semi-arid regions: prospective and challenges for the 21st century. Biosystems Engineering, 81, 3–34.

Rosenzweig C., Tubiello F.N. (1997). Impacts of future climate change on Mediterranean agriculture: current methodologies and future directions. Mitigation and Adaptation Strategies for Climate Change 1, 219–232.

Rosenzweig C., Strzepek K.M., Major D.C., Iglesias A., Yates D.N., McCluskey A., Hillel D. (2004). Water resources for agriculture in a changing climate: international case studies. Global Environmental Change, 14, 345–360.

Scholze M., Bondeau A., Ewert F., Kucharik C., Priess J., Smith P. (2005). Advances in Large-Scale Crop Modeling. Eos, 86, 26, 28 June 2005.

Sitch S., Smith B., Prentice I.C., Arneth A., Bondeau A., Cramer W., Kaplan J.O., Levis S., Lucht W., Sykes M.T., Thonicke K., Venevsky S. (2003). Evaluation of ecosystem dynamics, plant geography and terrestrial carbon cycling in the LPJ dynamic global vegetation mode. Global Change Biology, 9, 161-185.

Smith B., Prentice I.C., Sykes M. (2001). Representation of vegetation dynamics in modelling of terrestrial ecosystems: comparing two contrasting approaches within European climate space. Global Ecology and Biogeography, 10, 621-637.

Tubiello F.N., Ewert F. (2002). Simulating the effect of elevated CO2 on crops: approaches and applications for climate change. European Journal Agronomy, 18, 57-74.

Wolf J., Van Diepen C.A. (1995). Effects of climate change on grain maize yield potential in the European Community. Climate Change 29, 3, 299–331.

Chapter 2

2 Model evaluation and potential production

2.1 Introduction

The European Union's agriculture accounts for only 2% of its total Gross Domestic Product (GDP), but for 10% of global cereal and 16% of global meat production (Olesen and Bindi, 2001). The agricultural systems vary strongly among European countries, but they are currently connected within the same trading boundary, so local impacts may lead to a diffused response through the whole market. Furthermore, Europe has faced an increase in its average annual mean temperature of 0.8 °C over the last century (Beniston and Tol 1998), and further increases are expected as a consequence of the greenhouse gas concentration increase. New temperature and precipitation regimes will lead to a different distribution of meteorological conditions for crop growth in Europe (IPCC 2001a, Olesen and Bindi 2002). The CO_2 enriched atmosphere will also have a direct effect on the plant physiology, leading for some crops to better productivity and an enhanced water use efficiency (Van de Gejin and Goudriaan 1996, Tubiello *et al.* 1999). For this reason, climate change impacts on crops need to be assessed regarding two issues. First, how crop plant productivity will respond to the changing environment and, second, where the response will occur under the predicted new climate patterns.

Moreover, plants usually respond to a warmer environment with faster development. Therefore, the warmer climate will affect the crop phenology directly forcing the crops to develop faster and reach maturity earlier. The crop biomass production normally decreases with a shorter growth period due to diminished cumulative solar radiation interception during the active growing season (Abrol and Ingram 1996, Tubiello *et al.* 2000). In such a warming environment, the crop Net Primary Productivity (NPP) and the biomass yield

are expected to consequently decrease. Not only NPP can be affected by temperature through development, but also respiration can severly impact the biomass yield when temperature overcomes some specific threshold. However, NPP is also readily enhanced in a CO_2 enriched atmosphere, with a more substantial effect expected for C3 plants. Consequently the overall effect of climate change on crop development and biomass production would be a combined effect of the changes in temperature and atmospheric CO_2 concentrations, and could amount to an increase or reduction in biomass yield.

Crops are also included in the wider system of the biosphere, where changes in the biomass production of crops need to be included in any assessment of the carbon cycle at the continental scale. A new generation of Dynamic Global Vegetation Models (DGVMs) has been designed to simulate large-scale terrestrial vegetation dynamics, as well as the exchange of carbon and water between atmosphere and terrestrial biosphere (Kucharick *et al.* 2000, Smith *et al.* 2001, McGuire *et al.* 2001, Sitch *et al.* 2003). These models have been used to represent the transient terrestrial ecosystem responses to a rapid climate change forcing (Cramer *et al.* 2001), but only few of them have included crops as a dynamic part (Kucharick and Brye 2003, Donner *et al.* 2004). Small-scale agro-environmental impacts of climate change have been widely assessed using crop models (Tubiello and Ewert 2002). These have tremendous value for understanding crop behavior and predicting yields, but do not include detailed process-based descriptions of physiological and biophysical processes (Boote *et al.* 1997, Kucharick and Brye 2003), and require large numbers of crop specific parameters.

In this work, we incorporate crops and natural vegetation within a single modelling framework of a state-of-the-art Dynamic Global Vegetation Model (DGVM), LPJ (Lund-Potsdam-Jena) (Haxeltine and Prentice 1996a, Smith *et al.* 2001, Sitch *et al.* 2003) by introducing a crop carbon allocation scheme adapted from the WOFOST (WOrld FOod STudies) crop growth model (Van Diepen *et al.* 1988, Van Diepen *et al.* 1989, Supit *et al.* 1994, Boogard *et al.* 1998). All vegetation types use a common photosynthesis-assimilation scheme, while specific carbon dynamics rules are implemented for crop growth and development. This new version of the LPJ model includes crop-

specific carbon and water dynamics without model-dependent discontinuities when switching from natural vegetation to crops, but still maintains structural and dynamical differences between natural and crop plants. The crop compartment uses several parameters to drive the crop growth and simulation. A full non-linear optimization procedure is used to find the optimal crop parameters for the simulation in Europe.

The resulting optimal parameterization is used to run the model under several climate change scenarios to quantify impacts on the crop potential yields, and the patterns of productivity. In order to differentiate the effects of temperature changes from the direct effects of increased CO_2 concentrations on plant physiology, the assessment is performed using two modes, ``climate and $CO_2$ concentration change'' (*CCO2*) and ``climate change only'' (*CC*). In this way, it is possible to separate the response to the climate signal from the CO_2 fertilization effect. In this work, we exclusively focus on the climate change impacts of the major crop varieties simulated within a single model of natural and crop vegetation dynamics. The effects of technology change, cultivar adaptation, and irrigation will be reserved for later studies.

2.2 Methods

2.2.1 WOFOST

WOFOST is a semi-mechanistic model to simulate crop growth and development for potential and water limited production conditions, using climatic variables as driving forces, soil site characteristics, crop specific parameters and management options (Van Diepen *et al.* 1989,Van Ittersum *et al.* 2003). This model has been developed during the late 1980s following the pre-existing crop growth model SUCROS (Van Keuelen and Wolf 1986, Goudriaan and Van Laar 1994, Van Laar *et al.* 1997) at Wageningen University, The Netherlands. During the last 20 years the model has been continuously improved and widely applied in several monitoring (Boons-Prins *et al.* 1993, De Konig and Van Diepen 1992) and forecasting applications (Roetter 1993, Zinoni *et al.* 2004, Marletto *et al.* 2004). WOFOST calculates the daily rate of canopy CO_2 assimilation from daily incoming radiation, temperature, leaf area index (LAI), and canopy extinction coefficient (k). The model contains a set of subroutines to calculate the daily totals by integrating

rates of leaf CO_2 assimilation both over time and canopy profile. The crop production is structured in two hierarchical levels. First the potential production is calculated as the maximum production reachable by the crop assuming full availability of water and nutrients, and the absence of pests. After that, stress factors are applied to reduce the potential yields to water-limited and nutrient-limited. The water-stress reduction factor is evaluated using a detailed soil water balance model. Once the net biomass increase is defined, it is partitioned into four crop plant compartments (stems, leaves, roots and storage organs) according to crop specific partioning factors, the values of which depend on the development stage.

2.2.2 LPJ

The LPJ Dynamic Global Vegetation Model adopts a large-scale and process-based representation of terrestrial ecosystem dynamics taking into account carbon and water cycling in vegetation and soil, vegetation structural and compositional dynamics, and disturbance by fire. A comprehensive description of the model is given by Sitch *et al.* (2003). Representations of plant physiological and canopy biophysical processes are inherited from the BIOME3 equilibrium biogeography model (Haxeltine and Prentice 1996a). The vegetation of each modelled area or grid cell is represented as a combination of Plant Functional Types (PFTs), differentiated by physiological, dynamical and structural attributes as well as bioclimatic constraints for survival. Monthly climate data, and atmospheric CO_2 concentration drive the simulation for each grid cell, characterised by a prescribed soil type. Vegetation structure and dynamics are explicitly included and populations of PFTs compete for light and water. The soil is divided into two layers and contains three carbon pools with different carbon decomposition rates. Photosynthesis is modelled based on a version of the Farquhar model (Farquhar and Von Caemmerer 1980, Farquhar and Von Caemmerer 1982) readapted for global modelling purposes (Collatz et al. 1991, 1992). In this model the Rubisco activity is assumed to vary both seasonally and within the canopy in order to always maximize the net assimilation at leaf level (Haxeltine & Prentice 1996b). Under this ``strong optimality'' hypothesis (Dewar 1996, Haxeltine and Prentice 1996b) it is possible to predict the light-use efficiency from environmental factors. Even

Figure 2-1 Relation diagram of the LPJ-C, in green the crop compartment.

though the underlying mechanism are not completely understood (El Maayar *et al.,* 2005), the photosynthetic acclimation (or downregulation) to increased CO_2 concentration can lead to overestimation of assimilation at leaf level, especially for crops (Tubiello *et al.,* 2000). LPJ does not take into account such a process; on the other hand, El Maayar *et al.* (2005) demonstrated that acclimation would be taken into account only for small decrease in global net primary productivity.

2.2.3 LPJ-Crop

One of the main differences between wild and crop plants is the biomass allocation within the structural parts. Genetic selection of agricultural plants designed much higher biomass allocation into the compartments with economic value, i.e. roots or grain, but several studies show that the basic

biochemical patterns and ecophysiological processes are only slightly different (Singaas *et al.*, 2001).

Table 2-1 List of the experimental datasets used in the optimization. Lon and Lat refer to the nearest CRU TS 2.0 grid point used in the procedure.

Location	Lon	Lat	Years	Vars	Reference
			MAIZE		
Toulouse, France	1.5	43.5	1985, 1986	TAGB, DVS	Boons-Prins *et al.* 1993
S. Prospero, Italy	11.0	44.0	1997	TAGB, DVS	Ceotto 1999
Zaragoza, Spain	0.5	41.0	1995, 1996	DVS	Cavero *et al.* 2000
Settima, Italy	9.5	44.5	1997, 1998, 1999	DVS	Dal Monte *et al.* 2002
Vasto, Italy	14.0	42.0	1997, 1998	DVS	Dal Monte *et al.* 2002
			WHEAT		
Helecine, Belgium	5.0	50.5	1985	TAGB, DVS	Boons-Prins *et al.* 1993
De Bouwing, The Netherlands	6.0	52.0	1983, 1984	TAGB, DVS	Boons-Prins *et al.* 1993
Lelystad, The Netherlands	5.5	52.5	1983, 1984	TAGB, DVS	Boons-Prins *et al.* 1993
Rothamsted, UK	0.0	52.0	1980, 1981	TAGB, DVS	Boons-Prins *et al.* 1993
S. Prospero, Italy	11.0	44.0	1994, 1995	TAGB, DVS	Ceotto 1999
Settima, Italy	9.5	44.5	1998, 1999	DVS	Dal Monte *et al.* 2002
Vasto, Italy	14.0	42.0	1997, 1998, 1999	DVS	Dal Monte *et al.* 2002

Agro-ecosystems are generally monocultural and often consist of annual plants. One result is that short and intense drought can impose severe reduction on the crop yield within a period of few weeks. That implies that the time scale of the vegetation processes also needs to be considered differently in the modelling of crops, compared to natural vegetation. In its original version, LPJ only considers perennial PFTs, while in this work we describe crops exclusively as annual plants. Therefore, separate carbon allocation schemes with different time steps were implemented in this study for modelling of natural vegetation and crops (Figure 2-1). For natural vegetation, the standard LPJ biomass production scheme with a yearly time step for the allocation and the consequent LAI calculation was adopted. For crop development, a daily time step was adopted for all the processes. The

adapted LPJ model thus provides a day-by-day quantitative description of the growing season of the crop, while preserving the more computationally efficient scheme for natural vegetation. In this model version, we only simulate potential crop production; the water demand is always fulfilled, so that the plant productivity is always at the maximum achievable level under the constraining light and temperature condition. The crop carbon allocation scheme is derived from the WOFOST model as described in the Appendix I. As mentioned above, the integration of the water stressed production will be reserved for a later study.

2.2.4 Crop Data

Experimental crop observations were gathered from several maize and wheat field experiments in Europe (Table 2-1; Figure 2-2). Phenological records and biomass data were taken from the PHENAGRI project (Dal Monte *et al.* 2002), the Crop Growth Monitoring System (CGMS) of the European Community (Boons-Prins *et al.* 1993) and from some published field experiments (Ceotto 1999, Cavero *et al.* 2000). Since the model simulates potential production, only sites with predominantly non water-stressed conditions were selected for the optimization procedure. All data sets have previously been used for the validation of other crop growth models (Marletto *et al.* 2004, Zinoni *et al.* 2004). Using the available information we have set up two data sets. The first consists of phenological records showing the date of emergence, flowering and maturity of the crop experiment. Since no information on crop phenology is provided by CGMS, the day of the maximum measured LAI was taken as the date of anthesis. The second data set consists of Total Above Ground Biomass (TAGB) recorded during the growing season. When no specific data were available, the day of the last TAGB record was considered the maturity day.
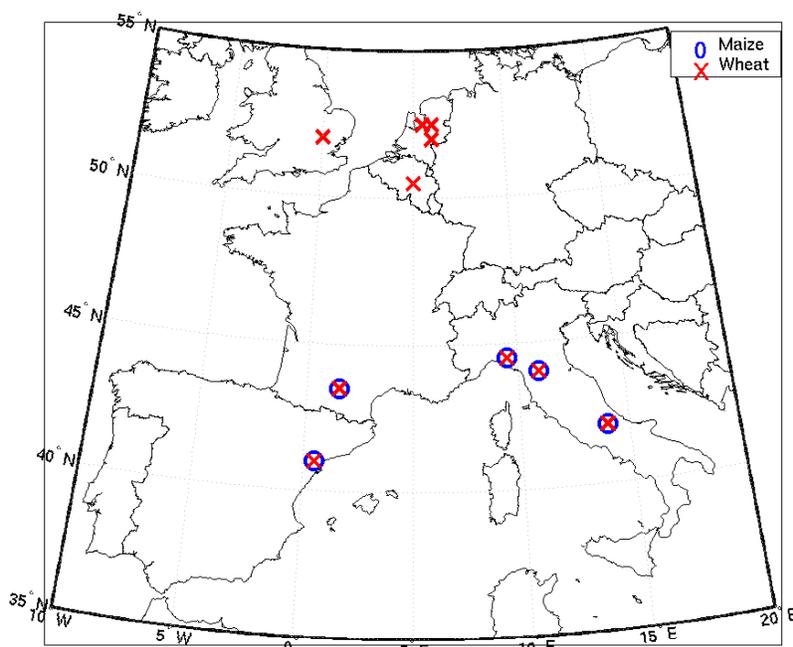
Figure 2-2 Locations of the experimental fields (Table 1) providing data for this work.

2.2.5 *Environmental forcings and experimental design*

The CRU TS 2.0 (Mitchell *et al.* 2004) global climate data set was used for the parameter optimization and to drive the simulations for the period 1901-2000. It provides monthly fields of observed mean temperature, precipitation and cloud cover on a 0.5° x 0.5° global grid over land. The complete set is one of the high-resolution gridded data sets of the Climate Research Unit of University of East Anglia and the Tyndall Center. The TYN SC 2.0 (Mitchell *et al.* 2004) is also part of the same data source; this data set was used to force the model for the future climate scenarios for the period 2001-2100. It consists of monthly climate data for the period 2001-2100 simulated by General Circulation Models (GCMs), covering the global land surface on the same 0.5° x 0.5° grid as the CRU TS 2.0. This set includes 16 scenarios of projected future climate representing all combinations of four SRES emissions scenarios and four GCMs, covering 93% of the range of uncertainty in global warming in the 21st century published by the Intergovernmental Panel on Climate Change (IPCC 2001b). We choose HadCM3 and CGCM2 outputs,

both under the SRES-B2 and SRES-A1 scenarios. A1 and B2 are the opposite representation of the world development within the SRES group. In the A1, the world is highly globalized and emphasis is on global economic growth rather than environmental protection and sustainability; we consider the particular case of A1FI, which is the "Fuel Intensive" sub-scenario where fossil fuels remain the main energy source. In the B2, on the contrary, Europe searches local solution for better solve ecological and social problems. The choice of the HadCM3 and the CGCM2 scenarios was motivated by their behaviour over Europe, which are characteristic for two clusters/families of scenarios in the IPCC analysis. HadCM3 is considered one of the reference GCMs within the IPCC framework and shows a clear increase in temperature over Europe (IPCC 2001a). In the IPCC simulations CGCM2 shows a marked slowdown of the North Atlantic thermohaline circulation (IPCC 2001a), so that heat transport to the North Atlantic and Europe tends to decrease. CGCM2 thus shows a less intense temperature increase until 2100. The land included within the borders 10.0° W and 50.0° E in longitude, 35.0° N and 70.0° N in latitude is defined as the study area. Mean climate and atmospheric CO_2 are shown in Figure 2-3, where HadCM3 temperature increases by 0.63° C per decade in the A1, and 0.24 °C in the B2 scenario, while for CGCM2 it is only 0.43 °C per decade in the A1, and 0.17 °C in the B2 scenario. Monthly climate data are interpolated to obtain quasi-daily series to drive the simulations. Mean global CO_2 concentration were taken from McGuire *et al.* (2001) covering the period 1901-1992, derived from ice cores and averaged observations from Mauna Loa and South Pole monitoring stations (Keeling *et al.*, 1995, Etheridge *et al.*, 1996). For the remaining period 1993-2100, mean global CO_2 concentration corresponding to the SRES-A1 and SRES-B2 scenarios (Schlesinger and Malyshev, 2001) were used.
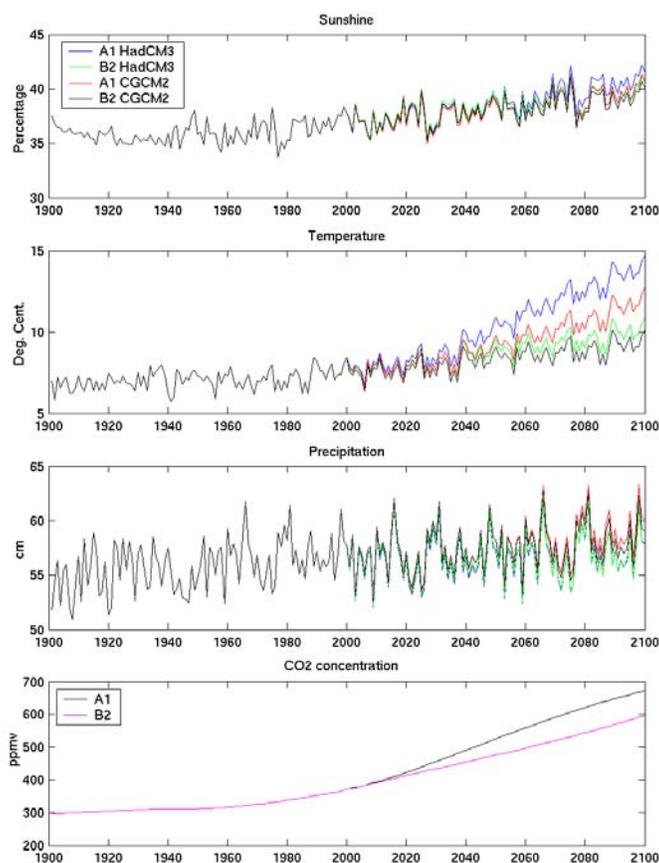
Figure 2-3 Climate annual means over the study area (10.0°W - 50.0°E, 35.0°N - 70.0°N.

Soil texture data were based on the FAO soil data set on a global 0.5° x 0.5° grid, as described by Sitch et al. (2003). A crop map with a global resolution 0.5° x 0.5° derived from Ramankutty and Foley (1998), was used as a mask to delimit crop areas on the grid. The Ramankutty and Foley data sets give a gridded representation of the global cropland distribution of the year 1992. The value of each grid point represents the fractional area covered by crops, expressed as an index from zero to one. The index is associated also to qualitative classes ranging from "other vegetation" (index zero) to "crops" (index one). Cells with an index from 0.15 to 1.0 (from class ``other vegetation and crop mosaic'' to ``crops'') have been selected for Europe from the original data set (Figure 2-4). Two Crop Functional Types (CFT), maize and wheat, were simulated, the latter based on parameter optimization (see
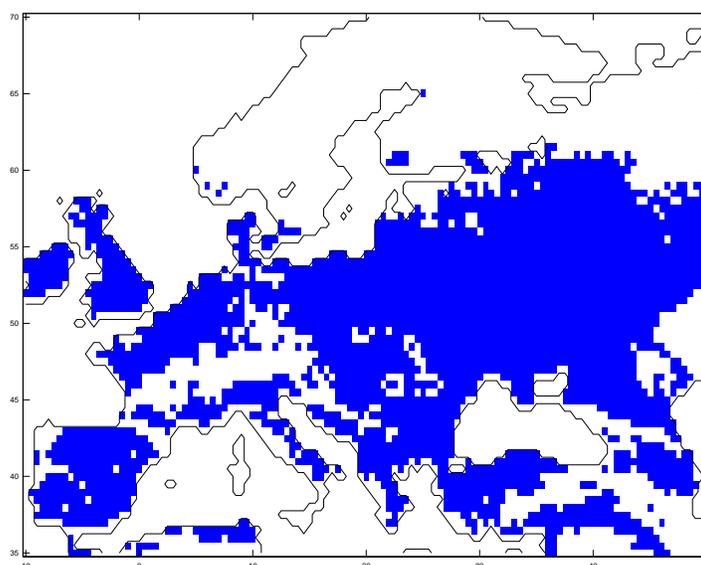
Figure 2-4 The applied crop mask; maize and wheat are free to grow on the mask with no competition for resources. No natural vegetation is allowed to grow on this grid and the grid remains constant over the whole simulation period.

next section). No natural vegetation was allowed to grow over grid points designated as crops according to the crop mask. Development of maize and wheat were simulated independently for each grid cell, with no assumption of competition for resources between these crop types.

The model was forced with each of a set of eight scenarios of future climate and atmospheric CO_2 concentrations: for each climate scenario (HadCM3-A1, HadCM3-B2, CGCM2-A1 and CGCM2-B2), separate runs were perfomed changing climate and CO_2 together (*CCO2* mode) or climate alone (*CC* mode). In the *CC* mode, the CO_2 concentration is fixed at the pre-industrial level of 280 ppmv for the whole simulation period, while the climate varies according to observation (until 2000) and to predictions (from 2001). For the *CCO2* simulations, the climate forcing is still the same to the *CC*, but CO_2 varies together with climate.

2.2.6 Crop parameter optimization procedure

The geographical distribution of crops is linked to many factors such as irrigation and fertilization techniques, cropping systems, soil management and

genetic characteristics of the cultivars. In this model, we represent a mean maize and wheat plant described by specific model parameter sets (Table 1 in Appendix I). Since it should be suitable for large scale simulations, our strategy was to find the best parameter set that minimizes the mean squared error between simulated values and regionally distributed point observations. The model was run for all points where crop data were available (Table 2-1; Figure 2-2). In the absence of site measurements of weather variables, data from the nearest CRU TS 2.0 grid point were used as climate forcing. The optimization procedure was applied to the crop parameterization in order to minimize the mean squared error (MSE), defined as follows, over all the simulated and the observed local data.

$$MSE(Parset) = \frac{\sum_{n}^{i}(k_{n,i} - x_{n,i}(Forc_i, Parset))^2}{N}$$

$k_{n,i}$: measured quantity number *n* on the field experiment number *i*

$x_{n,i}$: simulated quantity number *n* on the field experiment location number *i* as a function of forcing and the set of parameters

Forc_i: climate and soil forcing of the simulation for the field experiment location number *i*

Parset: crop parameter set used in all the simulations

N: number of samples

The result of this procedure is an optimized crop parameter set that allows the model to simulate the crop growth as closely as possible to the observed values within the study region.

Crop growth is characterized by dry matter production whilst development is characterized by crop phenology (Goudriaan and Van Laar, 1994). In the model, the phenology is represented by the development stage (see Appendix I), which depends only on past air temperature and on three crop parameters, the heat requirement sums for each of the growth phases (*tsum1*, *tsum2*), and the effective development response to temperature (*dtsmtb*). The heat requirement sums (*tsum1*, *tsum2*) determine the length of the growing season. Since the length of the growing season has an important impact on the biomass production, *tsum1* and *tsum2* play a dominant role for the biomass production when compared to the effective development response to

temperature (*dtsmtb*). The day of the emergence, i.e. the beginning of the development stage, is calculated using a simple 10-days running mean temperature threshold set to the parameter *t_eme* for maize, while it is fixed at the first day of the year (see Appendix I) for wheat. Biomass production is a complex process driven by the development stage involving light interception, photosynthesis, carbon allocation and mortality. Since in the model the crop phenology is completely independent from the biomass production, the development stage optimization was performed first, then, using the results, the optimization of the biomass.

2.2.7 Optimization of the development stage submodel

The phenological data sets contain the dates of emergence, flowering and maturity in day of the year (DOY). The development stage submodel not only describes the development in time, but also identifies the DOY of the flowering and maturity. Since all the phenological data are expressed in days, the MSE can be expressed in days. In addition to that, the maize emergence date has to be optimized in order to set the starting date for the maize development stage calculation. In fact, the maize emergence depends on a 10-day running mean temperature (*t_eme*) and is completely independent from the development stage (see Appendix I). Thus, before the beginning of the optimization of the maize development stage, the optimal mean temperature for emergence (*t_eme*) has to be found through a separate procedure.

In order to find the optimal parameter set, we used an unconstrained non-linear optimization procedure applied to the MSE function: a Matlab routine based on the simplex direct search algorithm (Lagarias *et al.* 1998) starting from a user-specified point with a specified tolerance. The beginning points of the search were set to literature values found (Boons-Prins *et al.* 1993) and a minimum and a maximum parameter increment (max increment 100.0 °C day, min increment 10.0 °C day) were set to speed up the search algorithm. No increments were set for the maize emergence temperature parameter optimization. Since the effective development response to temperature (*dtsmtb*) plays a secondary role in the development stage calculation, we included in the optimization only the heat requirement sum (*tsum1*, *tsum2*).

2.2.8 Optimization of the production model

Detailed information on the biomass in all the plant compartments is usually unavailable; only the total above ground biomass (TAGB) is present for all sites contributing data to this study. The biomass production depends directly on the net primary productivity (NPP), which depends in turn on the light interception as a basic process for carbon assimilation. We optimized the three parameters that define the assimilation at leaf-scale: the light extinction coefficient (*Kcrop*), the specific leaf area (*sla*), and the LAI at emergence (*LAIeme*). *Sla* and *LAIeme* drive and initialize the LAI development that controls leaf assimilation. *Kcrop* defines the capacity of the crop canopy to intercept light depending on LAI. The selected parameters have numerical limits, so the optimization has to be constrained within boundaries (see Appendix I). Therefore, a constrained non-linear optimization procedure was used to find the optimal parameters that minimize MSE. The strategy and the technical procedure was the same as for the development stage optimisation, except that a constrained search was applied. In this case, the MSE represents the mean squared error between the observed and simulated TAGB.

2.2.9 Climate change impact analysis

Since the model simulates the potential production of crops, only temperature and radiation drive the crop growth during the growing season. Radiation is the dominant factor in the biochemical processes at leaf level, but usually it is not a limiting factor for the development (Goudriaan and Van Laar 1994). The enriched CO_2 atmosphere can lead plants to improve their photosynthetic efficiency, so the joint effects of temperature and CO_2 concentration are expected to interact on crop productivity. The two crops do not always reach physiological maturity over the whole crop simulation grid, so the grid distribution of the potentially useful points changes in time. We apply our analysis only to the grid points where maize and wheat reach their full maturity and are theoretically ready to be harvested. Therefore, our assessment is divided in two parts, an analysis of the effects on crop productivity and another on the geographical patterns where crops reach full maturity.

The interannual variability of the total productivity over the study area has a component related to the change in distribution as well. In order to exclude it and to take into account only changes in plant productivity, we analyse the means over a fixed number of grid points during all the simulation years. We selected those points where maize and wheat reach full maturity at the first year of simulation, and we refer to this area as the "fixed reference area" of both crops. In this way, when we describe the interannual variability of the means, we represent the interannual variability referring to the initial state excluding any components due to area change. The initial maize distribution is shown in the Figure 2-9. Wheat reaches maturity over virtually the entire crop mask already at the beginning of the simulations.

Here, we analyse the effect on both the growing season length effect and the Harvest Index (HI) defined as:

$$HI = \frac{SO}{TAGB}$$

SO: Biomass storage organs [kgC/m2]

TAGB: Total above ground biomass [kgC/m^2]

HI expresses the yield efficiency in the carbon distribution within the above ground parts of the plant. The assimilated carbon begins to be allocated to the grain compartments only during the grain-filling phase, i.e. after flowering. Therefore, a high HI means that the plant has allocated more carbon to the grain and did so during the grain-filling phase. Biomass growth is coupled to photosynthesis, so a high HI indicates growth conditions favourable to production during the second part of the development.
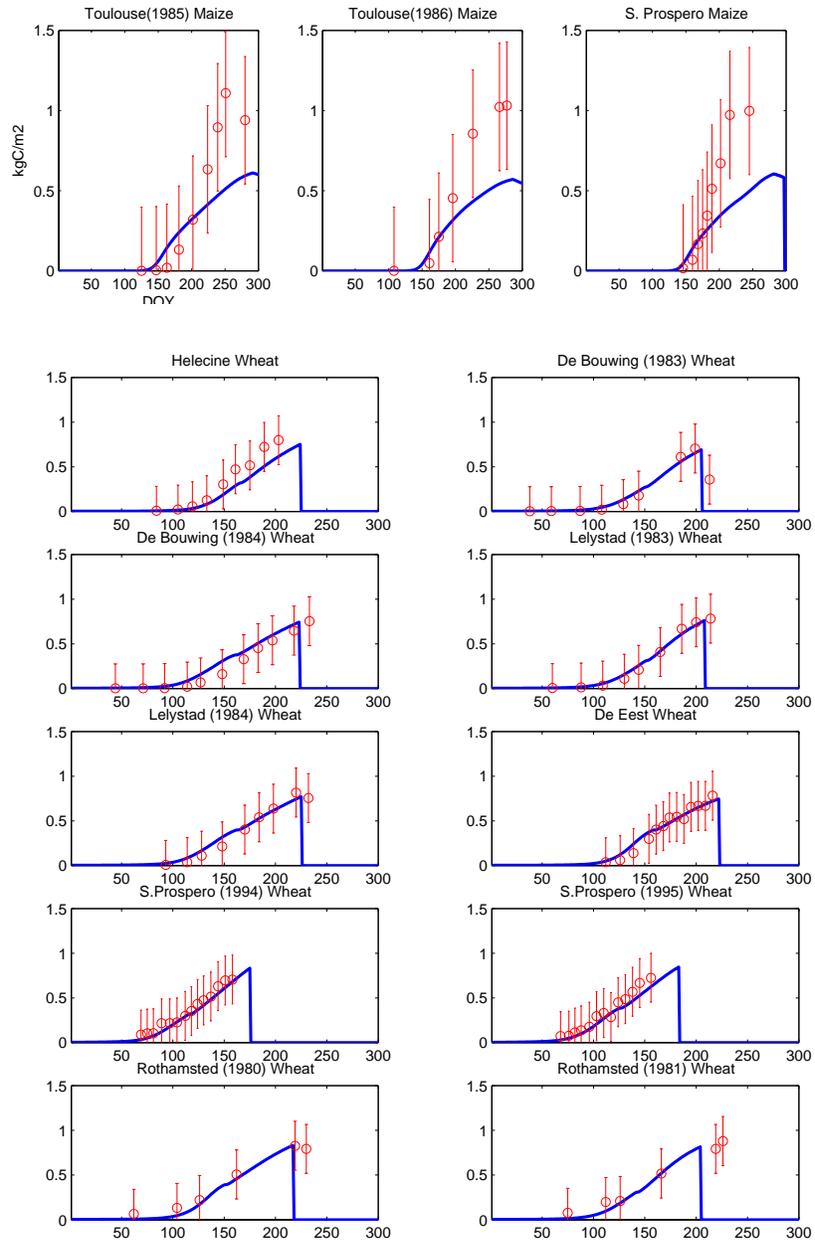
Figure 2-5 Optimization results for the biomass production model. Error bars show the standard deviation within all the data from the field experiments for wheat and maize.

Table 2-2 Results of development stage (DVS) submodel optimization, refer to Table 1 in Appendix I for input variable description.

	Maize DVS		Wheat DVS		Maize emergence
Parameters	tsum1	tsum2	tsum1	tsum1	t_eme
Beginning point	693.0	768.0	1255.0	909.0	6.0
Optimal point	1718.0	1135.0	1004.0	954.0	13.7
MSE [d^2]	344.7		429.9		411.8

Table 2-3 Results of the production model optimization, refer to Table 1 in Appendix I for input variable description.

	Maize			Wheat		
Parameters	Kcrop	sla	LAIeme	Kcrop	sla	LAIeme
Beginning point	0.50	0.0020	0.50	0.50	0.0020	0.13
Higher limit	0.99	0.0080	0.99	0.99	0.0080	0.099
Lower limit	0.03	0.0010	0.001	0.03	0.0010	0.01
Optimal point	0.81	0.0070	0.038	0.81	0.0070	0.099
MSE [(kgC/m^2)^2]	0.225			0.051		

2.3   Results

2.3.1   Optimal crop parameter sets

The summary and results of the DVS optimization set are given in the Table 2-2. The maize optimal points generally deviate more from the starting points than for wheat. Wheat MSE is also larger then maize, which reflects the intrinsic variability in the phenology data set, where the date of full maturity have a much larger variability then in the maize case.

The results of the production model optimization are given in Table 2-3. According to Figure 2-5 and the results in the table, the wheat simulations fit better then those for maize. In this case, the shape of the simulated curves does not fit the observed data, and during the final phase the simulated values are up to 50% smaller then the recorded data. For wheat, the observed and simulated curves show a much better fit.

The delay in the emergence and day of maturity depends on the development stage optimization. Maize reaches simulated maturity around DOY 300, with a constant delay of mostly 10 days against the last record. Wheat has a larger variability in the simulated day of maturity then maize. In the case of maize, only three stations do not seem to be sufficient to fully characterize the crop, while the ten data sets of wheat lead to a better optimization. The optimization results could be improved, hence, with the use of more experimental data, especially from CO_2 enriched experiments as ESPACE-wheat (Bender *et al.*, 1999) or FACE experiment (Tubiello *et al.*,

1999; Kimball *et al.*, 2002). The photosynthesis submodel of the LPJ standard version has been already tested in the NPP response to atmospheric CO_2 increase (Bacelet *et al.* 2003, Hickler *et al.* 2003), but in this context a more detailed test has to be carried out before planning an optimization procedure with CO_2 enriched atmosphere data. We reserve, therefore, this issue for a further study.
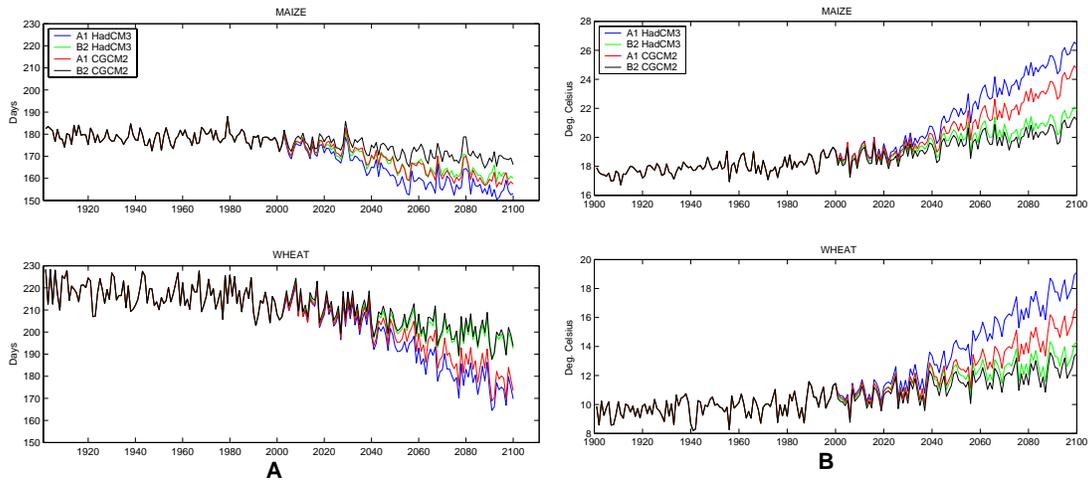
Figure 2-6 A, the mean length of the growing season, in B mean annual temperature over the fixed reference area.
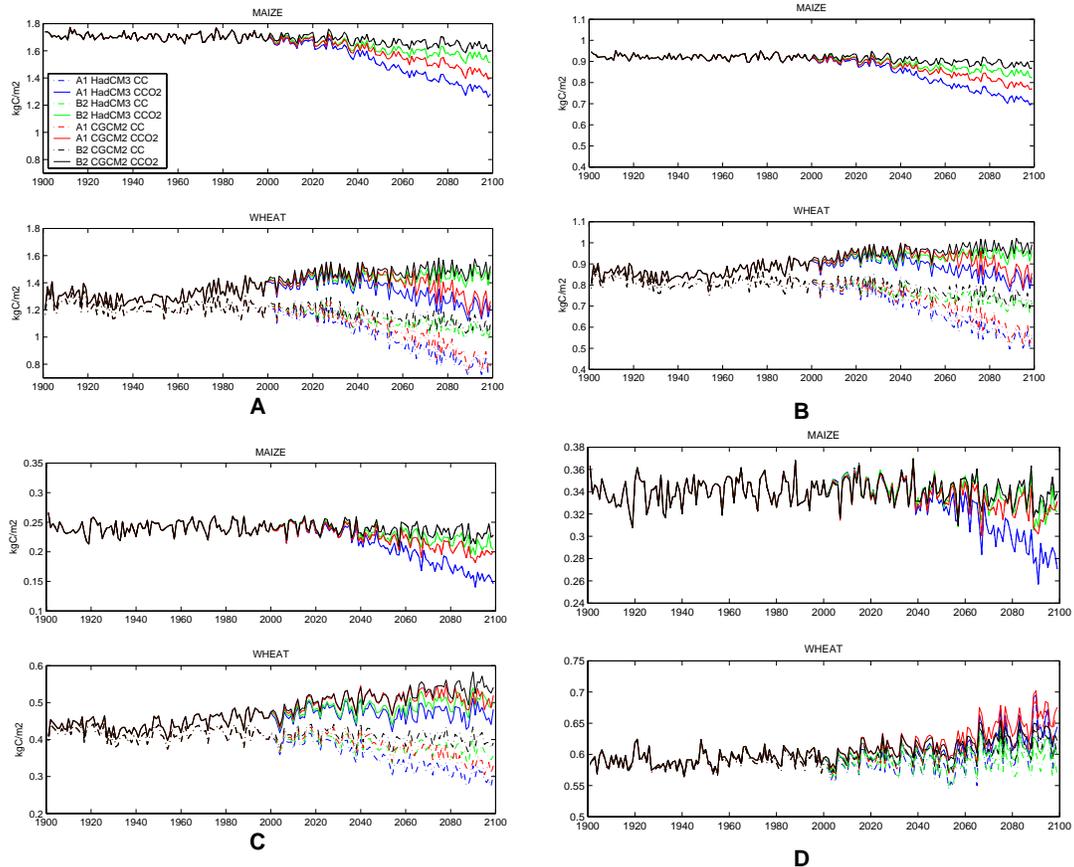

Figure 2-7 Mean crop production over the fixed reference area. In A the annual net primary productivity, in B the total carbon biomass, in C the grain carbon biomass and in D the harvest index. In B,C and D the values are referred to the end of the growing season. The model shows a non linear response to the temperature increase in the HadCM3 A1. Only in this case maize grain biomass and harvest index strongly decrease, while the total biomass decrease is more homogeneous in all the maize simulations. Wheat productivity is clearly related to the length of the growing season shown in the Figure 2-6-A.

2.3.2 Climate change effect on crop development and growth

The length of the growing season of maize (Figure 2-6-A) tends to oscillate around 180 days with an interannual variability within 10 days during the last century. The change within the period 2001-2100 depends on the warming conditions of the corresponding scenario (Figure 2-6-B). Thus, in the warmest scenario HadCM3 A1, the growing season length decreases by more then 20 days by the end of the simulation, while in the coldest, CGCM2 B2, the decrease is less then 10 days. The increased temperatures lead to higher levels of maintenance respiration, so annual NPP (ANPP, Figure 2-7-A) tends to decrease in all the scenarios. As described before, the shorter growing season leads NPP to decrease as well, so the current NPP decline is the result of the combined effect of faster development and higher respiration costs. Since maize is a C4 plant, the enriched CO_2 atmosphere does not affect NPP significantly. Since no external stress is simulated, total biomass tends to proportionally follow the decrease in ANPP (Figure 2-7-A). The grain carbon mass and the HI decrease during the same period as well (Figure 2-7-C and D). Further, the maize HI remains more or less stable for all the simulations, but it decreases severely in the warmest scenario, i.e. HadCM3 A1. In this case, the assimilated carbon is allocated more to the stems and leaves than to the grain. Since the grain allocation begins only after flowering, less biomass in the grain compartment means that the plant assimilates less carbon during the grain-filling period.

Figure 2-8 shows on the left side the decadal increment in monthly temperatures from April to September over the fixed maize reference area. The grain-filling phase corresponds mostly to the mid or late summer (July, August, September), when temperature shows a steep increase. In other words, the temperature of the months corresponding to the grain-filling period increases faster then these of the vegetative months (April, May and June) after 2000. Consequently, the development after flowering becomes faster and the grain-filling covers a shorter part of the full development cycle. The HadCM3 A1 shows the steepest increase, over 0.5 °C by the end of the scenario, compared to initial conditions. This simulation alone is associated with a strong decrease in grain biomass as well. While temperature increases
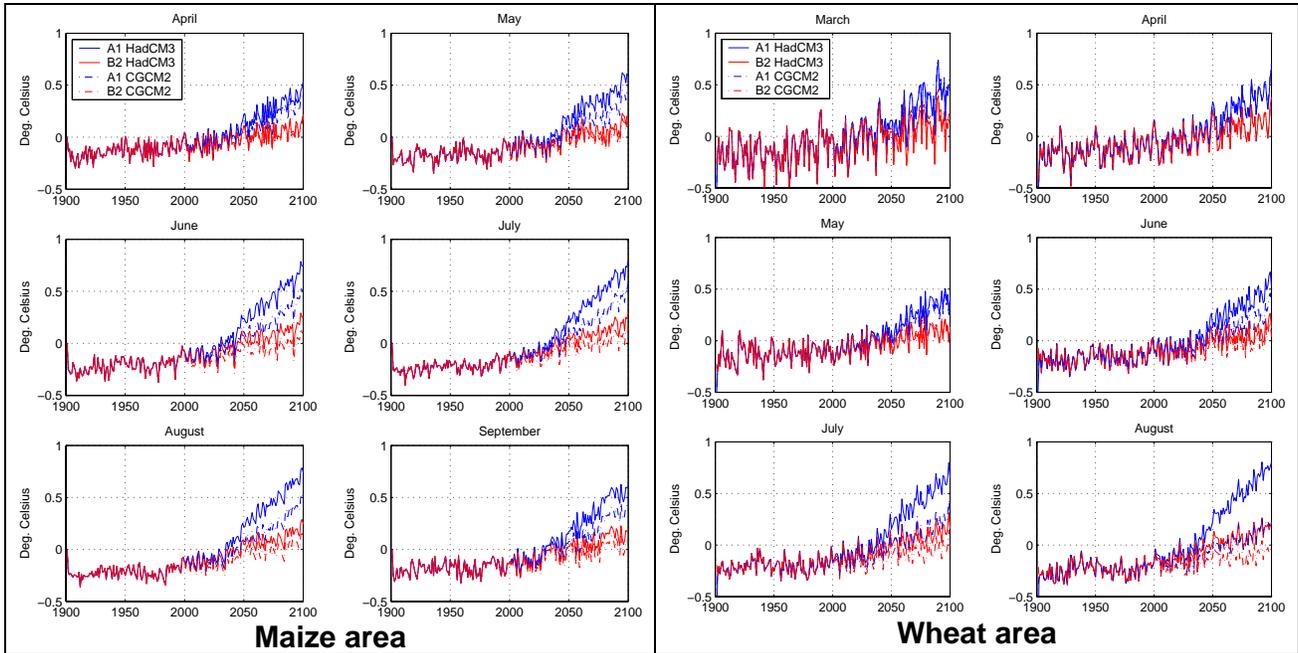
Figure 2-8 Decadal increment in monthly mean temperature over the fixed reference area. The increment is calculated as the difference between the month of the current year and the climatological mean of the month over the whole simulation period.

in all the scenarios, only for HadCM3 A1 the grain biomass production tends to collapse. This indicates that the model shows a response related to an internal temperature threshold. When the driving temperature is above this limit, the development becomes so fast that a clear impact on the maize biomass has to be expected in addition to the respiration cost.

The temperature increase has an even stronger impact on wheat growing season. The length decreases in all the simulations (Figure 2-6-A) as in maize, but the rate of decrease is much more intense: for HadCM3 A1 it goes from around 220 days to 170, a decrease of 50 days. Figure 2-8 on the right side also shows that the increase in April, May, and June during the wheat season are very similar across the scenarios. Only in July HadCM3 A1 temperature increases faster, but the development during this month is mostly completed or in its very final part. Therefore, large differences in grain biomass and HI are not as clearly evident among the simulations as it is for maize (Figure 2-7-C and D).

When the fertilization effect of increased CO_2 concentrations is excluded (*CC* scenarios), wheat NPP decreases more markedly than maize. In this case, not only respiration, but also the strong shortening of the growing period
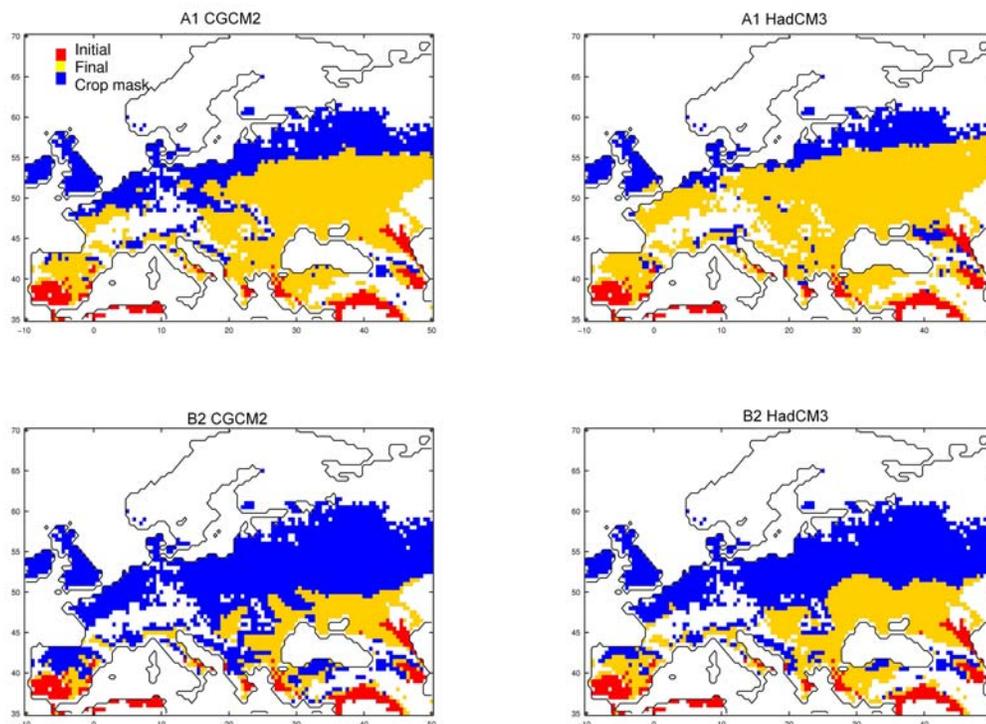
37

Figure 2-9 Change in the maize maturity distribution. Maize can freely grow on the crop mask (Figure 4). In red, the initial area occupied at the beginning of the simulations (1901). In yellow, the relative increase at the end (2100), the final distribution is is the yellow and red areas together. In blue, the remaining free crop mask.

plays a role. The two groups of simulations, *CCO2* and *CC*, show that A1 and B2 scenarios are clearly separated for wheat (Figure 2-7-A, B and C). Revisiting Figure 2-6-A, it is possible to note that also here there is a clear separation between A1 and B2 groups of wheat growing season length. This confirms that, apart from respiration, the length of the growing season controls the ANPP and the consequent total biomass. The fertilization effect applies to wheat, a C3 plant, so ANPP and total biomass increase in *CCO2* (Figure 2-7-A), but starts to decrease in the A1 group when the high temperature causes higher respiration. Grain biomass and HI increase in all the simulations, this means that carbon is allocated more efficiently to grain and final yield always improves.
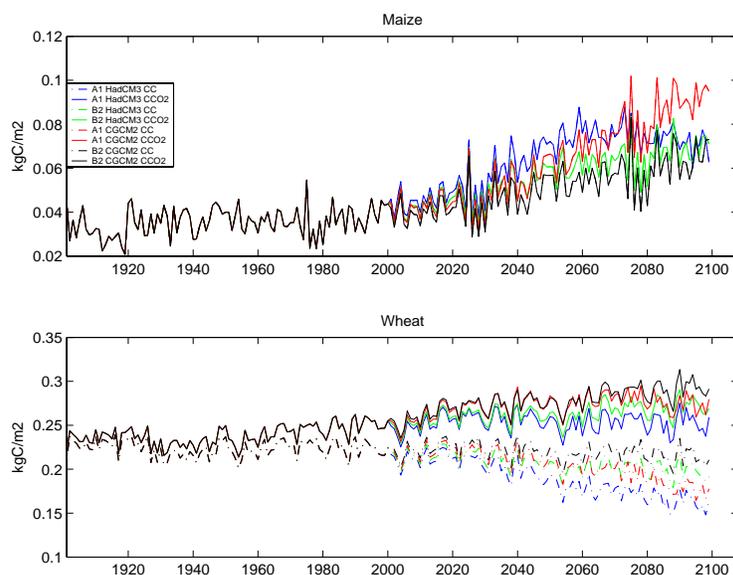
Figure 2-10 Mean grain biomass over the study area at the date of maturity. The mean is calculated over the whole applied crop mask.

2.3.3 Climate change effect on the geographical distribution

One of the most interesting climate change impacts for Europe is the predicted effect on grain yield distribution (IPCC 2001a, Olesen and Bindi 2001). In this study, both maize and wheat are set on the same crop mask over Europe (Figure 2-4) and free to grow with no competition. In this way, climate is the only forcing that determines the geographical distribution over the study area through its impact on phenology.

Figure 2-9 shows the areas where maize reaches full maturity. At the beginning of the simulation maize reaches full development only in southern Europe, but at the end, the central and eastern parts become largely suitable. While the climate warms, the suitable conditions for maize development follow the temperature paths by moving towards north and east. The largest differences are between emissions scenarios rather than GCMs. Both A1 scenarios provide suitable conditions for maize maturity over the majority of the crop mask, while for B2, some large area in north and central Europe remain still unsuitable. Not only the areas of full maturity, but also the areas with higher grain yield move from southern towards central and Eastern Europe. If we consider the quantitative biomass change between the end and

the beginning of the simulations, we notice that the grain biomass does not vary uniformly. In Figure 2-10, the mean of maize grain biomass increases rapidly over the whole continent as a consequence of the areal expansion. As we see in Figure 2-11-A, while the change in maize grain biomass is mostly positive, in some parts of southern Europe it is actually negative. Therefore, the carbon biomass decreases in the grain compartments in some points of the initial crop area, confirming what was shown before for the plant productivity impacts.

In each simulation year, wheat reaches full development mostly over the whole crop mask, but the growing season becomes always shorter so that NPP decreases. Since wheat is a C3 plant, the CO_2 concentration has a clear effect on the assimilation efficiency. In Figure 2-10, the mean wheat grain biomass decreases in *CC*, but slowly increases in *CCO2*. Since the mean in the figure is calculated over the whole crop mask and wheat covers always almost all mask, the curves in the figure reflect the same behaviour shown in Figure 2-7-C. The change in the grain biomass is mostly negative in all the *CC* simulations, but in the *CCO2* it is positive almost everywhere in Europe. This difference is more evident in the A1 runs (Figure 2-11-B). In both HadCM3 A1 and CGCM2 A1, the absolute grain biomass change for *CCO2* (Figure 2-B, on the right) is negative only in some points in southern Europe, while it is mostly negative over the whole continent for *CC* (Figure 2-B, on the left). Figure 2-11-B also shows that the areas with the largest decrease in wheat grain biomass in *CC* correspond to the areas with the smallest increase in *CCO2*. It is particularly evident in the eastern central region, where temperature increases most. The shorter growing season and the high respiration lead to a decrease in biomass accumulation. In *CCO2*, the CO_2 fertilization effect counterbalances this effect and the biomass tends still to increase slightly, while in *CC* clearly decreases. Furthermore, in both the cases, some parts of southern Europe show always a decrease in grain biomass, as in the case of maize.
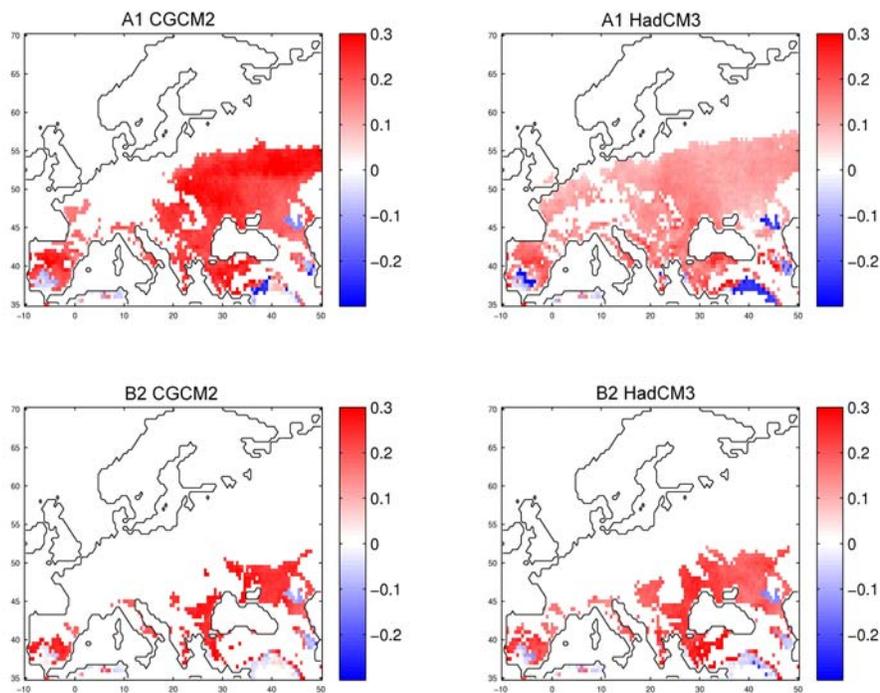
A
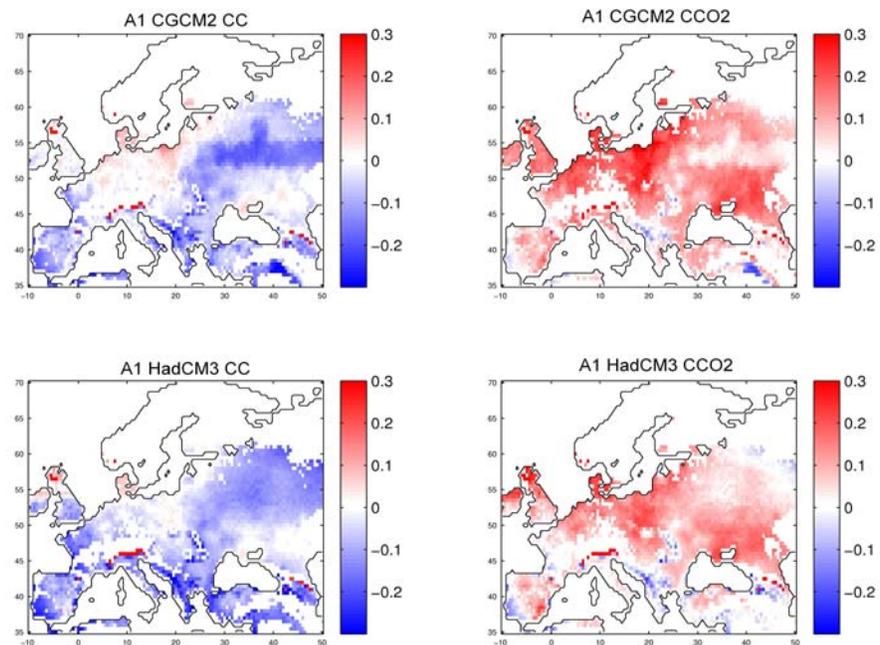
B

Figure 2-11 Change in grain biomass [kgC/m2] at the date of maturity. The change corresponds to the absolute difference between the last (2100) and the fist (1901) year of simulation. A, maize, large areas are zero because maize does not reach maturity at the first year. B, wheat, relative to the A1 scenarios runs only.

2.4   Discussion

Our model simulations with LPJ-C show that climate change will impact crop productivity of maize and wheat in different ways. Maize yield will only slightly decrease due to the impact of temperature on respiration, but when temperature reaches very high values, a non-linear response is expected. In this case, the maize grain production tends to collapse as a result of both respiration increase and shortening of the growing season. Wheat yield will also suffer from the negative impact of a shorter growing season, but the CO_2 fertilization effect will compensate this effect and lead to a net improvement of production efficiency.

The geographic distribution of both phenology and potential yield will be affected as well. Faster growth, driven by increased temperature, will force plants to produce less biomass and affect the harvest index. The eastern central European region will be affected by a relatively low increase in wheat yield, while maize will have a clear improvement. By contrast, both crops will experience a decrease in productivity in southern Europe. Therefore, maize could become more valuable in some central and northern regions, while southern Europe will suffer of a lack of productivity. These conclusions are comparable to those reached by Olsen and Bindi (2002) and the IPCC predictions (IPCC 2001c). In those studies, northern European regions are expected to have some positive effects through the introduction of new crop varieties and the CO_2 fertilization effect, but in southern Europe the disadvantages might be predominant. New policies have to be found to adapt the cropping system to the new climate regimes. In this sense, we agree that new crop distribution patterns will have to be expected as the result of climate change, and new adaptation strategies will have to be applied to maintain high yields especially in the more vulnerable regions such as the Mediterranean area. In this work, we give for the first time a geographical and quantitative description of the potential impacts of climate change using a Dynamic Global Vegetation Model. The approaches used in previous works (Olsen and Bindi 2001, Tubiello and Ewert 2002, Wolf *et al.* 2003, Fuhrer 2003, Van Ittersum *et al.* 2003) were typically based on information obtained from crop growth model simulations at a number of sites and extrapolated to larger regions. The modelling approach developed in the present study

provides the potential to simulate both natural vegetation and crop production on large regions using a single integrated approach. Furthermore, such an integrated model enables to estimate the ecosystem-scale carbon budget including soil organic pools.

LPJ-C simulates only potential production and crops are free to grow on the whole crop mask. In the real world, crop allocation is driven by economic values and land suitability. To help choose crop types and area distributions according to their economic profitability, a land use model should be integrated in the LPJ-C scheme. Water stress would have to be taken into account in the simulation of the production processes. Additionally, no extreme events are simulated in the current study, while they are considered to have a high-impacts potential in the European agro-ecosystem. The variety of crops through Europe is quite large, and wheat cultivars in particular differ in plant structure, development and physiological requirements. In this work, we selected only one general representation of a single wheat and maize cultivar through an optimization procedure. In this context, there is also some room for optimization improvement using more experimental data coming also from CO_2 enriched experiments; additionally, more then one single cultivar for each crop could be included in the input parameterisation set. This aspect is still in debate within the biosphere modelling community. For each crop cultivar a parameterisation set has to be used as model input, so that the amount of information to be provided increases quickly depending on the crops and their cultivars. An important advantage of DGVM is the limited amount of input parameters to be provided; therefore, if a larger number of crop cultivars should be included, the simplicity in input parameters should be also preserved. As a preliminary modelling framework, we decided to include only one single general parameterisation per crop, but a more detailed regional agronomic study should be reserved for future works.

Furthermore, agricultural systems are under continuous technological and genetic improvement, and such improvements could be taken into account when assessing the future evolution of the agro-environments. However, we assume that the change in cultivars and all the adaptation strategies will be applied to maintain the productivity as near as possible to the potential level.

The potential production, therefore, can be assumed to be close to the optimal production resulting from the constant adaptation and improvement.

In conclusion, this model framework can be considered as a baseline on which one can build a grid-based modular system to assess in an integrated way the potential impacts of the changing climate on agricultural production in Europe. Our study demonstrates clearly that European agriculture is likely to undergo major changes as a result of climate change through the 21st century. The results of our spatially distributed simulations generally support the conclusions of earlier point wise studies of climate change effects on agro-ecosystems in Europe.

2.5   Conclusions

Climate and atmospheric change over the coming century will have direct impacts on cropping systems in Europe. Improved productivity in the central and northern regions could lead to an enhanced food production. Our study shows that potential crop productivity in southern Europe is likely to decrease. According to the IPCC, the Mediterranean region will be affected by more intense droughts in the future, and this would exacerbate the negative impact of climate change on crop productivity in this region. In order to mitigate the impacts, new agro-ecological strategies have to be implemented by policy makers. This model represents a valid tool to simulate crop productions and natural vegetation within a single model framework, and after some further development, could be used as a tool to support agro-environmental policies needed to plan adaptation and mitigation to climate change.

2.6 References

Abrol Y.P., Ingram K.T. (1996) Effects of higher day and night temperatures on growth and yields of some crop plants. In: Global Climate Change and Agricultural Production (eds. Bazzaz F and Sombroek WG), FAO, Rome Italy and John Wiley & Sons, Chichester, England, 123-140.

Bachelet D., Neilson R.P., Hickler T., Drapek R.J., Lenihan J.M., Sykes M.T., Smith B., Sitch S., Thonicke K. (2003). Simulating past and future dynamics of natural ecosystems in the United States, Global Biogeochem. Cycles, 17, 1045, doi:10.1029/2001GB001508.

Bender J., Hertstein U., Black C.R. (1999). Growth and yield responses of spring wheat to increasing carbon dioxide, ozone and physiological stresses: a statistical analysis of 'ESPACE-wheat' results. European Journal of Agronomy, 10, 185–195.

Beniston M., Tol R.S.J. (1998). Expected Climate Change Impacts in Europe. Energy & Environment, 9, 365-381.

Boons-Prins E. R., de Koning G. H. J., van Diepen C. A., and Penning de Vries F. W. T (1993). Crop-specific parameters for yield forecasting across the European Communtiy. Wageningen, The Netherlands. Simulation Reports CABO-TT.

Boogard H.L., van Diepen C.A., Roetter R.P., Cabrera J.M.C.A., van Laar H.H. (1998). User's guide for the WOFOST 7.1 crop growth model and WOFOST Control Center 1.5, Technical Document 52, Wageningen Agricultural University, Wageningen, The Netherlands.

Boote K.J., Pickering N.B., Allen L.H. (1997). Plant modelling: advantages and gaps in our capability to predict future crop growth and yield in response to global climate change. In: Advances in carbon dioxide research (eds. Allen Jr. L.H., Kirkham M.B., Olszyk D.M., Whitman C.E.). ASA Special Publication 61, Madison, WI, 179-228.

Cavero J., Farre I., Debaeke P., Faci J.M. (2000). Simulation of maize yield under water stress within the EPICphase and CROPWAT models. Agronomy Journal, 92, 679-690.

Ceotto E. (1999) Exploring cropping systems of the low Po Valley using the systems approach. MSc Thesis, Wageningen Agricultural University, Wageningen, The Netherlands.

Collatz J.G., Ball J.T., Grivet C., Berry J.A. (1991). Physiological and environmental regulation of stomatal conductance, photosynthesis and transpiration: a model that includes a laminar boundary layer. Agricultural and Forest Meteorology, 54, 107-136.

Collatz J.G., Ribas-Carbo M., Berry J.A. (1992). Coupled photosynthesis-stomatal conductance models for leaves of C4 plants. Australian Journal of Plant Physiology, 19, 519-538.

Cramer W., Bondeau A., Woodward F.I., Prentice I.C., Betts R.A., Bronvik V., Cox P.M., Fisher V., Foley J.A., Friend A.D., Kucharik C., Lomas M.R., Ramankutty N., Sitch S., Smith B., White A., Young-Molling C. (2001). Global response of terrestrial ecosystem structure and function to CO2 and climate change: results from six dynamic global vegetation models. Global Change Biology, 7, 357-373.

Dal Monte G., Cali A., Buttarazzi M. (2002). Censimento e database di dati agrofenologici. Acts of National Meeting ``Fenologia per l'agricoltura'', Rome, 5-6 december 2002.

De Koning G.H.J., Van Diepen C.A. (1992). Crop production potential of rural areas within the European communities. IV. Potential, water-limited and actual crop production. Working document W68, Netherlands Scientific Council for Government Policy, The Hague, The Netherlands.

Dewar R.C. (1996). The correlation between plant growth and intercepted radiation: an interpretation in terms of optimal nitrogen content. Annuals of Botany, 78, 125-136.

Donner S.D., Kucharik C.J., Foley J.A. (2004). Impact of changing land use practices on nitrate export by the Mississippi River. Global Biogechemical Cycles, 17, 1085-2004.

El Maayar M., Ramankutty N., Kucharik C. J. (2005). Modelling global and regional net primary production under elevated atmospheric CO2: on a potential source of uncertainty. In press: Earth Interactions.

Etheridge D.M., Steele L.P., Langenfelds R.L., Francey R.J., Barnola J.M., Morgan V.I. (1996). Natural and anthropogenic changes in atmospheric CO2 over the last 1000 yearsfrom air in Antartic ice and firn. Journal Geophysical Research, 101, 4115-4128.

Farquhar G.D., Von Caemmerer S., Berry J.A. (1980). A biochemical model of photosynthetic CO_2 assimilation in leaves of C3 species. Planta, 149, 78-90.

Farquhar G.D. and Von Caemmerer S. (1982). Modelling of photosynthetic response to environmental conditions. In: Physiological Plant Ecology II: Water Relations and Carbon Assimilation (eds. Nobel PS, Osmond CB, Ziegler H), Springer, Berlin.

Fuhrer J. (2003). Agroecosystem responses to combinations of elevated CO_2, ozone, and global climate change. Agriculture Ecosystems and Environment, 97, 1-20.

Goudriaan J. and van Laar H.H. (1994). Modelling Potential Crop Grwoth Processes, Current Issue in Production Ecology, Kluwer Academic Pub, Dordrecht, The Netherlands.

Heemst van H. (1988). Plant data values required for simple and universal simulation models: review and bibliography. Simulation reports CABO-TT, Wageningen.

Haxeltine A., Prentice I.C. (1996a) BIOME3: an equilibrium biosphere model based on ecophysiological constraints, resources availability and competition among plant functional types. Global Biogeochemical Cycles, 10, 693-709.

Haxeltine A., Prentice I.C. (1996b) A general model for the light-use efficiency of primary production, Functional Ecology, 10, 51-561.

Hickler T., Prentice I.C., Smith B., Sykes M.T. (2003). Simulating the effects of elevated CO_2 on productivity at the Duke Forest FACE experiment: a test of the dynamic global vegetation model LPJ. EGS - AGU - EUG Joint Assembly, Abstracts from the meeting held in Nice, France, 6 - 11 April 2003, abstract #9347.

Houghton R.A., Hackler J.L., Lawrence K.T. (1999) The US carbon budget: contributions from the land use change, Science, 285, 574-578.

IPCC (2001a) Climate Change 2001: Working Group I: The Scientific Basis. Contribution of the Working Group I to the Third Assessment Report of the Intergovernmental Panel on Climate Change (eds. Houghton JT et al.), Cambridge University Press, Cambridge, UK and New York, USA.

IPCC (2001b) Special Report on Emissions Scenarios (eds. Nakicenovic N and Swart R), Cambridge University Press, Cambridge, UK and New York, USA.

IPCC (2001c) Climate Change 2001: Working Group II: Impacts, Adaptation, and Vulnerability. Contribution of the Working Group II to the Third Assessment Report of the Intergovernmental Panel on Climate Change (eds. McCarthy JJ et al), Cambridge University Press, Cambridge, UK and New York, USA.

Keeling C.D, Whorf T.P., Wahlen M., Vanderplicht J. (1995). Interannual extremes in the rate of rise of atmospheric CO_2 measurements, Nature, 375, 666-670.

Kimball B., Kobayashi K., Bindi M. (2002). Responses of agricultural crops to free-air CO_2 enrichment. Advances in Agronomy, 77, 293-368.

Kucharik C.J., Brye K.R. (2003). Integrated Biosphere Simulator (IBIS) yield and nitrate loss predictions for Wisconsin maize receiving Varied Amounts of nitrogen fertilizer. Journal Environmental Quality, 32, 247-268.

Kucharik C.J., Foley J.A., Delire C., Fisher V.A., Coe M.T., Lenters J.D., Young-Molling C., Ramankutty N., Gower S.T. (2000). Testing the performance of a Dynamic Global Ecosystem Model: water balance, carbon balance, and vegetation structure. Global Biogeochemical Cycles, 14, 795-825.

Kucharik C. J., (2003). Evaluation of a process-based agro-ecosystem model (Agro-IBIS) across the U.S. cornbelt: Simulations of the inter-annual variability in maize yield. Earth Interactions, 7, 14, 1–33.

Lagarias J.C., Reeds J.A., Wright M.H., Wright P.E. (1998). Convergence Properties of the Nelder-Mead Simplex Method in Low Dimensions. SIAM Journal of Optimization, 9, pp112-147.

Leff B., Ramankutty N., Foley J.A. (2004). Geographic distribution of major crops across the world. Global Biogeochemical Cycles, 18, 10, DOI:10.1029/2003GB002108.

Lloyd J., Taylor J.A. (1994). On temperature dependence of soil respiration. Functional Ecology, 8, 315-323.

Marletto V., Zinoni F., Criscuolo L., Fontana G., Marchesi S., Morgillo A., van Soetendael M.R.M., Ceotto E., Andersen U. (2005) Evaluation of downscaled DEMETER multi-model ensemble seasonal hindcasts in northern Italy by means of a model of wheat growth and soil water balance. Tellus A, 57, 488-497.

McGuire A. D., Stich S., Clein J.S., Dargaville R., Esser G., Foley J., Heimann M., Joos M., Kaplan J., Kicklighter D.W., Meier R.A., Melillo J. M., Moore III B., Prentice I.C., Ramankutty N., Reichenau T., Tian H., Williams L.J., Wittenberg U. (2001). Carbon balance of the terrestrial biossphere in the tweniteh century: analyses of CO2, climate and land use effects with four processes-based ecosystem models. Global Biogeochemical Cycles, 15, 183-206.

Mitchel T. D., Carter T. R., Jones P. D., Hulme M., New M. (2004). A comprehensive set of high-resolution grids of monthly climate for Europe and the globe: The observed record (1901-2000) and 16 scenarios (2001-2100). Technical report, no. 5. Norwich, UK, Tyndall Centre for Climate Change Research, University of East Anglia.

Olesen J., Bindi M. (2002). Consequences of climate change for European agricultutral productivity, land use and policy. European journal of Agronomy, 16, 239-262.

Ramankutty N. and Foley J.A. (1998). Characterizing patterns of global land use: an analysis of global croplands data. Global Biogeochemical Cycles, 12, pp. 667-685.

Roetter R. (1993). Simulation of the biophysical limitations to maize production under rainfed conditions in Kenya. Evaluation and application of the model WOFOST. Materiel zur Ost Afrika-Forschung, Heft 12, 261 pp +Hannex.

Schlesinger M.E., Malyshev S. (2001) Changes in near-surfaces temperature and sea-level for the Post-SRES CO2-stabilization scenarios. Integrated Assessment, 2, 95-110.

Singaas E.L., Donald R.O., DeLucia E.H. (2001) Variation in measured values of photosynthetic quantum yield in ecophysiological studies, Oecologia, 128, 15-23.

Sitch S., Smith B., Prentice I., Arneth A., Bondeau A., Cramer W., Kaplan J., Levis S., Lucht W., Sykes M., Thonicke K., Venevsky S. (2003). Evaluation of ecosystem dynamics, plant geography and terrestrial carbon cycling in the LPJ dynamic global vegetation model. Global Change Biology, 9, 161-185.

Sitch S. (2000). The role of vegetation dynamics in the control of atmospheric CO2 content. PhD Thesis, Lund University, Sweden.

Smith B., Prentice I.C., Sykes M. (2001). Representation of vegetation dynamics in modelling of terrestrial ecosystems: comparing two contrasting approaches within European climate space. Global Ecology and Biogeography, 10, 621-637.

Sombroek W.G., Gommes R. (1996). The climate change - Agriculture conundrum. In: Global Climate Change and Agricultural Production (eds. Bazzaz F and Sombroek WG), FAO, Rome Italy and John Wiley & Sons, Chichester, England, 1-14.

Supit I., Hoojer A.A., van Diepen C.A. (1994). System Description of the WOFOST 6.0 Crop Simulation Model Implemeted in CGMS, JRC European Commission, 148 pp.

Tubiello F.N., Rosenzweig C., Kimball B.A., Pinter P. Jr., Wall G.W., Hunsaker D.J., Lamorte R.L., Garcia R.L. (1999). Testing CERES-Wheat with FACE data: CO2 and water interactions. Agrononomy Journal, 91, 1856–1865.

Tubiello F.N., Ewert F. (2002) Simulating the effect of elevated CO2 on crops: approaches and applications for climate change. European Journal Agronomy, 18, 57-74.

Van Diepen C.A., Rappoldt C., Wolf J., van Keulen H. (1988). Crop growth simulation model WOFOST documentation version 4.1. Center for World Food Studies, Wageningen, 299 pp.

Van Diepen C.A., Wolf J., Van Keulen H., Rappoldt C. (1989). WOFOST: a simulation model of crop production. Soil Use and Management, 5, 16-24.

Van de Gejin S., Goudriaan J. (1996). The effects of elevated CO2 and temperature change on transpiration and crop water use. In: Global Climate Change and Agricultural Production, (eds. Bazzaz F and

Sombroek WG), FAO, Rome Italy and John Wiley & Sons, Chichester, England, 101-122.

Van Ittersum M.K., Leffelaar P.A., van Keuelen H., Kropff M.J., Bastiaans L., Goudriaan J. (2003). On approaxches and applications of the Wageningen crop models. European Journal of Agronomy, 18, 201-234.

Van Keulen H., Penning de Vries F.W.T., Drees E.M. (1982). A summary model for crop growth. In: Simulation of Plant Growth and Crop Production (eds. Penning de Vries FWT, Van Laar HH), Simulation Monographs, Pudoc, Wageningen, The Netherlands, 87-98.

Van Keulen H., Wolf J. (1986) Modelling of agricultural production: weather soils and crops. Simulation Monographs, Pudoc, Wageningen, The Netherlands, 479 pp.

Van Laar H.H., Goudriaan J., Van Keulen H. (1997). SUCROS97: Simulation of crop growth for potential and water-limited production situations. Quantitative Approaches in Systems Analysis, No. 14, C.T. de Wit Graduate School for Production Ecology and Resource Conservation, Wageningen, The Netherlands, 52 +Appendices.

Wolf J., Bindraban P.S., Luijten J.C., Vleeshouwers L.M. (2003). Exploratory study on the land area required for global food supply and the potential global production of energy. Agricultural Systems , 76-3, 841-861.

Zinoni F., Marletto V., Fontana G., Criscuolo L., Morgillo A., Marchesi S., Ceotto E. (2004). Demeter seasonal hindcasts and potential wheat yield forecasting. In: Proc. VIII ESA Congress, 11-15/7/2004, Copenhagen, Denmark (eds. Jacobsen S.E., Jensen C.R., Porter J.), 2004, 353-354.

3 Irrigation demand and drought risk

3.1 Introduction

During the last 200 years, the atmospheric CO_2 concentration had an increase by about 37%, reaching its current level of nearly of 380 μmol mol^{-1} (Keeling and Whorf, 2000). Land use change and anthropogenic emissions from the burning of fossil fuels has led to a rapid increase of CO_2 concentration in the atmosphere. If no change to the current use of fossil fuels occurs within the next years, the predicted CO_2 concentration will almost double by the middle of the 21st century (Alcamo *et al.* 1997; IPCC 2001c). One of the main consequences is a warming of the surface temperature. Current predictions show an increase on average by 0.4-0.6 °C per decade within the next 100 years (IPCC, 2001a), with associated change in precipitation regimes (Giorgi *et al.* 1998). Precipitation variability has already shown differentiated patterns during the 20th century between the Northern and the Southern parts of the European continent. The precipitation anomalies referring to the 1951–1980 period indicate that, between 1981 and 1994, there has been an increase in the northern areas, while less precipitation occurred in the Mediterranean (Hurrell and van Loon, 1997). According to the Intergovernmental Panel on Climate Change (IPCC), the effect of the increased concentration of greenhouse gases will reinforce this trend during the current century and lead to an increase in the frequency of extreme events (IPCC, 2001c). In some Mediterranean areas the predicted precipitation reduction will reach 20%, with some higher percentage during the summer (Ragab and Proudhomme, 2002; Chartzoulakis and Psarras, 2005).

Many assessments have been carried out to study potential impacts of climate change on the agricultural system in Europe (Kenny *et al.*, 1993; Parry *et al.*, 1992; Harrison *et al.*, 1995; Chartzoulakis and Psarras, 2005), including potential productions (Wolf and van Diepen, 1995; Criscuolo *et al.*, 2005) with

adaptation strategies (Rosenzweig and Tubiello, 1997; Tubiello *et al.*, 2000; Olesen and Bindi, 2002). All those studies suggest that yields will generally increase in the north, but decrease in the Mediterranean area. This differentiated yield pattern is the result of the combined effects of the increasing temperature, the change in precipitation regimes and a CO_2 enriched atmosphere.

A warmer climate generally leads to a faster crop development, which leads to a shorter growing season and a shorter photosynthetic period. Hence, seasonal net primary productivity can decrease in a warming environment, so that the final yield decreases. A possible adaptation strategy is to use slow-growth cultivars, which stay longer in the field. On the other hand, longer periods in a warmer climate lead to longer evapotranspiration periods. The CO_2 fertilization effect might improve the water use efficiency (WUE), increasing again the productivity; however, more extended irrigation may be needed to satisfy the increased seasonal demand of the extended evapotranspiration. Tubiello *et al.* (2000) found that the increased evaporative demands due to climate change will require 60–90% more irrigation to maintain grain yields of maize and soybean at current levels in some area of the Italian peninsula.

Crops, however, are only one component of the ecosystem, where many other elements play key roles. Carbon and water cycling, fire events, runoff, water availability, land use and soil carbon storage are important aspects often neglected. Furthermore, none of the studies mentioned above were based on a dynamic process-based model applied on regular grid. A new generation of models is now available to perform general ecosystem service assessments of regional and global scales. Several Dynamic Global Vegetation Models (DGVMs) give an integrated representation of both natural vegetation and crops taking into account carbon and water within a single grid-based modelling framework (Kucharik and Brye 2003, Criscuolo *et al.* 2005).

In this paper, we perform an assessment of the crop water requirement for different climate change scenarios using a state-of-the-art DGVM, the Lund-Potsdam-Jena (LPJ) model. We analyze how much water supply will be required to maintain maize and wheat productivity at the potential level in

Europe. A complete assessment of the water requirement, water use efficiency and crop yield is performed using a combination of two General Circulation Models (GCMs) under two IPCC scenarios. Additionally, we analyze the change in frequency of extreme yield failures of wheat production in comparison with a reference period for the past century.

3.2   Methods

3.2.1   The model

The LPJ Dynamic Global Vegetation Model represents the large-scale and process-based dynamics of terrestrial ecosystem taking into account carbon and water cycling in vegetation and soil, structure and composition of vegetation, and fire disturbance. A comprehensive description of the model is given by Sitch *et al.* (2003). For the crop growth compartment, see Criscuolo *et al.* (2005). The vegetation of each grid cell is represented as a combination of Plant Functional Types (PFTs), differentiated by physiological, dynamical and structural attributes as well as bioclimatic constraints for survival. Vegetation structure and dynamics are explicitly included, and populations of PFTs compete for light and water. The soil is divided into two layers and contains three carbon pools with different carbon decomposition rates. Photosynthesis is based on a version of the Farquhar model (Farquhar and Von Caemmerer, 1980; Farquhar and Von Caemmerer, 1982) readapted for global modelling purposes (Collatz *et al.* 1991, 1992). Crop Functional Types (CFTs) are included as annual plants with separate carbon allocation schemes.

Two CFT parameterisations have been used, one for maize and the other for wheat. The parameter sets are based on an optimization procedure applied for Europe. Crop growth can be simulated under both potential and water-limited conditions. No competition for resources occurs between CFTs, no natural vegetation can grow where crops are allowed to develop.

3.2.2   The experiment

The gridded global crop map by Ramankutty and Foley (1998) was used to derive the crop mask on the European grid (Figure 3-1). This data set consists of a global map with a resolution of 0.5° x 0.5°, in which each grid point
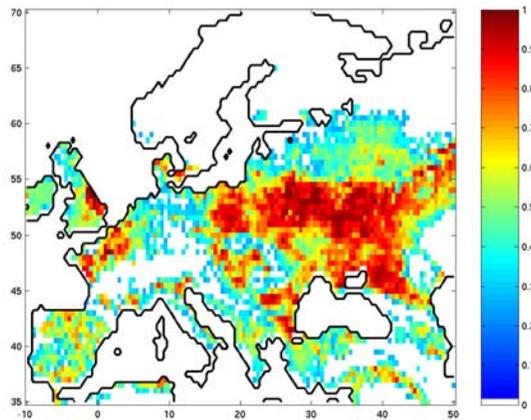
Figure 3-1 The crop mask derived from Ramankutty and Foley (1998).

represents the fractional area covered by crops for the year 1992. Indices vary from "other vegetation" (index zero) to "crops" (index one). Cells with an index from 0.15 to 1.0 (from class ``other vegetation and crop mosaic'' to ``crops'') have been selected for Europe and have been used to scale the production according to the grid area occupied by crops. Soil texture data were based on the FAO soil data set on a global 0.5° x 0.5° grid, as described by Sitch *et al.* (2003).

The model experiment consists of two sets of four simulations, each with two modes of the LPJ model combined with four GCM scenarios. In a "CO_2 changing" mode (COy), climate and atmospheric CO_2 concentration change according to the scenario. In a "CO_2 fixed" mode (COn), its concentration is fixed at the preindustrial level (280 ppmv). Such an experimental design allows analysing the CO_2 fertilization effect on the vegetation productivity separately from the climate change influence.

The simulation time covers the period 1901-2100: from 1901 to 2000 observed climate and CO_2 concentration (for COy) are used as model forcings, from 2001 to 2100 predicted climate scenarios are used together with the correspondent CO_2 concentration scenario (for COy).

Mean global CO_2 concentrations for the period 1901-1992 were taken from McGuire *et al.* (2001), derived from averaged observations of Mauna Loa stations and from South Pole ice cores (Keeling *et al.*, 1995; Etheridge *et al.*, 1996). For the remaining period 1993-2100, mean global CO_2 concentrations
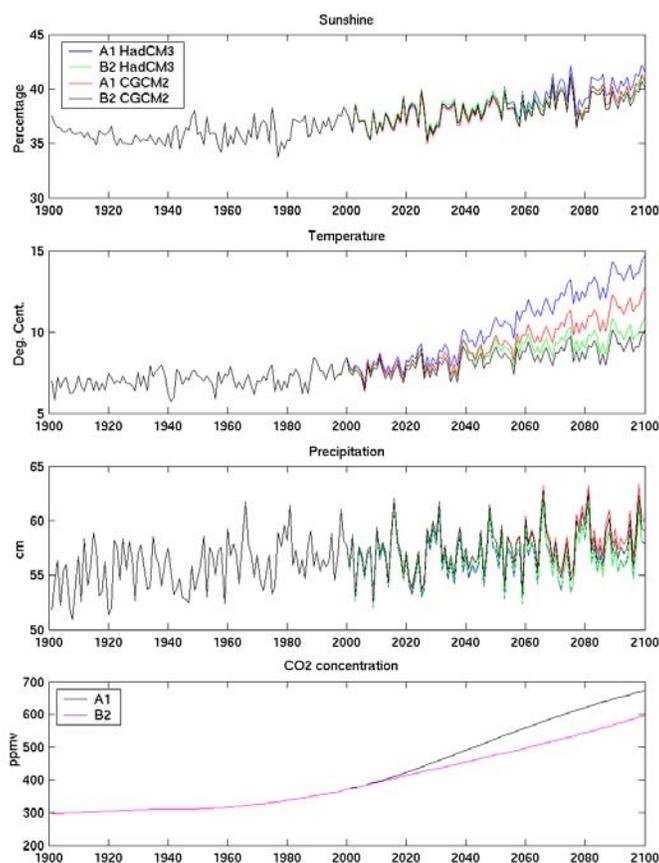
Figure 3-2 Annual means of climate variables and CO$_2$ over the study area (10.0°W - 50.0°E, 35.0°N - 70.0°N, land points only)

were derived from the integrated assessment of Schlesinger and Malyshev (2001).

Observed climate data for the 1901-2000 period were derived from the CRU TS 2.0 global climate data set (Mitchell *et al.*, 2004). This data set provides monthly fields of observed mean temperature, precipitation and cloud cover on a 0.5° x 0.5° global grid over land. Scenario climate data were derived from the TYN SC 2.0 data set (Mitchell *et al.*, 2004) for the period 2001-2100. This data set consists of monthly climate data for the period 2001-2100 simulated by General Circulation Models (GCMs), covering the global land surface on the same 0.5° x 0.5° grid as the CRU TS 2.0. This set includes 16 scenarios of projected future climate representing all combinations of four SRES emissions scenarios and four GCMs. The climate

variability is obtained superimposing the observed variability of the 20th century on the mean changes projected for the 21st century.

We selected the SRES-B2 and SRES-A1 scenarios from HadCM3 and CGCM2 GCMs outputs. A1 and B2 are the extremes of the SRES group. In A1, the emphasis is on global economic growth rather than environmental protection and sustainability; we consider the particular case of A1FI, the "Fuel Intensive" sub-scenario, in which the use of fossil fuels is maintained as highly as they are available. In B2, on the contrary, Europe searches local solution to better solve ecological and social problems within a less globalized world (IPCC 2001b). The choice of the HadCM3 and the CGCM2 was motivated by their behavior over Europe characteristic of two distinct groups of climate response in the IPCC analysis. In the IPCC simulations, CGCM2 shows a marked slowdown of the North Atlantic thermohaline circulation (IPCC 2001a), so that heat transport to the North Atlantic and Europe tends to decrease. CGCM2 thus shows a less steep temperature increase compared to HadCM3 (Figure 3-2). Furthermore, HadCM3 is currently considered one of the reference GCMs within the IPCC framework (IPCC 2001a).

Our analysis takes into account two representative periods, 1961-1990 marked as "observation period", and 2071-2100 as the "climate change state" of the simulations. This is also consistent with TYN SC 2.0, in which the first time interval is considered the reference period for the climatic conditions of the last century; the second is representative for the conditions at the end of the current century.

We consider the cumulative actual evapotranspiration of the growing season as the water requirement (WR) and the water use efficiency (WUE) as the ratio between the WR and the final carbon biomass.

3.2.3 Analysis of water requirement

The LPJ model can simulate both potential and water-limited crop production; for a description of the crop scheme, see Criscuolo *et al.* (2005). We use this feature to calculate how much water is required to increase production from water-limited to potential over the whole simulation grid. For potential, we assume no limitation to the water supply, i.e. demand is fully satisfied. The water-limited simulation is the current baseline; all the grid cells
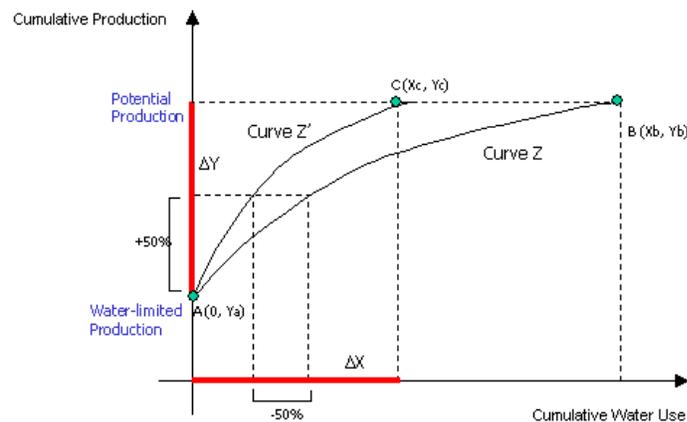
Figure 3-3 Cumulative yield increase as a function of the cumulative water use. This figure is only for illustrative purposes (see text).

are analysed in a hierarchical order, from the highest to the lowest WUE. The unlimited water supply is allocated following the hierarchy to switch the yield of the grid cell to potential. The procedure iterates until all the cells have been evaluated and converted to potential. The cumulative sum of grain carbon biomass always increases as the correspondent amount of water is allocated to the grid. The expected curve is steeper at the beginning, becoming increasingly flatter towards the end.

Figure 3-3 shows a general example of the expected relationship between the cumulative water use and the cumulative yield. The two curves in the Figure represent a hypothetical water requirement analysis referring to cases Z and Z'. The first point of the curve Z (point A, in Figure 3-3) corresponds to the water-limited cumulative yield (Ya) when no additional water is given. Last point (point B, in Figure 3-3) defines a complete shift to potential production: the X component (Xb) represents the amount of water to be added to the grid, the Y component (Yb) is the correspondent cumulative potential yield. In the experiment Z' the water-limited baseline is the same of Z (point A, in Figure 3-3). The curve Z' reaches the same potential yield as for Z (point C, in Figure 3-3), but less water is allocated (Xc). This graphical way of describing the relationships gives a conceptual picture of a hypothetical farmer's options. For example, if the farmer would increase the water-limited productions (Ya) by 50%, and the production conditions lead either to the Z' and Z cases, our

analysis shows that 50% less water has to be used in the Z' case compared to Z.

Table 3-1 Observed records of water allocated to the agriculture sector in the EU and simulated potential irrigation demand. The m*ean water allocation* (Lallana, 2003) is calculated as the ratio between the total water abtraction and the total irrigated land, relative to the 4 selected European regions. The *regional potential irrigation demand* (see text) is shown for COn and COy; with observed as fraction of potential we describe the ratio of *regional potential irrigation demand* and *mean water allocation* in percentage. Also the related standard deviations are given.

	Observation			
	Mean water allocation (m3/ha/year)			
	WSEur	**WCNEur**	**ExtSEur**	**ExtNEur**
1993	6819	1763	4440	1250
1994	7010	1787	5810	1024
1995	7349	1767	5789	827
1996	7357	1655	6267	859
1997	7199	1542	6453	478
1998	7500	1770	6560	579
1999	7424	2123	6576	488
St Dev.	244.58	177.97	756.46	290.18

	COn							
	Potential irrigation demand (m3/ha/year)				**Observed as fraction of potential [%]**			
	WSEur	**WCNEur**	**ExtSEur**	**ExtNEur**	**WSEur**	**WCNEur**	**ExtSEur**	**ExtNEur**
1993	534	164	1142	441	7.83	9.30	25.72	35.28
1994	657	436	1268	1049	9.37	24.40	21.82	102.47
1995	789	404	1017	680	10.74	22.86	17.57	82.21
1996	842	285	1387	547	11.45	17.22	22.13	63.66
1997	457	105	1214	376	6.35	6.81	18.81	78.67
1998	566	92	874	222	7.55	5.20	13.32	38.35
1999	606	194	981	900	8.16	9.14	14.92	184.35
St Dev.	138.16	138.66	179.21	294.14	56.49	77.91	23.69	101.37

	COy							
	Potential irrigation demand (m3/ha/year)				**Observed as fraction of potential [%]**			
	WSEur	**WCNEur**	**ExtSEur**	**ExtNEur**	**WSEur**	**WCNEur**	**ExtSEur**	**ExtNEur**
1993	523	141	1135	374	7.67	8.00	25.56	29.92
1994	651	418	1260	1031	9.29	23.40	21.69	100.71
1995	782	380	1011	662	10.64	21.50	17.46	80.04
1996	827	253	1382	543	11.24	15.28	22.05	63.19
1997	441	93	1205	357	6.13	6.03	18.67	74.69
1998	556	83	871	214	7.41	4.69	13.28	36.97
1999	595	179	977	881	8.01	8.43	14.86	180.46
St Dev.	139.07	134.60	177.96	296.71	56.86	75.63	23.53	102.25

West South (WSEur): France, Greece, Italy, Portugal, Spain
West Centr North (WCNEur): Austria, Belgium, Denmark, Germany, Netherlands, Norway, United Kingdom, Finland, Sweden
Extended South (ExtSEur): Turkey, Cyprus
Extended North (ExtNEur): Bulgaria, Czech Rep, Estonia, Hungary, Latvia, Lithuania, Romania, Slovak Rep., Slovenia

We consider the difference of the water requirement between potential and water-limited simulations as the "potential irrigation demand". In this way the term "irrigation" assumes the meaning of water to be allocated per unit of surface to improve the basic water-limited productivity up to the potential, with no constraints to the water supply. We compare the simulated irrigation against a set of irrigation records of the European Environment Agency (Lallana, 2003). This study combines Eurostat, FAO and national information of water resources allocated to irrigation in the EU agricultural sector during 1993-1999. The mean water allocation data are calculated as the ratio between total water withdrawal and the total irrigated land surface, aggregated on four regions in which Europe is divided. In order to compare the results, we also grouped the simulation data into four regions (See Table 3-1 for details of the regions). For each region, we consider simulated total water withdrawal as the sum over all the cells of the potential irrigation demand times the surface occupied by the crop. The irrigated land surface corresponds to the sum of the cell surface occupied by the crop. Since the crop mask is constant in time, the irrigated surface is constant as well. We define, therefore, the regional potential irrigation demand (RPID) for each year as:

$$RPID = \frac{\sum_{n=1,N} PID_n * S_n}{\sum_{n=1,N} S_n}$$

$$PID = WR_{pot} - WR_{wl}$$

$$S = A * c$$

Where, N is the number of grid cells of the region, PID is the potential irrigation demand, WR_{pot} and WR_{wl} are the water requirements, calculated as actual evapotranspiration under potential and water-limited conditions, S is the surface occupied by the crop, A the total surface of the grid cell and c the coefficient of the correspondent cell of the crop mask.

3.2.4 Extreme loss frequency analysis

We define an extreme loss event when the grain yield is below a specific threshold derived from the variability of the annual yield during 1961-1990. We set this threshold at each grid cell as the average of the third and the fourth

lowest annual yield simulated during the period 1961–1990. The frequency of extreme loss events is the number of years in which an extreme loss event occurs divided by the number of years considered. Consequently, the frequency for 1961-1990 is 1/10 for each grid point, or conversely, we arbitrarily define a threshold that corresponds to an extreme event occurring every 10 years within the reference period. The assumption is that a farmer, or a regional planner, will base his projections on the passed risk. Next, we calculate the frequency of extreme loss again for each grid cell for the climate change period (2071-2100), maintaining the same thresholds. The change in frequency, then, gives an indication of the change in risk of crop failure in the absence of adaptation. Note that the climate forcings of the scenarios do not differ in the interannual variability (Figure 3-2), but in their long-term means, so that changes in risk are exclusively created by changes in the mean towards or away from the threshold.

As we illustrate further, maize does not always reach maturity in water-limited simulations, so we exclude it from our frequency analysis. We also exclude wheat simulations with constant CO_2 from this analysis (COn simulations).
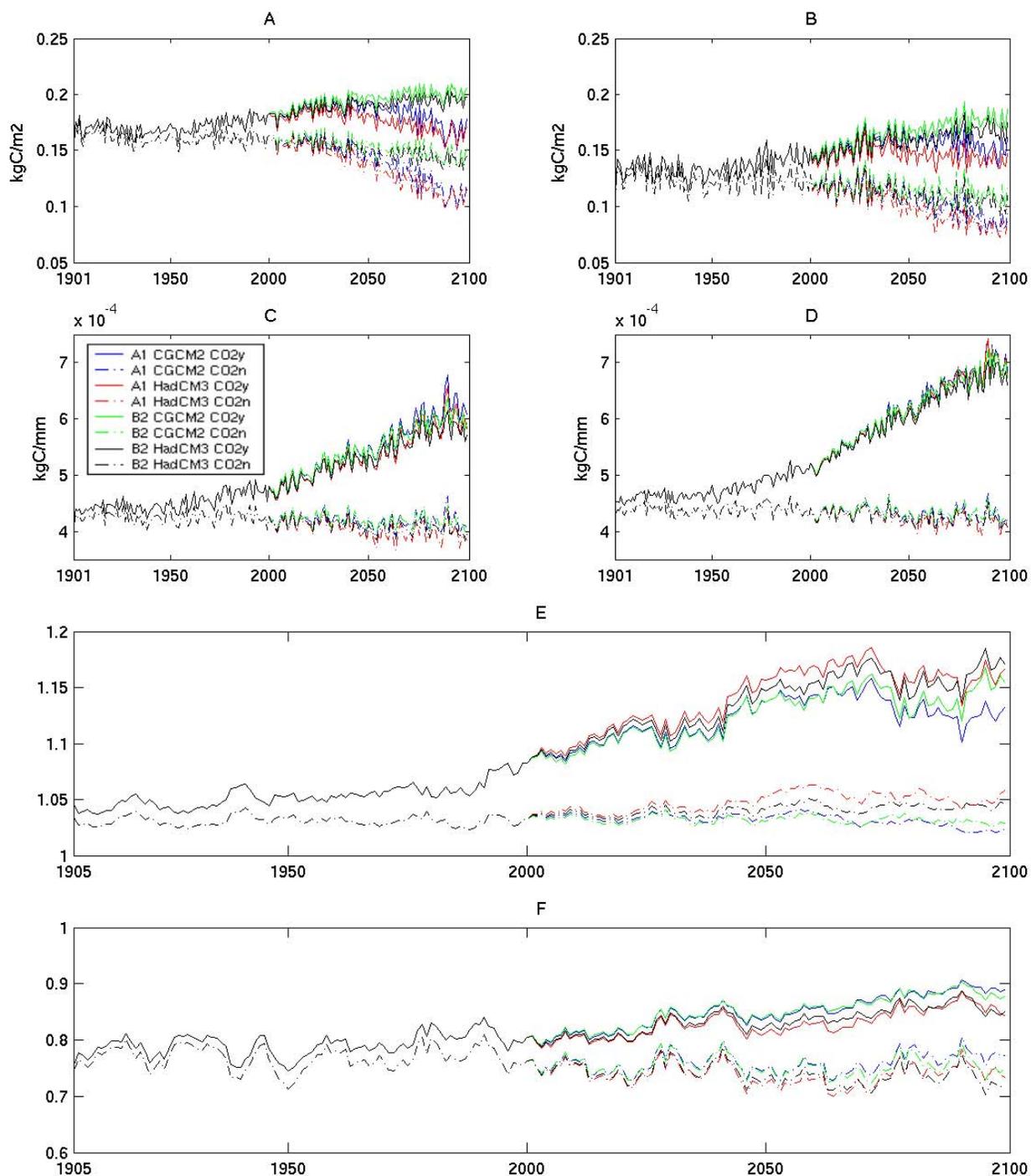
Figure 3-4 Annual average of total carbon biomass and WUE of wheat over the study area. The averages are calculated over the entire European grid. In A, carbon biomass of potential production and in B of water-limited; in C, WUE of potential production, in D of water-limited. In E, the ratio between water-limited and potential conditions WUE (5-years-running mean); in F, same as in E, but for total carbon biomass.

3.3 Results

3.3.1 Wheat

The simulated annual carbon biomass gain is highly scenario dependent. In Figure 3-4-A, the potential production shows four groups of mean carbon biomass curves, B2 and A1 runs are grouped in two sets of two lines, each for COn and COy. The B2 groups increase under the fertilization effect and tend slightly to decrease without; the A1 group initially increase in COy, but decreases after 2030, while COn decreases immediately after 2000. The higher scenario temperatures force the growth to be faster, so that the growing season becomes shorter and the consequent Net Primary Productivity (NPP) decreases (see Criscuolo *et al.*, 2005). The enriched CO_2 atmosphere counterbalances this effect up to a certain temperature threshold. The temperature forcing of A1 overcomes this level; consequently the shortening effect prevails against the fertilization. The four groups are less evident in the water-limited case (Figure 3-4-B), while the gap between COn and COy is more pronounced. The water stress, hence, tends to reduce the differences between scenarios, but to enlarge the difference between non-fertilizing and fertilizing atmosphere. The WUE is higher in water limited than in potential production conditions (Figure 3-4-C, D). The plant responds to water deficit reducing the water conductance with the stomata partial closure, which tends to increase the WUE (Jones, 1983). Therefore, giving the plant the same CO_2 concentration but different water stress (COn cases), the WUE tends to be larger in the more water-limiting environment, within certain stress level. When the CO_2 concentration is increased in a water-limiting environment, the WUE is even more improved by the fertilizing effect (COy cases). The ratio between WUE in water-limited and potential production conditions is mostly around 1.03 in COn (Figure 3-4-E, shaded lines), but increases to mean of around 1.12 in COy (Figure 3-4-E, solid lines). WUE is, therefore, always larger in water-limited conditions and even larger when CO_2 fertilization effect is active. The ratio between the water limited and the potential carbon biomass varies between 0.7-0.8 in COn (Figure 3-4-F, shaded lines). By comparison, this ratio increases to 0.85-0.9 in the CO_2 fertilized runs (Figure 3-4-F, solid lines), showing again that the differences
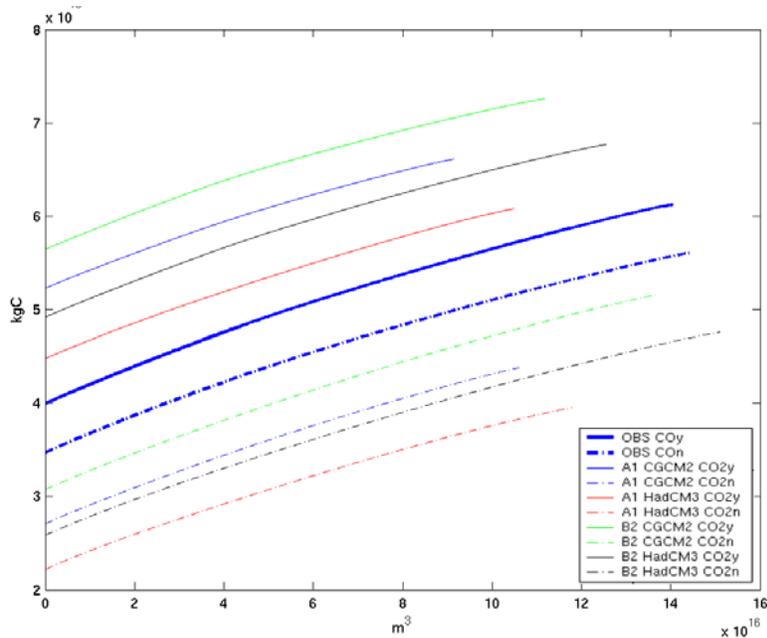
Figure 3-5 The wheat yield increment as a function of the water used, assuming water is allocated gradually from the highest WUE grid cell to the lowest; OBS represents the 1961-2000 period, the others the 2071-2100, the yield is scaled by the crop fraction and the area of the grid cell. Three groups of lines are visible, four COy curves referring to 2071-2100 at the top, two curves for 1961-2000 in the middle, and four COn again for 2071-2100 at the bottom.

between water-limited and potential production are decreased through the CO_2 fertilization effect. In the case with constant CO_2 (Figure 3-4-F, shaded lines), however, we see a slight decrease, which shows that the climate becomes more adverse to non-irrigated agriculture. This effect is overcompensated by the effect of CO_2 fertilization, if the fertilization is indeed as strong as it is simulated by LPJ.

Europe-wide totals of wheat yield as a function of total water use are shown in Figure 3-5 for both 1961-1990 (OBS, bold lines) and 2071-2100 (thin lines). For the non-fertilized runs (dashed lines), the curve using the observed climate of 1961-1990 (OBS COn), reaches approximately $5.7*10^{10}$ kgC at the final point, i.e. the point of potential production where all grid cells are fully irrigated. The simulation with CO_2 fertilization, which uses current CO_2 levels instead of pre-industrial ones, achieves a markedly higher potential yield above $6*10^{10}$ kgC (60 mill. tons of carbon). The diagram also shows that the potential yield without the extra effect of CO_2 fertilization since the pre-industrial requires a total of $14*10^{16}$ m^3 of water for irrigation, while the same amount can by produced with only $9*10^{16}$m^3 with CO_2 fertilization switched on (OBS, COy). In other words, 35% of water is saved due to the additional CO_2

fertilization from anthropogenic emissions during the observation period. For 2071-2100, not surprisingly, the effect is much stronger. For example, fertilization improves potential grain yield of B2 CGCM2 (green lines) by 44% compared to COn, saving additionally 20% of water; this proportion is almost the same for all the scenarios. Furthermore, there are large differences in the potential yield and water requirement between the scenarios. A1 CGCM2 COn reaches around $4*10^{10}$ kgC as potential production with the use of $10.2*10^{16}$ m^3, while B2 CGCM2 COn reaches the same level with about $7.2*10^{16}$ m^3, i.e. there is 33% water saved relatively to A1. Applying the same analysis to A1 HadCM3 COn and B2 HadCM3 COn, we find a slightly smaller difference, about 28%. In this case we can conclude that the mean "scenario effect" is around 30% of water saved when switching from A1 to B2 with constant CO_2 and at constant levels of grain production.

For simulations where the increased CO_2 level is factored into the production, i.e. those assuming full CO_2 fertilization, we compare scenario simulations (COy) with the simulation using observed climate (OBS COy). We find that the combined effect of increasing CO_2 and climate change from today to what is projected for the end of the century leads to between 25 and 80% of water saved assuming constant grain production at the potential level of reference observed climate. If we compare the potential productions, we find a slight decrease (A1 HadCM1) and an approximately 18% increase (B2 CGCM2), but in all cases a reduction in water consumption. The "best" scenario in absolute terms of impacts on water use is B2 CGCM2 COy. The combination of lowest temperature increase and relatively high precipitation leads to the best ratio between yield and water used. The water amount required to reach the potential production level of the observation period is the smallest for this scenario: to reach $6*10^{13}$ kgC, $2.2*10^{16}$ m^3 of water have to be used in B2 CGCM2 COy (80% less, relatively to OBS), while $5.0*10^{16}$ m^3 in A1 CGCM2 COy (64% less), $6.6*10^{16}$ m^3 in B2 HadCM3 COy (52% less), and $10.0*10^{16}$ m^3 A1 HadCM3 COy (28% less). Finally, the fully water-limited production with no irrigation water always increases with CO_2 fertilization, but always decreases without.

The mean observed water allocation, the regional potential irrigation demand and the observed as fraction of potential is shown in Table 3-1 (see

above and in Table capture for definitions). Appreciable differences are evident through regions and time rather than between constant and changing CO_2 simulations. As expected, the southern regions (ExtSEur and WSEur, see Table 3-1 for details) show much higher values for both the observed water allocation and the regional potential water demand. The eastern regions (ExtNEur and ExtSEur) show a high observed fraction of potential, reaching more 100% in northeastern Europe (ExtNEur). The ratio of standard deviation of the time series (last line of observed as fraction of potential) is also around 100% for this region. Consequently, not only the regional potential irrigation demand is close to the mean observed water allocation, but also its interannual variability is well reproduced, at least for the given time interval. The other two regions, WSEur and WCNEur, have much lower fraction; the standard deviation fraction is close to 100%, indicating that the interannual variability is well reproduced also in these cases. During 1993-1999, the difference of CO_2 concentration in COy and COn is between 59.5 ppmv (1993) and 73.4 ppmv (1999). This difference is reflected in the slightly lower fraction of potential of COy simulations. Since the fertilization effect decreases the water requirement, the regional potential irrigation demand for COy is smaller; therefore, the fraction of the observed mean water allocation is smaller for COy than COn.

In addition to that, agricultural production of Eastern Europe is based mainly on wheat and the calculated regional potential irrigation demand refers in this work only to wheat. This explains why the European region best simulated in terms of interannual variability and absolute values is ExtNEur. In Western Europe (WSEur and WCNEur), on the other hand, a large part of irrigation is dedicated to high valuable crops as tobacco, fruits, and olives, which are often much more water demanding than wheat (IEEP, 2000). Hence, our study represents only a part of the irrigation water use in the in Western Europe, so that our estimation is lower than the observed. To have a detailed analysis of the irrigation demands of wheat, crop specific irrigation data are needed; on the other hand, they are generally rare and usually not continuous in time (IEEP, 2000). This is a current limit in many irrigation studies on large-scale level, especially in spatial explicit DGVM frameworks as the LPJ.

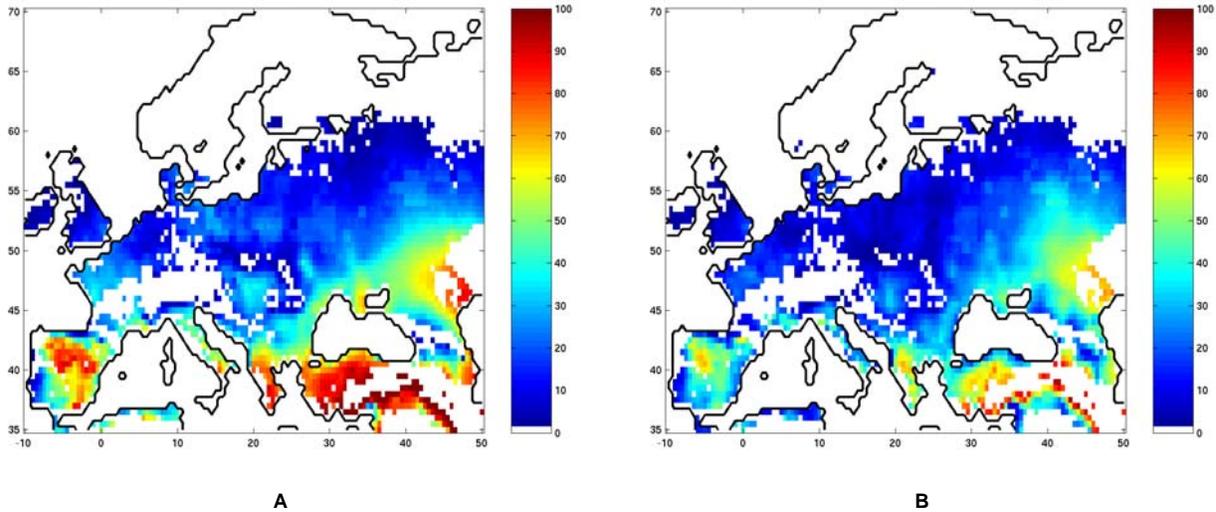A   B

Figure 3-6 A) Potential yield loss of wheat due to water stress, expressed as the difference between potential and water limited grain carbon biomass for the HadCM3 A1 COy relative to the to 1961-1990 mean [percentage]. The values are calculated as (Yield$_{pot}$-Yield$_{wl}$)/ Yield$_{pot}$*100. B) Same as A, but for 2071-2100.

We consider the difference between the potential and the water-limited yield as the potential yield loss; this value is representative for the grain carbon mass lost due to water stress. The largest potential yield loss is distributed in southern and central-eastern regions. The Mediterranean Europe, Turkey and a large area in central Eastern show the highest losses (Figure 3-6-A, B). Since the temperature forcing is the same between potential and water-limited simulations, wheat follows the same phenological development. Hence, wheat reaches mostly everywhere its full maturity, at the same moment in both potential and water-limited simulations. In addition to that, the water stress is never so intense to stop the development and kill the crop. Consequently, no differential impacts can be expected on the biomass production due to a change in the growing season length.
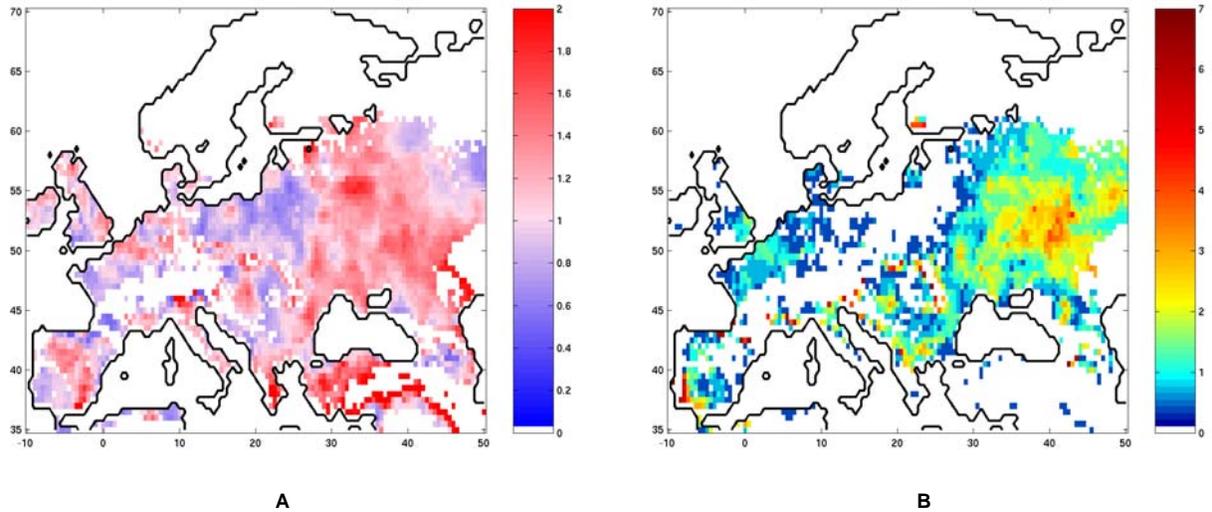
Figure 3-7 A) Ratio of yield standard deviations for HadCM3 A1 COy for 2071-2100 and 1961-1990. B) The ratio of the frequency of extreme yield loss events (see text) for 2071-2100 and 1961-1990, for HadCM3 A1 COy.

The potential yield loss is, therefore, related only to the water stress. The comparison of Figure 6-A and B gives a picture of how the potential yield loss changes between the observation period and the climate change state when the atmosphere is enriched by higher CO_2 concentration. The fertilization effect generally reduces the impact of the water stress, and the potential yield loss slightly decreases in most places, and even decreases strongly in the currently most water limited areas of southern Europe.

A further analysis of our results, using the HadCM2 A1 COy scenario, shows that large parts of the continent will be affected by an increase in the wheat yield variability. The ratio of the standard deviations of the wheat yield during the climate change period (2071-2100) divided by that for the observational period (1961-1990) is predominantly above one (Figure 3-7-A). In particular Anatolia, southern Greece and large parts of northeastern Europe increase the standard deviation up to 2 times the observation period. Some regions, however, e.g. the Baltic, or southern and western France, show a decrease in variability.

The analysis of the frequency of extreme loss events, still for the HadCM2 A1 COy scenario, gives a more complete picture of the possible impacts due to the changing climate in Europe. As we defined before, the change in

frequency of extreme loss events represents the change in risk of crop failure occurring at the end of the current century. The high potential yield loss of east-central Europe is associated with the highest increase of frequency of extreme loss events (Figure 3-7-B). This area shows a widespread increase in the frequency between the observation and climate change period up to 4-5 times. We can, therefore, conclude that east-central Europe is the area where the highest risk of crop failure may be expected in the next 70-100 years. This area is also associated with a relative increase in variability. Also the Mediterranean Basin is projected to suffer from increasing numbers of loss events, especially in Southern Spain and on the Balkan Peninsula. The high yield loss occurring in Anatolia and Southern Greece (Figure 3-6, A-B) is not associated to an increase in extreme events (Figure 3-7-B, white pixels), but the standard deviation is rather high (Figure 3-7-A). This lead to the conclusion that many non-extreme events will force the mean yield to constantly decline around the Aegean Basin. The Iberian Peninsula shows a sort of "dipole" behavior. Northern, eastern and central Spain are similar to the Aegean Basin, with frequent yield losses, high variability, but no increase in the frequency of extreme events. The southwestern area has high increase in frequency, but has relative low yield losses and a decrease in variability. In this area, therefore, the mean annual water-limited and potential yields have to be similar, low in quantity, rather constant, and close to the extreme event threshold. Central Europe and the Baltic regions show a decrease of frequency (Figure 3-7-B, values between 0 and 1), or simply no change is expected. No change in interannual variability between observed and projected climate scenario is available in the used climate data set. Consequently the change in frequency of extreme events reflects the shift in the mean status. However, the yield in water-limited conditions is the result of the complex interaction of the climate forcing and CO_2 concentration. Therefore, even though the interannual forcing variability is constant, the yield can have a non-linear response being above or below the selected threshold. This is the reason why different scenarios lead to differences in crop yield and frequency change.
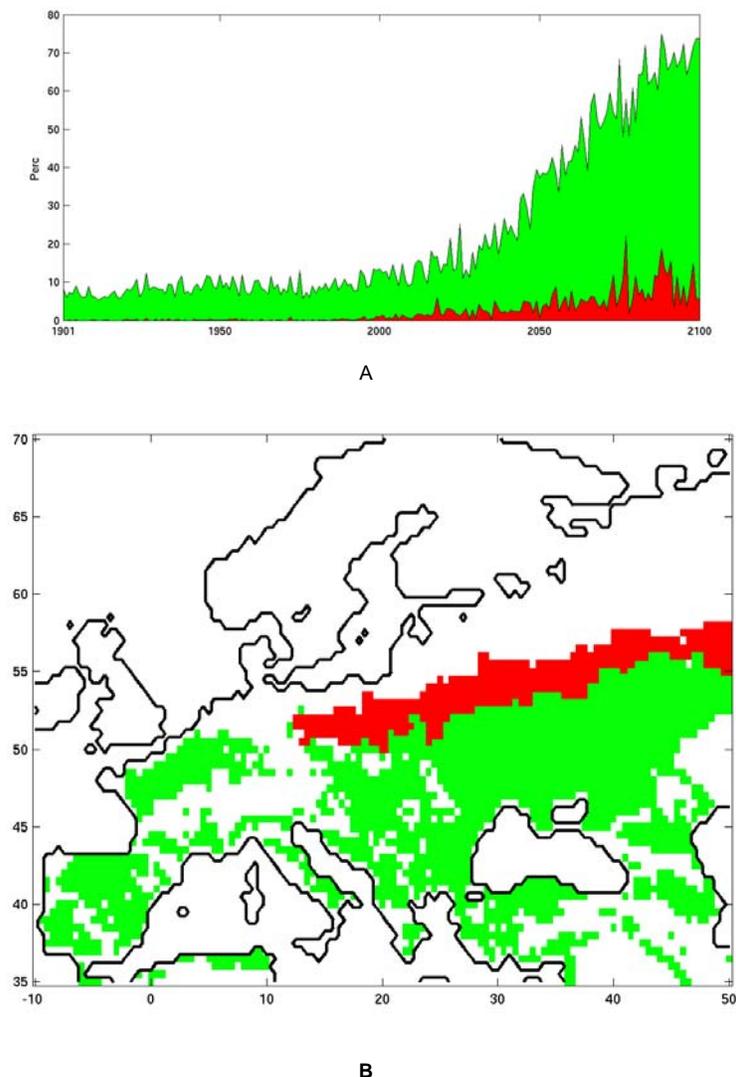
A

B

Figure 3-8 A) Percentage of the area of the crop mask where maize reaches full maturity, referring to HadCM3 A1 scenario. Red area for water-limited and green for potential production simulations. B) The areas of full maturity of maize HadCM3 A1 are shown as the mean of the last 10 years: the red area refers to water-limited simulation; the green and the red area together define the area of potential production.

3.3.2 Maize

Maize plants are largely unaffected by the CO_2 fertilization effect, but sensitive to temperature and highly water demanding. In all the water-limited simulations, the maize canopy can barely survive over the simulation grid. The potential production simulations show that the area of full maturity corresponds to southern Europe at the beginning, but tends to spread far northeast with the projected climate change. Temperature is, consequently, the only limiting factor in potential production, but water supply limits both
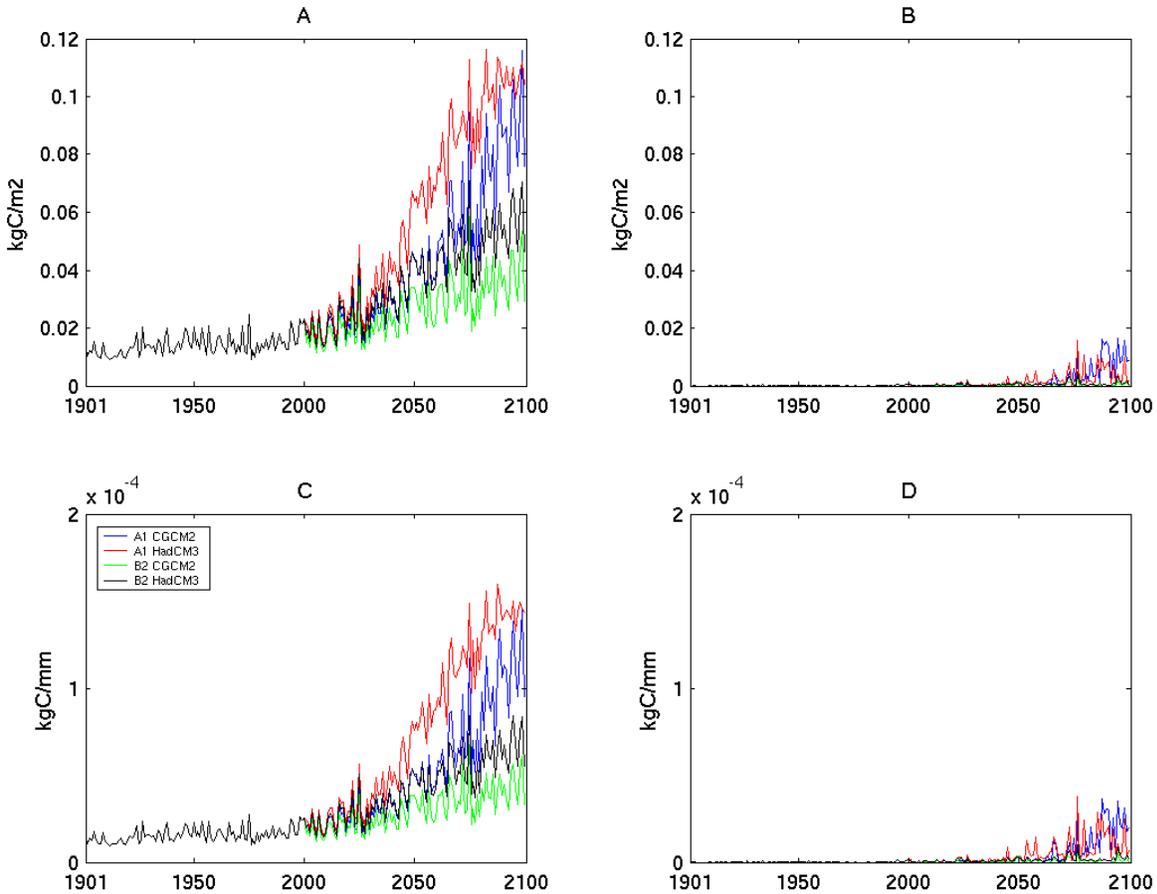
Figure 3-9 Annual average of total carbon biomass and WUE of maize over the study area. The averages are calculated for the entire European area. Total carbon biomass of potential production in A, and of water-limited one in B; WUE of potential production is given in C, and of water-limited one in D.

productivity and geographical distribution in water-limited conditions. The water stress is almost everywhere so intense that it will kill the crop. Figure 3-8-A shows the fraction of the area of the crop mask in which maize reaches full maturity using the HadCM3 A1 scenario.

The area for potential production is around 10% for the first 100 years, and increases constantly mostly to 70%. In other terms, temperature is always high enough to ensure development on a rather limited area until 2000, and largely favourable towards 2100. However, although temperature will be expected to allow crop development, the water supply is not enough to allow the growth in anything but 0 to around 5% of the study area until the second half of the current century. Around 2060-2080, the area slightly increases to around 10%. The geographical distribution for A1 HadCM3 A1 as the mean of the last 10 years is shown in Figure 3-8-B. These years have been selected
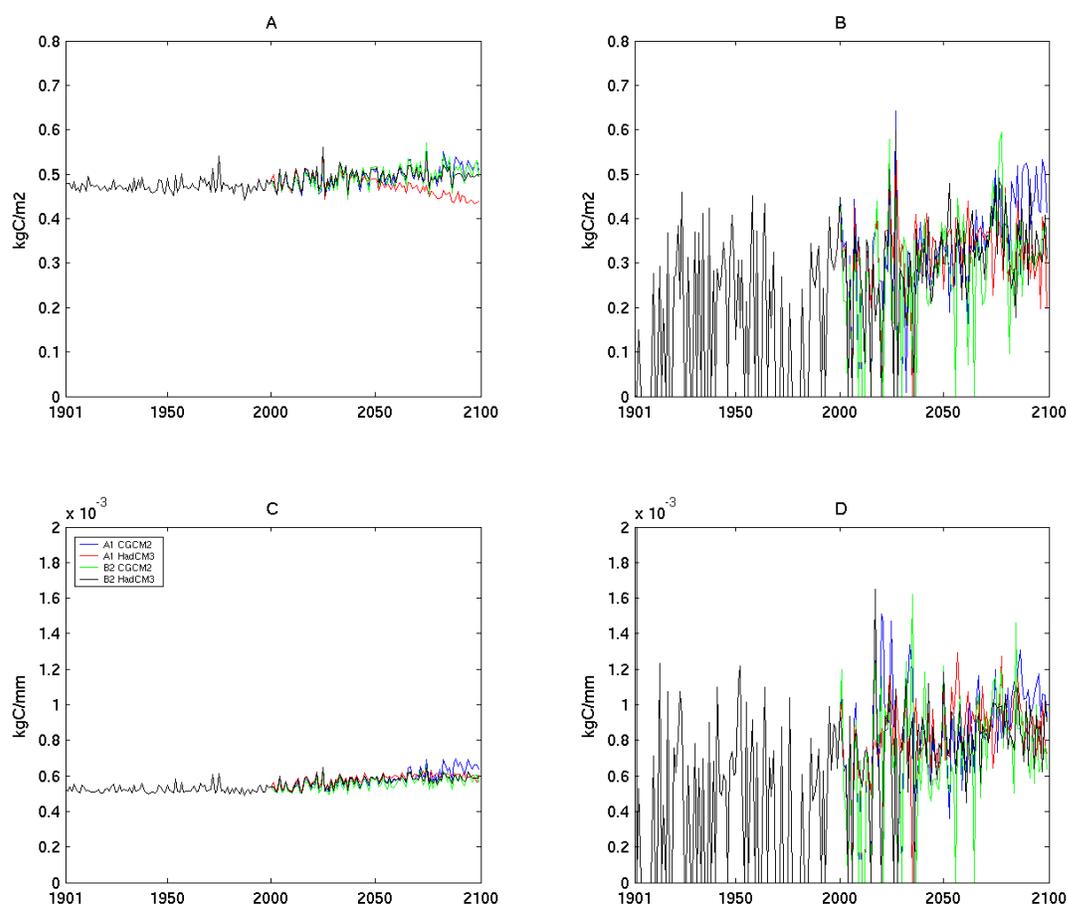
Figure 3-10 Annual average of carbon biomass and WUE of maize over the study area, considering only areas where maize reaches full maturity. Total carbon biomass for potential production in A, and for the water-limited case in B; WUE of potential production is given in C, and for the water-limited case in D.

as an example for the relatively high number of points where maize reaches maturity. Water stressed maize survives only within the red area, where the right combination of precipitation and temperature allows the growth and full development of the crop. The green area together with the red defines the potential production distribution. This scenario can be assumed to be typical for the future, using a rather extreme scenario of climate warming in Europe; the high temperature potentially allows the development everywhere, but only the northern and northeastern regions receive enough precipitation to satisfy the water demand for the growth.

The mean potential total carbon biomass over the whole study area is very The mean potential total carbon biomass over the whole study area is very small, but increases when the warming climate begins to force the northeastward spread after 2000 (Figure 3-9-A). The water-limited carbon

gain is very small until 2060-2080 when some grid points begin slightly to grow in carbon biomass (Figure 3-9-B). The mean WUE increases with the biomass production (Figure 3-9-C, D): unlike wheat, the WUE in water-limited simulations is much smaller than in potential production. When maize does not reach maturity, the model values in the corresponding grid cell are set to zero. We also include the average carbon gain over only the grid cells where full maturity is reached (Figure 3-10). Over the whole grid, A1 HadCM3 shows the largest potential production biomass increase (Figure 3-9-A); in the mean over the points where maturity is reached it shows the smallest production and a decline after 2050 (Figure 3-10-A). Also in this case, therefore, the shorter growing season and increased respiration lead to a decrease of NPP. On the other hand, the high temperature in A1 HadCM3 forces the largest geographical spread, leading to an increase in the total area of the carbon biomass production. The general variability is high in water-limited simulations, and the mean drops frequently to zero before 2050 (Figure 3-10-B). The WUE follows the oscillations in the carbon gain (Figure 3-10-C, D). As for wheat, water-limited WUE is larger than for the potential. The yield increment as a function of the water use is shown in Figure 3-11. The mean cumulative grain biomass gain over the reference period (OBS, bold line) is mostly zero for the water-limited simulation, and at potential production it is much smaller then the average over 2071-2100, independent of the scenario chosen. In addition to that, the cumulative potential biomass gain for the climate change period is almost the same throughout the scenarios, with values between 15 and $16*10^9$ kgC. Even though each scenario reaches almost the same grain potential production, the associated water use is quite different. In the CGCM2 simulations, switching from A1 to B2, about 25% less water is required to obtain about the same potential production; in HadCM3, on the contrary, 0.5% of water would be lost. In addition to that, A1 HadCM3, B2 HadCM3 and A1 CGCM2 reach the same level of cumulative grain biomass of $3.5*10^9$ kgC, using $10*e10^{16}$ m^3 of water. The potential production of 1961-1990 is on the same level with more water used. In this case, therefore, the climate change has a positive impact on maize productivity: the same quantity of grain biomass is obtained using less water. As for wheat, the "best" scenario is B2 CGCM2: the largest yield improvement with the
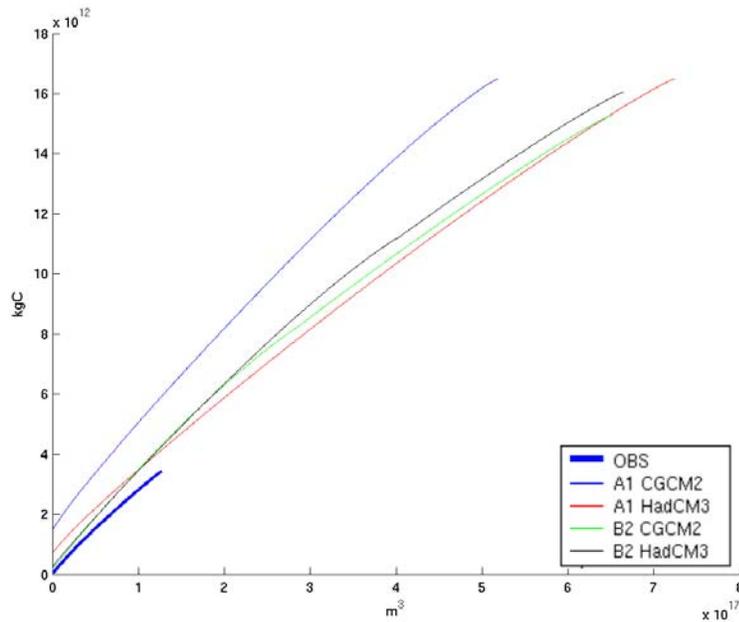
Figure 3-11 Maize yield increment as a function of the water used for four scenarios, assuming water is allocated gradually from the highest WUE grid cell to the lowest; OBS represents the 1961-2000 period, the others the 2071-2100, the yield is scaled by the crop fraction and the area of the grid cell.

minimum water use increase is found in this scenario. The difference between the potential production of 1961-1990 and 2071-2100 is 12.5×10^9 kgC, which corresponds to an increase by a factor of 3.5, the largest among scenarios. On the other hand, this large improvement is obtained increasing the water use 3.2 times, the smallest across scenarios. Additionally, the potential production of 1961-1990 is obtained in this scenario with the largest amount of water saved (50%).

The loss of potential yield for maize in general amounts to almost the entire potential production. As we already mentioned above, the water stress forces the maize plants to die mostly everywhere on the simulation grid. The mean potential yield loss for 1961-1990 is shown in Figure 3-12-A, and for 2071-2100 in Figure 3-12-B, where the figure is close to 100% almost everywhere, except near the northern biogeographical limit, where the right combination of precipitation and temperature frequently allows the growth and development even in water-limited simulations.

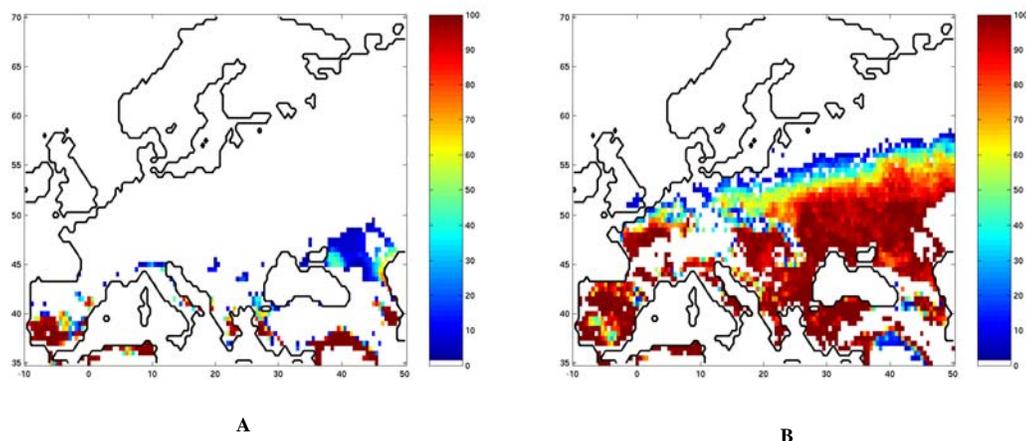A   B

Figure 3-12 A) Loss of potential yield for maize due to water stress, expressed as the difference between potential and water limited grain carbon biomass for the HadCM3 A1 COy relative to the 1961-1990 mean [kgC/m2]. The values are calculated as $(Yield_{pot}-Yield_{wl})/Yield_{pot}*100$. B) Same as A, but for 2071-2100.

3.4 Discussion and Outlook

Wheat and maize cultivation may face very different production scenarios in the future, depending on various factors. Climate change will lead to a potential spread of maize towards the north and east of the European continent, but the water demand will often not be satisfied by the natural precipitation regime. Therefore, climate change will have a strong impact on maize yields, unless largely improved irrigation will be installed. Since CO_2 fertilization will not likely affect maize productivity, consequent adaptations have to be quickly planned to face the possible impacts or to use the potential benefits. As a matter of fact, northern and central European countries could benefit from increased maize yields, but only under a satisfactory water supply system. The Mediterranean Basin shows a big yield loss due to water stress, and the shorter growing season will also not improve the yields.

Wheat yield will decrease following the shortening of the growing season due to the temperature rise. The CO_2 fertilization effect will improve the WUE and the productivity. Precipitation will partially satisfy the water demand, due also to the increased WUE. Therefore, the water stress will affect the yield relatively less than maize. Wheat will face an increase of crop yield variability, and also a higher frequency in extreme crop failures. In our scenarios, therefore, the combination of these two facts will make Southern Europe a very vulnerable area for wheat production.

The use of slow-growth cultivars is often highlighted as a possible adaptation to prevent a yield decrease in a warming climate. However, this adaptation strategy may not yield substantial benefits. In case of an extended growing season, more water will be transpired, increasing the seasonal water requirement, unless WUE is substantially improved. On the other hand, WUE is limited mainly by micrometeorology rather than genetic characteristics. Consequently, a slow-growth cultivar could increase the productivity, but also the water requirement. Furthermore, a summer slow-growth maize could extend its growing period throughout the summer. Current projections predict warmer and drier summer conditions especially in Southern Europe, where maize mainly grows. Slow-growth maize, consequently, could increase its water requirement not only for the extended growing season, but also for the increased atmospheric water demand. In this context, the use of slow-growth summer cultivars should be, consequently, carefully considered as a solution to maintain high yields.

The LPJ model is able to well reproduce the net ecosystem exchange (Sitch et al., 2003) and to correctly simulate the increase of WUE under water-limiting conditions for C3 and C4 crops. However, the response of the field crop to CO2 concentration may be small compared to model predictions (Tubiello et al., 2000; El Maayar et al., 2005). Crop plant adaptation and site-specific environmental characteristics can often decrease the CO2 fertilization effect. For this reason, we have designed our simulations with and without CO2 fertilization. However, our results of wheat COy simulations could be reviewed to a slightly lower WUE and yields. Our results show that the water requirement is highly scenario dependent. Switching from SRES-A1 to B2, 30% of water would be saved in wheat production. The best ratio between water use and crop yield corresponds to the best combination of the CO_2 fertilization effect and a relatively low increase in temperature, which is B2 CGCM2 COy. In this case, maize and wheat show the highest increase in yield with the lowest water requirements. At the end of the current century it is possible to achieve the same yield as at the end of last century, but with less water allocated to irrigation. Indeed, comparing the reference (1961-1990) to the climate change period (2071-2100), the "best combination" shows that the reference yield could lower irrigation up to 80% for wheat and 50% for maize.

We found that maize may increase potential yield by 12.5 MtonC, with an associated water requirement increase of 3.2 times, reaching 50 million m^3. The part of the water withdrawal used for agricultural in Southern Europe was already high in the period 1998-2002: France 9.81%, Italy 45.10%, Spain 68.03% and Portugal 78.24% (AQUASTAT, 2005). As mentioned already, these regions are projected to likely suffer from a decrease in precipitation and river discharge (EAA, 2004); additionally, the largest part of maize cropland is concentrated in this area. A further increase of three times in water agricultural use, as we predict, is likely to be unsustainable.

Some recent studies demonstrate the usefulness of extending DGVMs to crops for large-scale assessments, rather than the use of crop models (Scholze *et al*, 2005). Crop models have improved dramatically the understanding of biomass production and its behavior in the changing climate, but they rarely include the description of the soil carbon dynamics. In addition to that, the amount and detail of the input data limit their use to specific crops assessments in well-defined areas. Several DGVMs have been recently developed and tested to represent the biogeochemical cycles with agro-environmental aspects. Even though still in progress, those studies represent the latest challenge in biosphere modelling, giving a grid-based dynamic description of the vegetation processes. The Organizing Carbon and Hydrology in Dynamic Ecosystems model (ORCHIDEE), for instance, is a DGVM designed to include crops as part of land vegetation (Gervois et al., 2004; de Noblet-Ducoudré et al., 2005). ORCHIDEE was used to assess the current water and carbon budget in Europe.

This version of the LPJ model represents a step further in the development of DGVMs. The LPJ is now at the interface between crop and vegetation ecosystem modelling, maintaining its original potential for studies of the biogeochemical cycles. Not only crops and natural vegetation in a single tool, but also potential and water-limited production are included within the same crop scheme. This important new feature gives the possibility to perform water requirements and yield impact assessments in a spatially explicit way. This feature, combined to the detailed photosynthesis description, make this model a valid tool to simulate crop productions and water requirements within the

carbon and water cycle for general ecosystem impact assessments in climate change scenarios.

Further development could improve the representation of crop production including agro-environmental adaptations and crop distribution. Actual crop patterns are determined by both biophysical and agro-economic conditions. In order to better predict the impacts of the changing climate, the combined effect of crop yield and land use has to be included in an integrated modelling framework. Beside this, a comparison with experimental WUE data is needed to adjust the response to changing CO2 concentration. Experimental data of water-limited crop production are often a very complex issue. Not only the status of the canopy, but also that of the soil compartment needs to be accurately prescribed from data. Only validation of the potential production has been performed in a previous work (Criscuolo *et al.*, 2005). Further, the photosynthesis response of the LPJ standard version to atmospheric CO_2 and soil water has been already tested (Bacelet *et al.*, 2003; Hickler *et al.*, 2003) against data of the Duke Forest Free Air CO_2 Enrichment (FACE) experiment (DeLucia *et al.*, 1999). The model shows good agreement and an increase of CO_2 fertilization effect under water-limited conditions. As described before, photosynthesis in this LPJ version is computed in exactly the same way as in the standard LPJ model. We also put in evidence the need for common data sets consisting of all the necessary information to validate the crop-extended DGVMs. A common standardized data set of crop field data, would allow the DGVM community to test the results and cross compare the features of these challenging integrated models.

3.5 Conclusions

Water supply and demand for agricultural purposes is currently an important issue in the European continent. Climate change will reinforce the need for an efficient use of the water resources, especially in southern regions. The warming environment and the CO_2 enriched atmosphere could be an important opportunity for north and central European countries, but can lead also to highly unsustainable water consumption conditions in southern Europe. Guidelines for environmental impact analysis and management tools for the improved use of water resources should be developed to improve

water use in Europe. In this framework, the LPJ can be used as an important component in the integrated study of the crop production, water and carbon cycling.

3.6   Refernces

Alcamo J., Kreileman G.J.J., Bollen J.C., van den Born G.J., Gerlagh R., Krol M.S., Toet A.M.C., de Vries H.J.M. (1996). Baseline scenarios of global environmental change. Global Environmental Change, 6, 261–303.

AQUASTAT (2005). http://www.fao.org/ag/agl/aglw/aquastat/dbase/index.stm

Bachelet D., Neilson R. P., Hickler T., Drapek R. J., Lenihan J. M., Sykes M. T., Smith B., Sitch S., Thonicke K. (2003). Simulating past and future dynamics of natural ecosystems in the United States, Global Biogeochemical Cycles, 17, 1045, doi:10.1029/2001GB001508.

Chartzoulakis K., Psarras G. (2005). Global change effects on crop photosynthesis and production in Mediterranean: the case of Crete, Greece. Agriculture, Ecosystems and Environment, 106, 147–157.

Collatz J.G., Ball J.T., Grivet C., Berry J.A. (1991). Physiological and environmental regulation of stomatal conductance, photosynthesis and transpiration: a model that includes a laminar boundary layer. Agricultural and Forest Meteorology, 54, 107-136.

Collatz J.G., Ribas-Carbo M., Berry J.A. (1992). Coupled photosynthesis-stomatal conductance models for leaves of C4 plants. Australian Journal of Plant Physiology, 19, 519-538.

Criscuolo L., Knorr W., Ceotto E., Smith B. (2005). An assessment of climate change impacts on potential maize and wheat productivity in Europe using a Dynamic Global Vegetation Model. Submitted: Global Change Biology.

De Lucia E. H., Hamilton J.G., L. Naidu S.L., Thomas R.B., Andrews J.A., Finzi A., Lavine M., Matamala R., Mohan J.E., Hendrey G.R., Schlesinger W.H. (1999). Net primary production of a forest ecosystem with experimental CO2 enrichment, Science, 284, 1177–1179.

De Noblet-Ducoudré N., Gervois S., Ciais P., Viovy N., Brisson N., Seguin B., Perrier A. (2005). Coupling the Soil–Vegetation Atmosphere Transfer Scheme ORCHIDEE to the agronomy model STICS to study the influence of croplands on the European carbon and water budgets. In press: Agronomie.

EAA (2004). Impacts of Europe's changing climate an indicator-based assessment, EAA Report No 2/2004, European Environment Agency, Copenhagen, Denmark.

El Maayar M., Ramankutty N., Kucharik C. J. (2005). Modelling global and regional net primary production under elevated atmospheric CO2: on a potential source of uncertainty. In press: Earth Interactions.

Etheridge D.M., Steele L.P., Langenfelds R.L., Francey R.J., Barnola J.M., Morgan V.I. (1996). Natural and anthropogenic changes in atmospheric CO2 over the last 1000 yearsfrom air in Antartic ice and firn. Journal Geophysical Research, 101, 4115-4128.

Farquhar G.D., Von Caemmerer S., Berry J.A. (1980). A biochemical model of photosynthetic CO2 assimilation in leaves of C3 species. Planta, 149, 78-90.

Farquhar G.D. and Von Caemmerer S. (1982). Modelling of photosynthetic response to environmental conditions. In: Physiological Plant Ecology II: Water Relations and Carbon Assimilation (eds. Nobel PS, Osmond CB, Ziegler H), Springer, Berlin.

Gervois S., de Noblet-Ducoudré N., Viovy N., Ciais P., Brisson N., Seguin B., Perrier A. (2004). Including Croplands in a Global Biosphere Model: Methodology and Evaluation at Specific Sites. Earth Interactions, 8, 16, 1–25.

Giorgi, R., Meehl G.A., Kattenberg A., Grassl H, Mitchell J.F.B., Stouffer R.J., Tokioka T., Weaver A.J., Wigley T.M.L (1998). Simulation of regional climate change with global coupled climate models and regional modelling techniques. In R.T. Watson et al. (ed.) The regional impacts of climate change: An assessment of vulnerability. Cambridge University Press, New York.

Harrison P.A., Butterfield R., Downing T. (1995). Climate Change and Agriculture in Europe: assessment of Impacts and Adaptations. University of Oxford, UK Research Report No. 9. Environmental Change Unit.

Hickler T., Prentice I.C., Smith B., Sykes M.T. (2003). Simulating the effects of elevated CO2 on productivity at the Duke Forest FACE experiment: a test of the dynamic global vegetation model LPJ. EGS - AGU - EUG

Joint Assembly, Abstracts from the meeting held in Nice, France, 6 - 11 April 2003, abstract #9347.

Hurrell J.W., van Loon H. (1997). Decadal variations in climate associated with the North Atlantic oscillation. Climate Change, 36, 301-326.

IEEP (2000). The environmental impacts of irrigation in the European Union, a report to the Environment Directorate of the European Commission. Institute for European Environmental Policy, London, UK.

IPCC (2001a). Climate Change 2001: Working Group I: The Scientific Basis. Contribution of the Working Group I to the Third Assessment Report of the Intergovernmental Panel on Climate Change (eds. Houghton JT *et al.*), Cambridge University Press, Cambridge, UK and New York, USA.

IPCC (2001b). Special Report on Emissions Scenarios (eds. Nakicenovic N and Swart R), Cambridge University Press, Cambridge, UK and New York, USA.

IPCC (2001c). Climate Change 2001: Working Group II: Impacts, Adaptation, and Vulnerability. Contribution of the Working Group II to the Third Assessment Report of the Intergovernmental Panel on Climate Change (eds. McCarthy JJ et al), Cambridge University Press, Cambridge, UK and New York, USA.

Jones H.G. (1983). Plants and Microclimate. Cambridge University Press, Cambridge, UK and New York, USA.

Keeling C.D., Whorf T.P., Wahlen M., Vanderplicht J. (1995) Interannual extremes in the rate of rise of atmospheric CO2 measurements. Nature, 375, 666-670.

Keeling C.D., Whorf T.P. (2000). Atmospheric CO2 records from sites in the SIO air sampling network. In Trends: A compendium enriched aerial environment. Agronomy Journal, 81, 692–695.

Kenny G.J., Harrison P.A., Parry M.L. (eds) (1993). The effect of climate change on agricultural and horticultural potential in Europe. Environmental Change Unit. University of Oxford, Oxford, UK.

Kucharik C.J., Brye K.R. (2003). Integrated BIosphere Simulator (IBIS) yield and nitrate loss predictions for Wisconsin maize receiving varied amounts of Nitrogen fertilizer. Journal of Environmental Quality, 32, 247-268.

Lallana C. (2003). Mean Water Allocation for Irrigation in Europe, Indicator of the European Environment Agency, http://themes.eea.eu.int/Specific_media/water/indicators.

McGuire A., Sitch S., Clein J., Dargaville R., Esser G., Foley J., Heimann M., Joos F., Kaplan J., Kicklighter D., Meier R., Melillo J., Moore B., Prentice I., Ramankutty N., Reichenau T., Schloss A., Tian H., Williams L., Wittenberg U. (2001) Carbon balance of the terrestrial biosphere in the twentieth century: Analyses of CO2, climate and land use effects with four process-based ecosystem models. Global Biogeochemical Cycles, 15, 183-206.

Mitchel T. D., Carter T. R., Jones P. D., Hulme M., New M. (2004). A comprehensive set of high-resolution grids of monthly climate for Europe and the globe: The observed record (1901-2000) and 16 scenarios (2001-2100). Technical report, no. 5. Norwich, UK, Tyndall Centre for Climate Change Research, University of East Anglia.

Olesen J., Bindi M. (2002). Consequences of climate change for European agricultutral productivity, land use and policy. European journal of Agronomy, 16, 239-262.

Parry M.L., Carter T.R., Porter J.R., Kenny G.J., Harrison P.A. (1992). Climate Change and Agricultural Suitability in Europe. Environmental Change Unit, University of Oxford. Report No. 1. Oxford, UK.

Polley H. W. (2002). Implications of atmospheric and climatic change for crop yield and water use efficiency. Crop Science, 42, 131–140.

Ragab R., Prudhomme C. (2002). Climate change and water resources management in arid and semi-arid regions: prospective and challenges for the 21st century. Biosystems Engineering, 81, 3–34.

Ramankutty N., Foley J.A. (1998). Characterizing patterns of global land use: an analysis of global croplands data. Global Biogeochemical Cycles, 12, 667-685.

Ronneberger K., Tol R. S. J., Schneider U. A. (2005). KLUM: A simple model of global agricultural land use as a coupling tool of economy and vegetation. Hamburg, Germany. FNU Working paper.

Rosenzweig, C., Tubiello F.N. (1997). Impacts of future climate change on Mediterranean agriculture: current methodologies and future directions. Mitigation Adaptation Strategies Climate Change, 1, 219–232.

Rosenzweig C, Strzepek K.M., Major D.C., Iglesias A., Yates D.N., McCluskey A., Hillel D., 2004. Water resources for agriculture in a changing climate:internatio nalcase studies. Global Environmental Change, 14, 345–360.

Schlesinger M.E., Malyshev S. (2001). Changes in near-surfaces temperature and sea-level for the Post-SRES CO2-stabilization scenarios. Integrated Assessment, 2, 95-110.

Scholze M., Bondeau A., Ewert F., Kucharik C., Priess J., Smith P. (2005). Advances in Large-Scale Crop Modeling. Eos, 86, 26, 28 June 2005.

Sitch S., Smith B., Prentice I., Arneth A., Bondeau A., Cramer W., Kaplan J., Levis S., Lucht W., Sykes M., Thonicke K., Venevsky S. (2003). Evaluation of ecosystem dynamics, plant geography and terrestrial carbon cycling in the LPJ dynamic global vegetation model. Global Change Biology, 9, 161-185.

Tubiello F.N., Donatelli M., Rosenzweig C., Stockle C.O. (2000). Effects of climate change and elevated CO2 on cropping systems: model predictions at two Italian locations. European Journal of Agronomy, 13, 179–189.

Tubiello F.N., Rosenzweig C., Kimball B.A., Pinter P.J. Jr, Wall G.W., Hunsaker D.J., Lamorte R.L., Garcia R.L. (1999). Testing CERES-Wheat with FACE data: CO2 and water interactions. Agronomy Journal, 91, 1856–1865.

Wolf J., Van Diepen C.A.(1995). Effects of climate change on grain maize yield potential in the European Community. Climate Change, 29, 299–331.

4 Changes in agricultural land use and soil carbon storage in Europe

4.1 Introduction

The European continent faced important changes in agricultural production and land use over the last 50 years. The fast increase of land productivity, the enhanced efficiency in the production processes and the changing agro-economic markets led to a contraction of cultivated areas (Rabbinge *et al.,* 2000; Rounsevell *et al.,* 2003). The increase in crop productivity has counterbalanced the shrinkage of area so that the current food supply exceeds the demand (Ewert *et al.,* 2005). Thus, a stagnation or further decline of the current agricultural areas has to be expected also for the future (Rounsevell *et al.,* 2005). On the other hand, croplands made up nearly half of the terrestrial land surface of Europe in 1998 (EUROSTAT, 2005) and important quantities of carbon and water fluxes within the biosphere are regulated trough croplands. Therefore, agricultural land-use decisions severely influence directly carbon, nutrient and water fluxes between soil and atmosphere. Hence, changes in agricultural land use represent one of the essential links at the interface between biosphere and anthroposhere.

Furthermore, recent studies show that the climatic conditions of Europe have changed during the last hundred years. The average annual mean surface temperature has increased by 0.8 °C over the last century (Beniston *et al.,*1998); also the precipitation variability has shown differentiated patterns during the 20th century between the Northern and the Southern parts of the European continent (Hurrell *et al.,*1997). According to the Intergovernmental Panel of Climate Change (IPCC), the effect of the increasing concentration of greenhouse gases will reinforce this trend during the current century and increase the frequency of extreme events (IPCC, 2001a). Current predictions show an average mean surface temperature increase of up to 6 °C within the

next 100 years (IPCC, 2001b), and a reduction in precipitation by up to 20% in the Mediterranean areas (Ragab *et al.,* 2002; Chartzoulakis *et al.,* 2005).

The impact of the changing climate on current crop yield patterns in Europe has been assessed in recent studies with a new generation of Dynamic Global Vegetation Models (DGVMS) (Criscuolo *et al.,* 2005). These models provide an integrated representation of both natural vegetation and crops, taking into account carbon and water cycles within a single grid-based modelling framework. In these studies the combined effects of the increasing temperature, the change in precipitation regimes and the enriched CO_2 atmosphere force the crop potential productivity to generally increase in the north, but decrease in the Mediterranean area.

During the last years, an increasing emphasis is given to the possibility of storing carbon from the atmosphere to terrestrial ecosystems to reduce the amount of atmospheric CO_2 emitted from fossil fuel burning. For agricultural lands, decreased tillage and efficient use of irrigation and fertilizers have been considered as strategies to increase soil organic carbon (SOC) and decrease atmospheric CO_2 (West and Marland, 2003). Once agricultural land is abandoned and the area is colonized by natural vegetation again, not only carbon is accumulated back in the living pools and in the soil, but also the new vegetation has a fertilized growth according to the previously stored SOC (Caspsen *et al.*, 2000). Therefore, the assessment of the SOC in agricultural land is an important issue, especially to quantify the potential impacts of the global warming. Even though new methodologies to estimate the SOC have been recently proposed (Jones *et al.*, 2005), the impacts of climate change on agricultural soil has been neglected in most large-scale modelling studies. In this context, DGVMs offer the opportunity to assess not only the impact and interaction of vegetation and crops within the carbon cycle, but also the changes in SOC.

Actual crop patterns are determined by both, the biophysical as well as the agro-economic conditions. To understand the combined effect of these factors on land-use decisions, an integrated modelling framework is required to represent essential biophysical and economic processes. Current approaches to simulate large scale land-use changes still tend to over-emphasize either the geographic or the economic aspect, neglecting their interactions

(Heistermann *et al.,* 2005). Geographic models are commonly based on detailed biophysical characteristics of land. They focus on the dynamics of spatial patterns of land-use types by analysing land suitability and spatial interaction. Projections of human actions are based rather on observed behaviour than on underlying theoretical economic motivations. This limits their capability to represent the impact of market interactions, such as economic competition among land intensive sectors (for more details on geographic land-use models see e.g.Veldkamp *et al.,* 2001). In economic models, land is usually implemented as a constraint in the production of land-intensive commodities and the focus is more on market impacts and resulting emissions of land-use than on its allocation. The limitation of these models mainly manifests itself in the representation of land, which is treated as homogeneous and space-less, ignoring biophysical characteristics and spatial interactions (for more details on economic land-use models see e.g. Balkhausen *et al.,* 2004; van Tongeren *et al.,* 2001). A number of integrated approaches try to overcome these weaknesses by combining economic rationale and biophysical assessment in an integrated framework (Heistermann *et al.,* 2005). In the ACCELERATES project, for example, the farming model SFARMOD is coupled to the crop model ROIMPEL (Rounsevell *et al.,* 2003; ACCELERATES, 2004). SFARMOD determines the most profitable combination of crops based on yields under several management options and exogenously determined crop prices, while ROIMPEL provides the respective crop yields and management parameters. This is an agro-climatic and process-based simulation model, which uses climate data derived from GCMs and GIS-based soil data. Due to the detailed description of management options and impacts on farm level, the coupled framework depends on an enormous amount of input data.

In this work, we include the global agricultural land-use model, the Kleines Land Use Model (KLUM) (Ronneberger *et al.,* 2005) in a state-of-the-art DGVM, the Lund-Potsdam-Jena model for crops (LPJ-C) (Criscuolo *et al.,* 2005) to estimate the impacts of climate change on biosphere and economy for the EU25 countries. LPJ-C is an expanded version of the standard LPJ model (Sitch *et al.,* 2003) with an added crop growth compartment. It provides a dynamic representation of vegetation and crop growth. KLUM is a

coupling tool, designed to interlink global economic and vegetation models. By determining the most profitable crop allocation, based on crop prices and spatial explicit yields it reflects the essential biophysical and economic aspects of large-scale agricultural land-use changes.

Similar to the ACCELERATES-approach, this framework provides a link between dynamically modelled yield projections and economically motivated agricultural land-use decisions. In contrast to the ACCELERTAES approach, however, our system requires a less detailed input set, allowing large-scale applications and long-term predictions. Beyond, KLUM provides an interface to dynamically couple the framework to a state-of-the-art global trade model, in order to further enhance the integration of economics.

We demonstrate the potentials of the coupled system by studying the impact of two characteristic climate change scenario simulations on biomass production, crop distribution and soil carbon accumulation. In order to investigate the impact of the changing crop allocation on the SOC, we study the development of the soil carbon accumulation under fixed and dynamically simulated crop allocation. For the moment, we exclude hard predictable drivers such as management and demand changes with the intention to focus on the coupling effects. Therefore, crop production is simulated in potential production conditions and the crop prices are fixed to current values.

4.2   Modelling Framework

The KLUM@LPJ framework runs on a 0.5x0.5 longitude-latitude grid, with a time-step size ranging from one day to one year, depending on the modelled process. The framework is designed for global coverage and a possible time horizon of several centuries. In this study, however, we restrict our analysis to the area of the countries of the EU25. The two original models are dynamically coupled, exchanging data on a yearly basis.

4.2.1   The LPJ-C model

The LPJ-DVGM model is a representation of the terrestrial ecosystem with large-scale and process-based dynamics. The modelled dynamics take account of the carbon and water cycling in the vegetation and the soil, of the vegetation structure and the composition, and of fire disturbance. The LPJ-C

model incorporates crops and natural vegetation within a single modelling framework in which the two vegetation types use a common photosynthesis-assimilation scheme, while carbon dynamics and development are differently described. A comprehensive description of the general model is given by Sitch *et al.* (2003), and by Criscuolo *et al.* (2005) for the crop growth compartment. The natural vegetation in each grid cell is represented by a combination of plant functional types (PFTs). A PFT is a conceptual and numerical way to represent vegetation type inside a modelling framework. PFTs are differentiated by physiological, dynamical, and structural attributes as well as bioclimatic constraints for survival. Vegetation structure and dynamics are explicitly included and populations of PFTs compete for light and water. Photosynthesis is based on a version of the Farquhar model readapted for global modelling purposes (Farquhar *et al.,* 1980; Farquhar *et al.,* 1982).

The soil contains one litter pool for each PFT or CFT, and two SOC pools, the slow and the fast decomposing. A fraction of the litter is respired as CO_2 directly into the atmosphere with a decomposition rate at 10°C of 0.35 yr^{-1}. The remaining litter is divided in fast and slow SOC pools with a decomposition rate at 10°C of 0.03 yr^{-1} and 0.001 yr^{-1} respectively. These rates correspond to a turnover time of 2.86, 33.3 and 1000 yr. Decomposition depends explicitly on temperature (adopted from Lloyd and Taylor, 1994) and soil moisture (adopted from Foley, 1995), for details of SOC equations refer to Sitch et al. (2003). The crop biomass enters directly the litter pool; during this process a part of the carbon is moved to the atmosphere directly, while a certain quantity of SOC and the remaining litter are left in the soil. The amount of carbon moved to the atmosphere mainly depends on temperature; generally, a warm environment allows a larger flux of CO_2 to the atmosphere, leaving less SOC in the soil.

As natural vegetation is identified by the PFTs, crops are represented as crop functional types (CFTs) with specific carbon dynamics and canopy attributes. CFTs are modelled as annual plants with no competition for resources, and free to grow where no natural vegetation is allowed. The crop growth can be simulated under potential and water-limited conditions. No stress affects the plant in the first case, so that the growth is driven only by temperature and light; in water-limited simulations, water availability limits the

productivity. In this work, six CFTs (rice, wheat, maize, barley, potato, sugar beet) are simulated in potential production conditions. The crop parameterisation sets are derived from Boons-Prins et al. (1993) and adapted for the modelling requirements of LPJ. No specific calibration was performed on the crop parameters.

The harvest index (HI) is an important commercial and plant physiology index, giving a simple numerical representation of the carbon biomass distribution inside the plant structural components. Here we define the HI as the ratio of the storage organs and total biomass. In this study, we assume that only the storage organs are taken away from the field for harvest. The rest of the plant carbon biomass goes directly in the soil litter and follows the decomposition process. Tubers generally allocate much more carbon in the storage organs than cereals, which distribute the biomass more homogeneously in the plant compartments. Therefore, only a small part of the total carbon biomass of tubers (potatoes and sugarbeet, in this work) is conveyed to the soil carbon litter, but more than half of a cereal's biomass is transferred to the soil at the harvest day. Consequently, the HI also quantifies the part of the biomass transferred to the soil litter.

Since the SOC depends on the litter, the flux of biomass from the vegetation to the litter pool has to be analysed to determine the contribution of each single CFT. For this reason, we define the potential litter (PL) as the quantity of biomass per area of each crop moved from the vegetation to the soil pool every year, scaled by the area share. Consequently, the amount of biomass actually entering the soil litter (PLtot) in year n at the harvest is the sum of the crop PLs:

$$PLtot_n = \sum_k PL_{nk}$$

$$PL_{nk} = (TB_{nk} - SO_{nk})l_{nk} = (TB_{nk}(1 - HI_{nk}))l_{nk}$$

TB is the total biomass, *SO* is the biomass in storage organs pool at the harvest of year *n* and crop *k*, *HI* is again the harvest index and *l* is the area share. In the detail, the PL for the crop k represents the biomass transferred to its litter pool at the harvest day of the year n, taking into account of the land share. The litter of the year n represents the carbon litter accumulated and
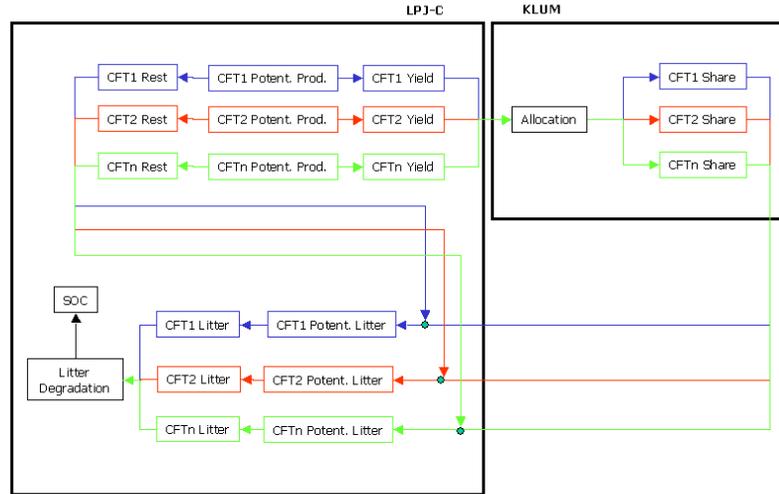
Figure 4-1 Coupling scheme of the KLUM@LPJ system; SOC indicates the soil organic carbon, CFTn the number n crop functional type and Rest the difference between total biomass and yield.

decomposed from the beginning of the simulation to the day of the current harvest; therefore, the PL represents the yearly increase of the litter pool, before performing the reduction due to decomposition and direct respiration (Figure 4-1 for a schematic representation).

4.2.2 The KLUM model

The global agricultural land-use model KLUM is designed to interlink economy and vegetation by reproducing the key-dynamics of global crop allocation (see Ronneberger *et al.* (2005) for a detailed description of the model). For this, the maximization of achievable profit under risk aversion is assumed to be the driving motivation underlying the simulated land use decisions. In each spatial unit, the expected profit per hectare, corrected for risk, is calculated and maximized separately to determine the most profitable allocation of different crops on a given amount of total agricultural area (see the Appendix II for mathematical formulation). In this, decreasing returns to scale is assumed. Mathematically the sum of these local optima is equivalent to the global optimum, assuring an overall optimal allocation.

Profitability of a crop is determined by its price and potential yield, which are the driving input parameters to the model. Furthermore, a cost parameter per crop and a risk aversion factor for each spatial unit are calibrated according to observed data. Risk is quantified by the variance of achievable profit, calculated according to preceding five yearly time steps.

For the current study, we recalibrated the original KLUM version to match the resolution of LPJ-C: the allocation of six crops (rice, wheat, maize/corn, barley, potato and sugar beet) on a 0.5°x0.5° grid of the area of the EU25 countries is simulated. For the calibration-procedure we used data of the years 1991-2001 on yields and planted area on NUTS2 level of the EUROSTAT database New Cronos (2005) and country level data on prices of the FAOSTAT (2005). We adjusted prices for inflation and converted them to 1995 US\$ by means of data of the Word Bank (2003). Prices are averaged to 5-year means and aggregated to three multi-national-regions (Western Europe, Eastern Europe and Former Soviet Union) as described in Ronneberger *et al.* (2005), matching the typical resolution of a global trade model in order to enable a possible coupling. We assigned each grid cell of the 0.5°x0.5° grid to a NUTS2 region according to the minimal distance of centers. The agricultural area in each grid cell is supposed to be an equal share of the agricultural area in the original region. Cost parameters are adjusted accordingly as described in Appendix II. To represent crops with insufficient data or not yet emerging crops (as e.g. maize or rice in Northern Europe) we adopted the cost parameters (again adjusted) and initial profit variability of adjacent or close-by units within the same world region[1] and with similar biophysical characteristics as indicated by the yield structure of the remaining crops. For NUTS2 regions with no data available we either used data on NUTS1- or even country-level for the calibration (for large parts of Germany, the UK, Portugal and Finland) or adopted the complete calibration of adjacent, biophysical similar regions (e.g. for Smalland and Västsverige, the calibration of Östra Mellansverige was adopted). For most of Finland yield data was only available on country level, whereas the planted area could be

---

[1] For the Former Soviet Union we had to adopt some prices and the complete calibration for rice from countries of Eastern Europe. In Finland for maize and rice in Latvia and Eszak-Alfold (Hungary) gave a better fit than all western European regions.
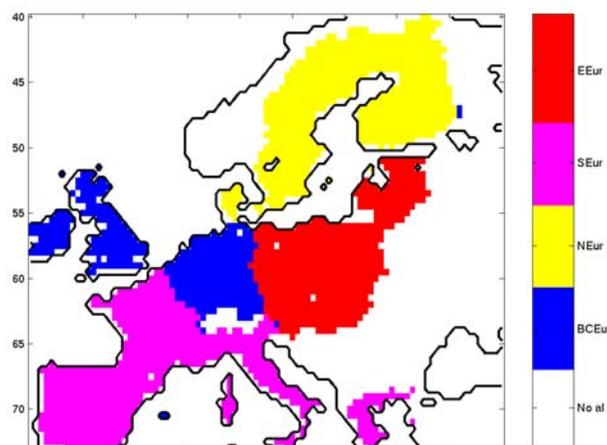
Figure 4-2 The reference grid and its sub-regions; the reference grids include the EU25 countries.

taken on NUTS2 level. Some crop prices for the region of the Former Soviet Union were missing, so we adopted slightly adjusted prices from Eastern Europe. NUTS2 regions, which are representing large city areas, such as London, Hamburg or Stockholm were left out of the calibration.

4.2.3 KLUM@LPJ

Conceptually, the two models are coupled via an exchange of potential yields and the crop allocation pattern. More concretely, KLUM calculates the share of the agricultural area to be allocated to each crop using their potential yields, as determined by LPJ-C. In order to provide KLUM with the potential productions of all the crops, in a first instance LPJ-C simulates all crops alternatively, as if they would occupy the entire grid cell without any interaction among the CFTs. Since in LPJ-C crops are not assumed to compete for resources, the only impact of the actual allocation pattern of the crops is on the soil carbon pool, which is determined by the accumulation of biomass in the plants litter. Thus, the area shares, as calculated by KLUM are used in LPJ-C to determine the contribution of the different crops to the soil carbon pool. The crop PL is scaled by the land allocation coefficients at the harvest

Table 4-1 Crop prices for the three economic regions (see text), used for the projection period 2001-2100.

$/ton	Wheat	Maize	Rice	Sugar beet	Potato	Barley
WEU	157.20	167.03	343.45	50.79	148.67	142.91
CEE	116.08	97.74	339.04	25.31	65.24	104.21
FSU	107.13	104.23	361.25	33.66	73.29	92.69

day and transferred into the soil litter, where it is finally decomposed according to the SOC sub-model. We technically realize the coupled system of LPJ-C and KLUM by directly implementing a C++ version of KLUM into the LPJ-C framework. In each yearly time step, the potential production and the allocation shares are exchanged between KLUM and LPJ-C, according to the above described scheme (Figure 4-1).

4.2.4 Design of model experiment

We use the coupled system to investigate the combined impacts of climate change on biomass production, changes in crop allocation and soil carbon accumulation. We chose the two extreme IPCC scenarios A1 and B2 to better highlight the different potential effects of temperature and atmospheric CO_2 on crops and allocation dynamics. To further separate the effect of crop allocation on the SOC, we performed the same simulations with fixed crop allocation. In this way, it is possible to distinguish the changes resulting from altering allocation from those due to climate forcing.

The simulation time covers the period 1991-2100. We use observed data for climate (precipitation, temperature and radiation), CO_2 concentration and crop prices for the period of 1991-2001. From 2001 to 2100 we use predicted climate scenarios together with the correspondent CO_2 concentration scenario. Crop prices are kept constant on the 5-year averages of 1995-2000 for the complete projection period (see Table 1). The 1991-2000 period is considered as a reference period in order to evaluate the performance of the modelling framework. To reach equilibrium in the SOC for the initial year, we spin up the model for 100 years using the 1961-1990 climatology provided in TYN 2.0 (Mitchel *et al.,* 2004) and observed CO_2 concentrations.
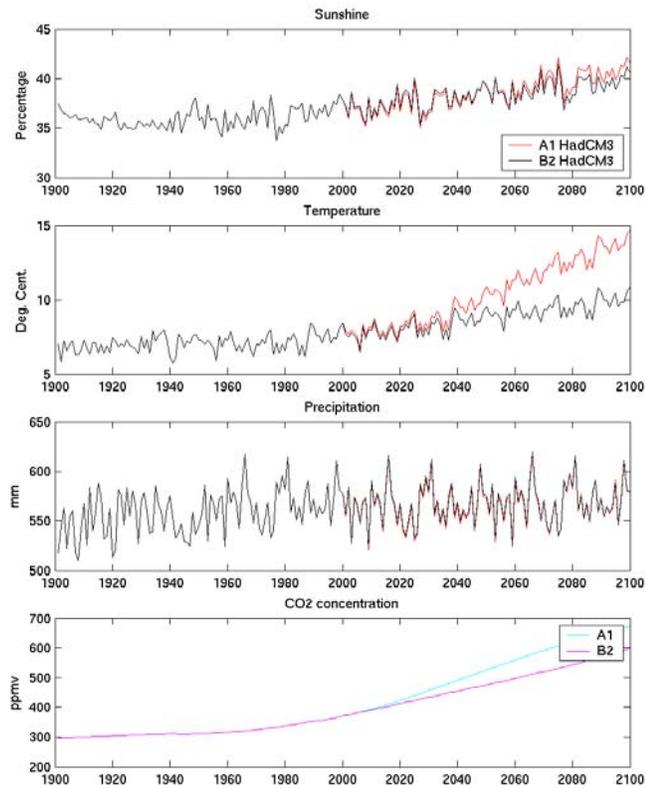
Figure 4-3 Climate means over the simulation grid.

We consider the area of the NUTS2 regions as "reference area". The reference area is also subdivided in four sub-regions for the regional analysis (Figure 4-2): British Islands and Central Europe (BCEur, including 344 grid cells), Scandinavia and Finland (NEur, including 574 grid cells), Southern Europe (SEur, including 605 grid cells) and Eastern Europe (EEur, including 463 grid cells). We refer to "regional mean" as the mean calculated over the grid cells corresponding to the regions.

4.2.5 The scenarios

We derive mean global CO_2 concentrations from McGuire *et al.* (2001), for the period 1991-1992, while data from the integrated assessment of Schlesinger *et al.* (2001) cover the remaining period after 1992. Soil texture data is based on the FAO soil data set on a global 0.5° x 0.5° grid, as described by Sitch *et al.* (2003). Observed climate data for the 1991-2000

period is derived from the CRU TS 2.0 global climate data set (Mitchel *et al.,* 2004). This data set provides monthly fields of observed mean temperature, precipitation and cloud cover on a 0.5° x 0.5° global grid over land. For the scenarios we use climate data from the TYN SC 2.0 data set (Mitchel *et al.,* 2004) for the period 2001-2100. This data set consists of monthly climate data for the period 2001-2100 simulated by General Circulation Models (GCMs), covering the global land surface on the same 0.5° x 0.5° grid as CRU TS 2.0. This set includes 16 scenarios of projected future climate representing all combinations of four SRES emissions scenarios and four GCMs. We select the SRES-B2 and SRES-A1 scenarios from HadCM3 (Figure 4-3). A1 and B2 are the extremes of the SRES group and give two very different CO2 concentration paths for the 2001-2100 period (IPCC, 2001c). The choice of HadCM3 is motivated by its behaviour over Europe, which is characteristic for a cluster of scenarios in the IPCC analysis. In the IPCC simulations, HadCM3 shows a clear increase in average temperature. Furthermore, HadCM3 is currently considered one of the reference GCMs within the IPCC framework (IPCC, 2001b).

4.2.6 Evaluation

In order to evaluate the performance of the coupled system we compare the resulting area shares and potential productions to observed data of the year 2000. We choose the final year of the reference period 1991-2000 for our evaluation, because the results of KLUM show strong perturbations for the first years of the simulation. This is a result of the differences in observed and simulated yield, which initially causes an unusual high variance in the profitability. The variance is calculated based on the profitability of the preceding five time steps and used in the algorithm as a risk estimator (see Appendix II). During the spin up period the land shares are kept constant and no calculations are carried out by KLUM. Thus, for the first years after the spin up period the variance is based on simulated as well as initialised observed yields and variances, causing the respective perturbations in the calculated variances and consequently also in the area shares. Only after around ten years the dynamic equilibrium is reached. As we discuss later on, this initialisation strategy could be reviewed, providing a longer spin up period.
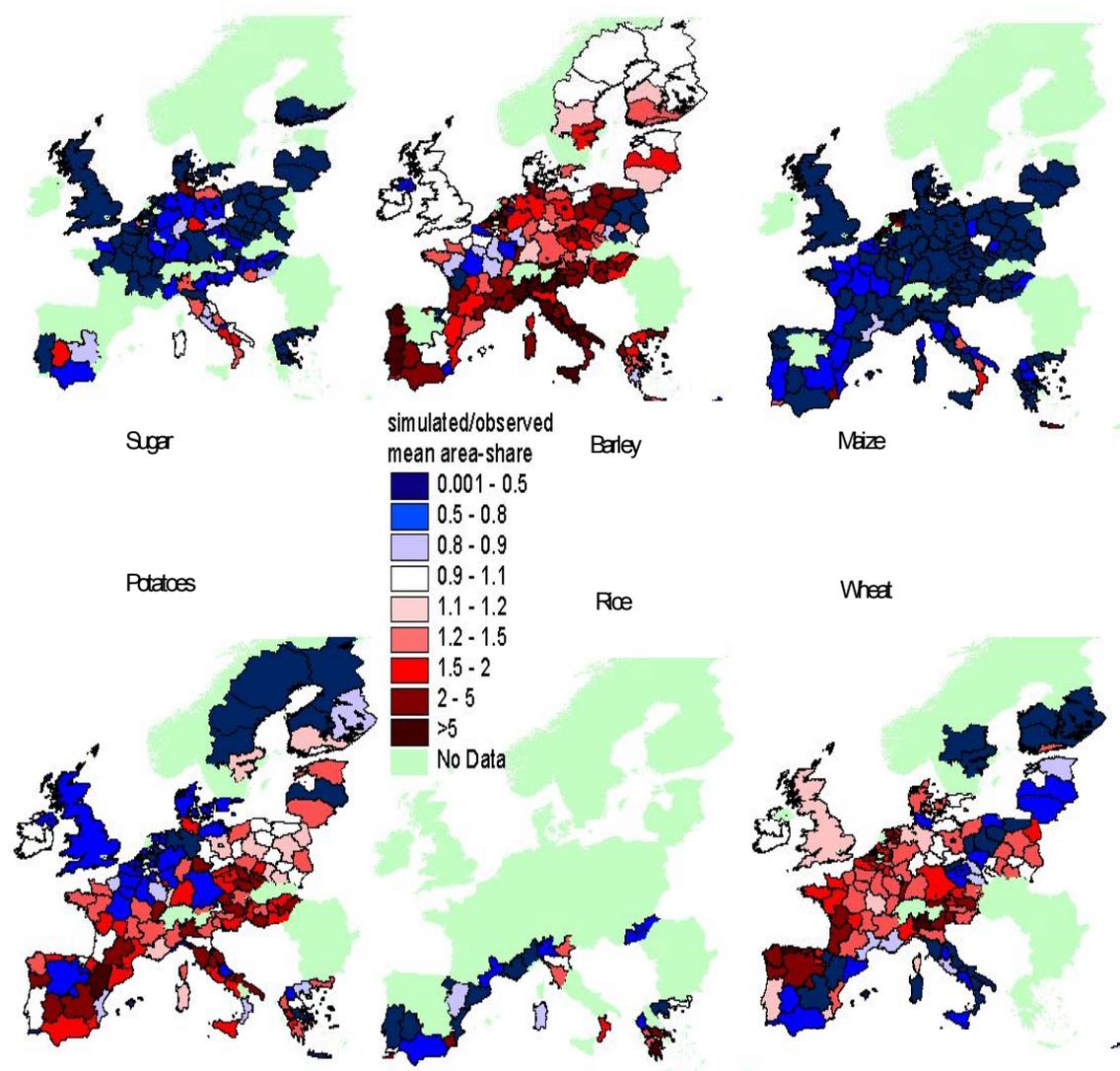
Figure 4-4 Ratio of simulated and observed area share for the year 2000. The values are compared on NUTS2 level, where the simulated values are averaged over all grid cells within one NUTS2 region. Overestimations are marked in red, underestimations in blue. White coloured grid cells match the observed value within a 10% error range.

Figure 4-4 and Figure 4-5 depict the ratio of simulated over observed values for yield and area shares of all crops for the year 2000. Blue colours indicate underestimated values whereas overestimated values are depicted in red. White areas indicate an accordance of simulated and observed values within a 10% range.
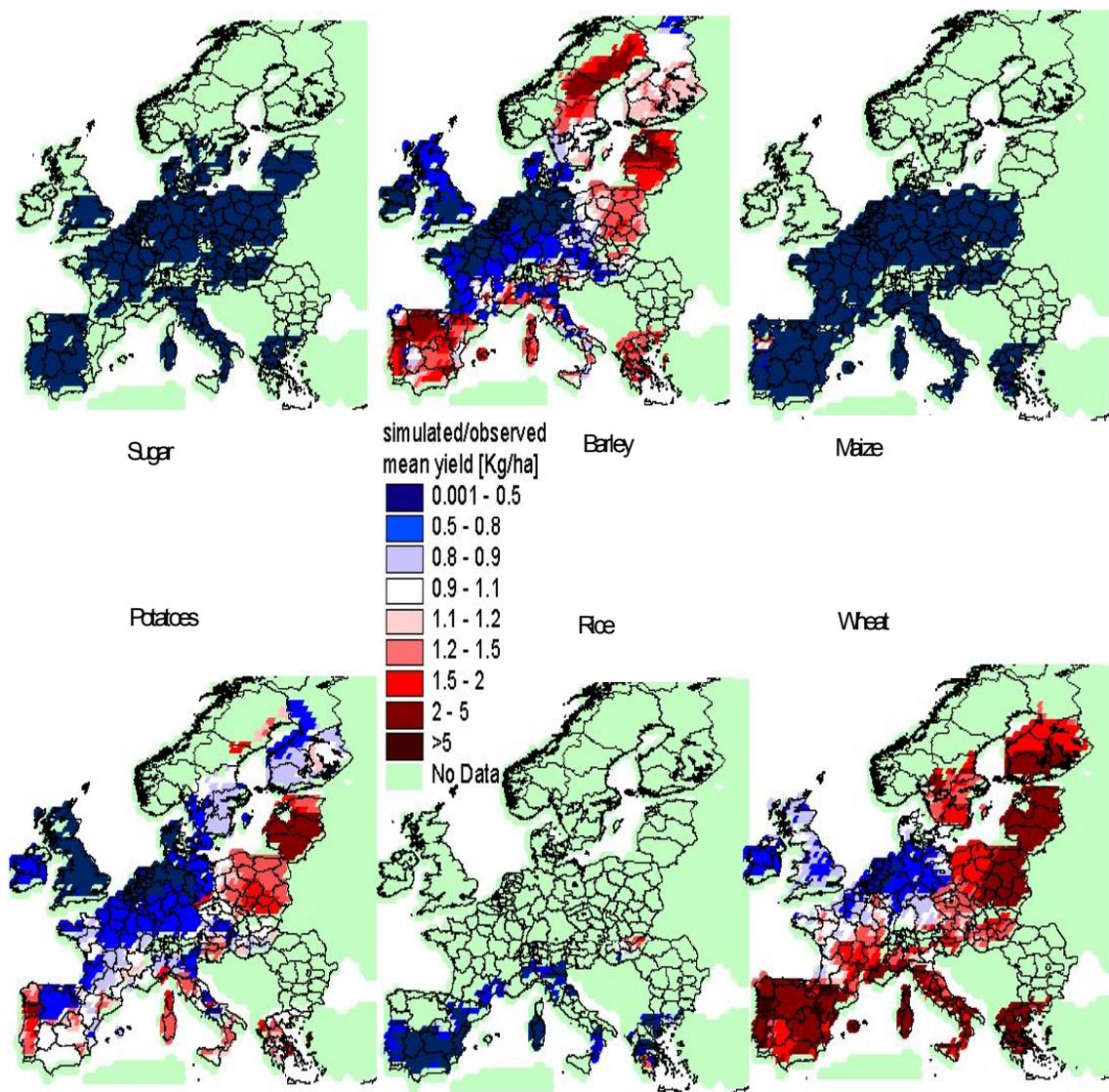
Figure 4-5 Ratio of simulated and observed yield for the year 2000. The values are compared on grid level, where the observed values of the NUTS2 region are assumed to be identical to in each grid of this region. Overestimations are marked in red, underestimations in blue. White colored grid cells match the observed value within a 10% error range.

In Figure 4-6, we show the frequency of occurrence of different percentage deviations among simulated and observed values. The colour bars depict for each crop the percentage share of all simulated data points that show a defined percentage deviation from the observed value. The length of a certain colour bar quantifies the share of data points, while the colour defines the respective deviation, where yellow to red colours mark positive and blue to green colours mark negative deviations. The simulated area shares are
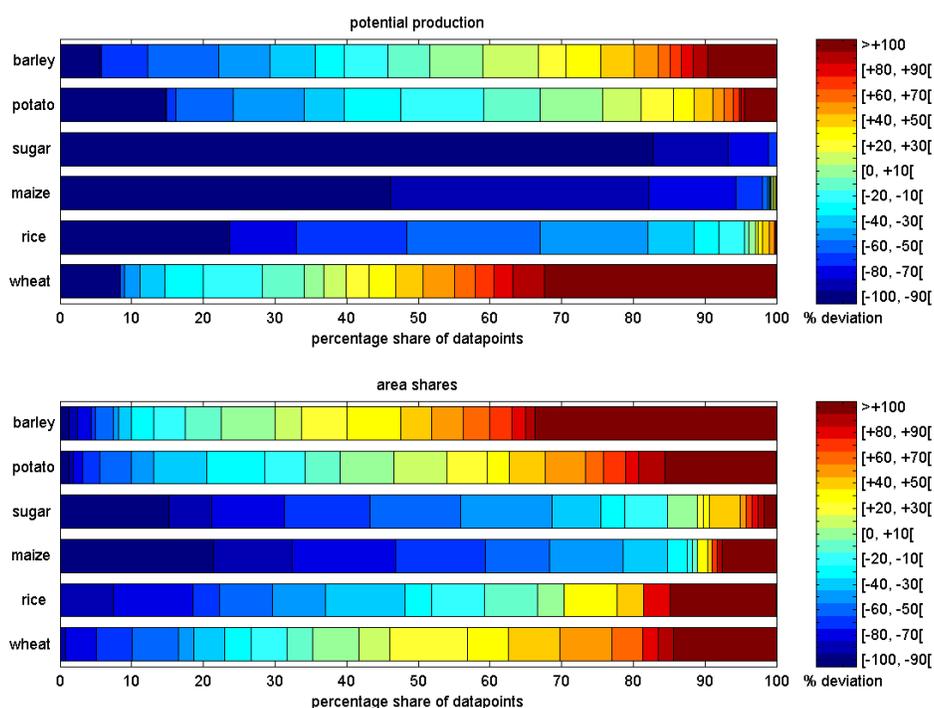
Figure 4-6 Frequency of occurrence of the different percentage deviations of simulated and observed for the year 2000; the colour characterizes the extent of the percentage deviation from simulated to the observed value. The length of the respective colour bar quantifies the percentage share of all simulated data points for this crop that lie within the marked range.

aggregated to the NUTS2 regional level in order to compare them to the observed values. For the evaluation of the simulated potential productions the comparison is performed on 0.5° x 0.5° resolution, where observed yields of the same NUTS2 region are assumed to be identical on all included grid cells.

The simulated potential production of nearly all crops does not exceed but underestimate the observed yields in the majority of simulated data points (Figure 4-6). For most crops the blue to green part of the bar clearly exceeds the 50 % mark, indicating that more than half of the simulated data points show a negative deviation from the observed values. Only for wheat the potential production is actually exceeding the observed yields for a majority of nearly 65% of the simulated data points, visualized by the yellow to red coloured bars starting from the 35% mark. The potential production represents the maximum production achievable under the forcing of a given radiation and

temperature. Thus, theoretically the simulated values should be always larger than the real world observation. The marked underestimation might be partly due to the fact that simulated yield is represented as dry matter. The observed harvested yields have a certain percentage of water, which increase the weight compared to the harvested dry matter. Furthermore, we do not apply any calibration to the crop parameters and we do not include any technological and cultivar improvements.

Figure 4-5 shows that the underestimated areas of potential productions for wheat and barley are concentrated in Central Europe and some parts of Southern Europe. For potatoes the area of underestimation shows a similar pattern but is a bit more spread also to Northern Europe. For both potential productions and area shares we observe the greatest underestimation for maize, sugar beets and rice. In Figure 4-6, a dark blue, indicating that the values are underestimated over nearly the entire grid, dominates the respective bars for the potential productions. For sugar beet 100% of the data points are underestimated by more than 60%; for maize and rice over 90% (maize) and respectively 60% (rice) of all data points are underestimated by more than 50%. For the area shares the picture looks slightly better. Here maize shows the largest share of underestimated data points with a share over 60% that is underestimated by more than 50%. For sugar beets and rice the shares of data points that are differing from the observed values by more than –50% lies at ~55% (sugar beet) and ~30% (rice). The underestimated area shares of these three crops are, on the one hand, a direct consequence of the underestimated yields. On the other hand it has been observed before that in KLUM the reproduction of minor crops is comparably weak (Ronneberger *et al.*, 2005). Yet, overall we observe more balanced proportions of underestimated and overestimated data points for the area shares.

The simulated area shares for wheat, barley and potatoes match comparably well with the observed values. It is interesting to note that the observed pattern of underestimated versus overestimated yields for wheat and barley is not reproduced in the results of KLUM. For the case of wheat it is even inverted, showing an overestimation of area shares in Central Europe and parts of South Europe. However, the underlying reason becomes evident

when looking at the relative shift of yields compared to the observed values. The yields of all crops are underestimated in Central Europe, yet for wheat the deviation from the observed value is the smallest, resulting in the highest profitability, when compared to the observed situation. In other words, compared to the observed situation for Central Europe the yield of wheat is least underestimated and thus for the simulated yield pattern the profitability of wheat relative to the other crops is increasing. Consequently, compared to the observed yield pattern more wheat is planted.

4.3 Results

For the projection period 2001-2100 the simulation of biomass production, crop allocation and soil carbon accumulation reveal clear interaction. According to the specific crop characteristics, the mean total carbon biomass over the reference area shows different time evolution for different crop typologies (Figure 4-7-A). As expected, the mean biomass of potatoes is generally way larger than of the rest of the simulated crops; additionally, the increase in biomass is larger for potatoes than for most other crops. The mean biomass increases constantly from around 1.00 to 1.20 kgC/m^2, with an increase slightly steeper for scenario A1 than for scenario B2. Potatoes are known to be a low temperature-demanding crop. In other terms, potatoes do not need high temperatures to complete the growth and, consequently, are a broadly spread crop; in our simulations the potential growing area covers mostly the whole reference area. A complete analysis shows that potatoes, at the beginning of the simulations, cover the whole continent with the exclusion of Northern-central Sweden. At the end of the simulation almost the complete simulation grid is covered.

Yet, the contribution to the reference means of this expansion is very small compared to the direct influence of the CO_2 fertilization effect and temperature on net primary productivity (NPP). We can conclude, hence, that the increase of mean potatoes biomass on the reference area in Figure 4-7-A is explained mainly by the CO_2 fertilization and the temperature effect. Wheat and barley accumulate comparably less biomass per plant, but the potential growing area covers almost the whole grid. The mean total biomass is around 30% smaller
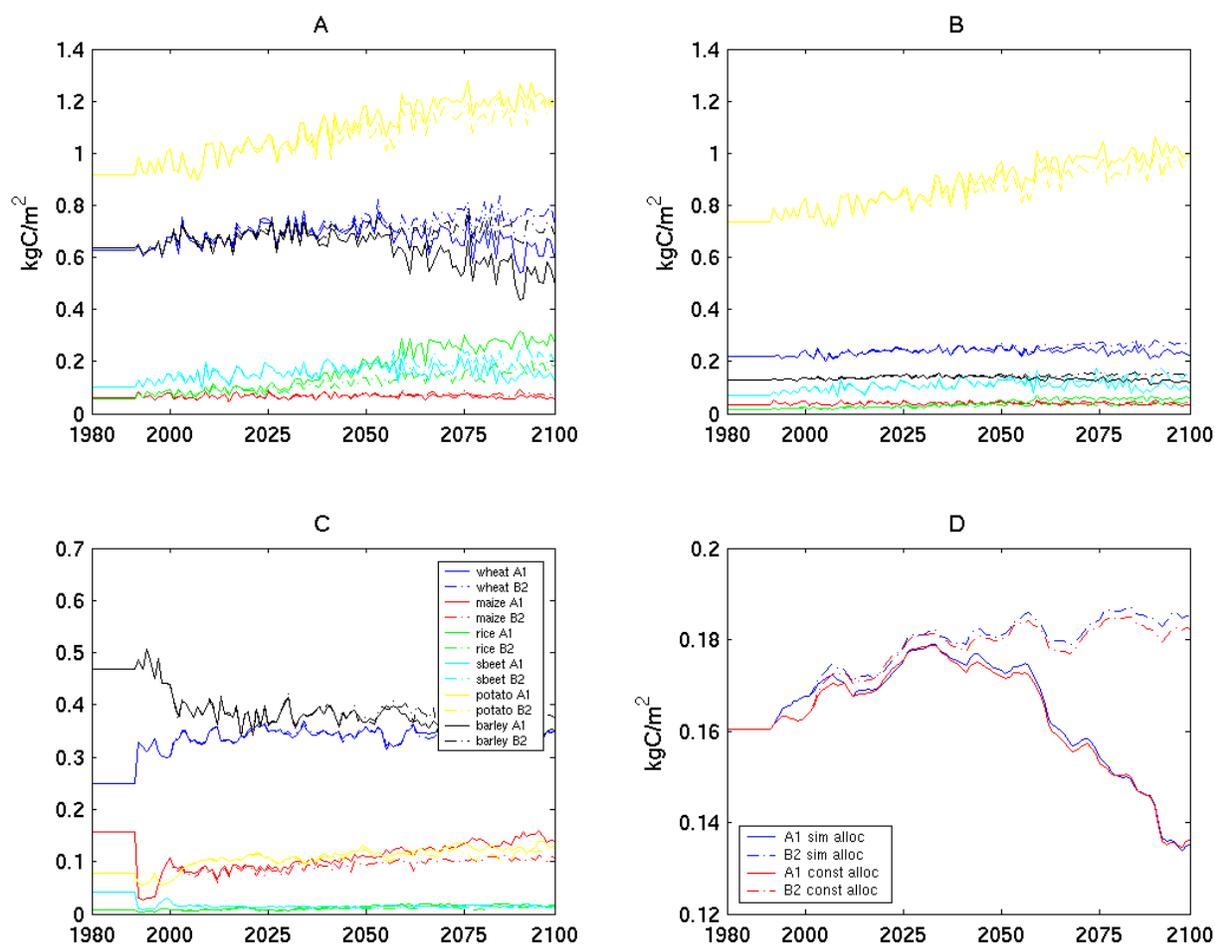
Figure 4-7 Means over the reference area (see text for details). In A, mean total carbon biomass; in B, mean storage organs carbon biomass; in C, mean land allocation coefficient; in D, mean soil carbon.

than for potatoes but around five times larger than for rice, maize and sugar beet, which are much more localized in the south and centre of Europe.

For C3 cereals, such as wheat, barley and rice, the mean carbon biomass tends to slightly increase until around 2040. After this period, for scenario B2 it is almost constant whereas in scenario A1 a clear decrease for "cold" C3 cereals (wheat and barley) and an increase for the "warm" C3 cereal (rice) can be observed. This difference in scenarios for wheat and barley is a result of the shortening of the growing season due to high surface temperature and the CO_2 enriched atmosphere. It has been demonstrated that an increase in mean temperature leads to a shortened growing season and a decreased

NPP (Criscuolo *et al.*, 2005). On the other hand, NPP is sustained by the CO_2 concentration increase, so that the final total biomass tends to slightly increase. In A1, the temperature effect prevails on the CO_2 fertilization effect after 2040. On the contrary, since rice is highly temperature demanding, the potential growing area of rice increases following the temperature increase. Thus, the mean total biomass of rice over the reference area consequently increases in A1. Maize increases constantly in both the scenarios, with a more pronounced steepness in B2. No CO_2 fertilization effect improves the maize NPP, as a C4 plant; hence, the mean biomass increase is related only to the temperature increase. Temperature affects the maize production mainly through the enlargement of the potential growing area, rather than the plant productivity (Criscuolo *et al.*, 2005). Sugar beet is mainly constant with a very low variability.

Potato and sugar beet allocate biomass mainly in the storage organs (tuber), and the associated HI is very high in our simulations, around 0.6-0.8. Maize is the third crop in the HI rank; wheat and rice are respectively the forth, the fifth and barley the sixth, with 0.35-0.40. The relationship is evident comparing the mean total carbon biomass and the storage organs (namely the yield) in Figure 4-7-A and B. As mentioned above, the fraction of the litter associated with the six crops is reflected in HI: for potatoes e.g. about 40-20% of the total biomass is moved to the soil carbon litter, whereas more than 60% of the barley biomass is transferred to the soil pool. For rice, we observe a large decrease in the HI: even though the mean biomass is largely increasing, the mean carbon allocated to the storage organs remains more or less constant, increasing the amount of carbon being transferred to the litter pool. When the biomass is moved to the litter, it is scaled by the land allocation coefficient to take into account of the actual share covered by the respective crop. The averaged land shares (Figure 4-7-C) show a high variability within the first ten years of the simulated allocation period due to the above-mentioned spin up strategy. Figure 4-7-D depicts the effect of land-allocation on SOC. The differences between fixed (green lines) and simulated (blue lines) allocation are not clearly evident, with the exclusion of the fist 10-15 years after the spin up period. The rapid changes in the land shares lead the litter to rapidly increase after the spin up; consequently the SOC tends to

increase following the increased biomass flux from the litter pool. This initial impulse, on the other hand, is relatively quickly adsorbed and the soil carbon reaches a new equilibrium after 10-15 years; moreover, the new equilibrium is similar to the one reached with fixed allocation. On the long term, the soil carbon shows a typical dependence of respiration on temperature (Lloyd and Taylor, 1994). As mentioned, the increase in biomass fluxes to the litter lead to an increase in SOC until about 2040. After this period the SOC decreases markedly in A1, while steady increases in B2. The intense temperature increase in A1 forces a faster decomposition after 2040, so that a large part of the litter and SOC are quickly released as CO2. At the end of the A1 simulation, the soil pool tends to slightly increase again, indicating a stabilization of the decomposition rate. In scenario B2, temperature increases as well, but not enough to counterbalance the increased biomass flux to the soil pool caused by the higher respiration rate.

Still, the development of the mean soil carbon pool shows a certain dependency on the mean allocation share on regional level, especially during the first years after the spin up. To better clarify this issue, we show regional means of SOC and of the PL with simulated allocation respectively in Figure 4-8 and Figure 4-9. SOC increases within the 10-15 years in all the regions, NEur excluded (Figure 4-8).
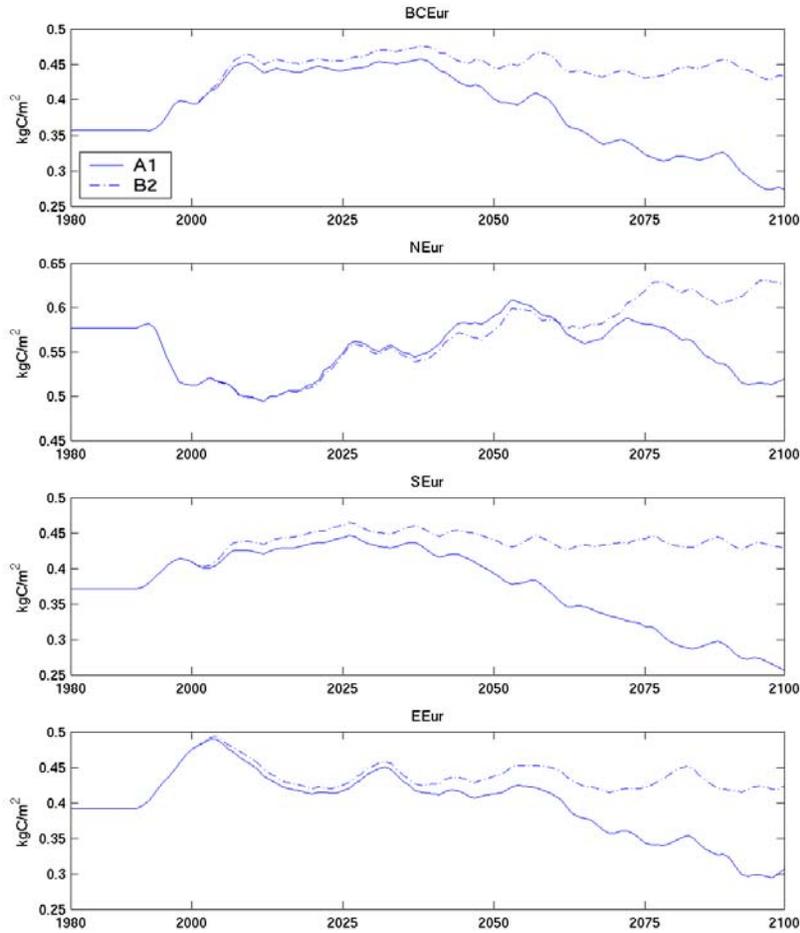
Figure 4-8 Mean soil carbon pool over the selected four regions.

The initial impulse is related to the initial increase in the PLtot (Figure 4-9). This increase indicates a larger flux of biomass to the litter, due to the initial change in allocation and biomass production (see above for PL definition). Yet, an increase in litter is generally reflected in an increase in SOC with a delay of some years; in NEur, however, a slight decrease of SOC is evident. During the spin up period, the complete reference grid is initialised with the observed allocation patterns. When KLUM receives the simulated yield from LPJ-C after the spin up, the simulated yields are zero for a number of grid cells, especially in large part of the north. Consequently, no crops are allocated in these cells and the respective PL is set to zero, leading to a stop of the biomass flux to the litter in these grid cells. At the same time the allocation coefficient of barley as well as the biomass of the plant rests (TB-
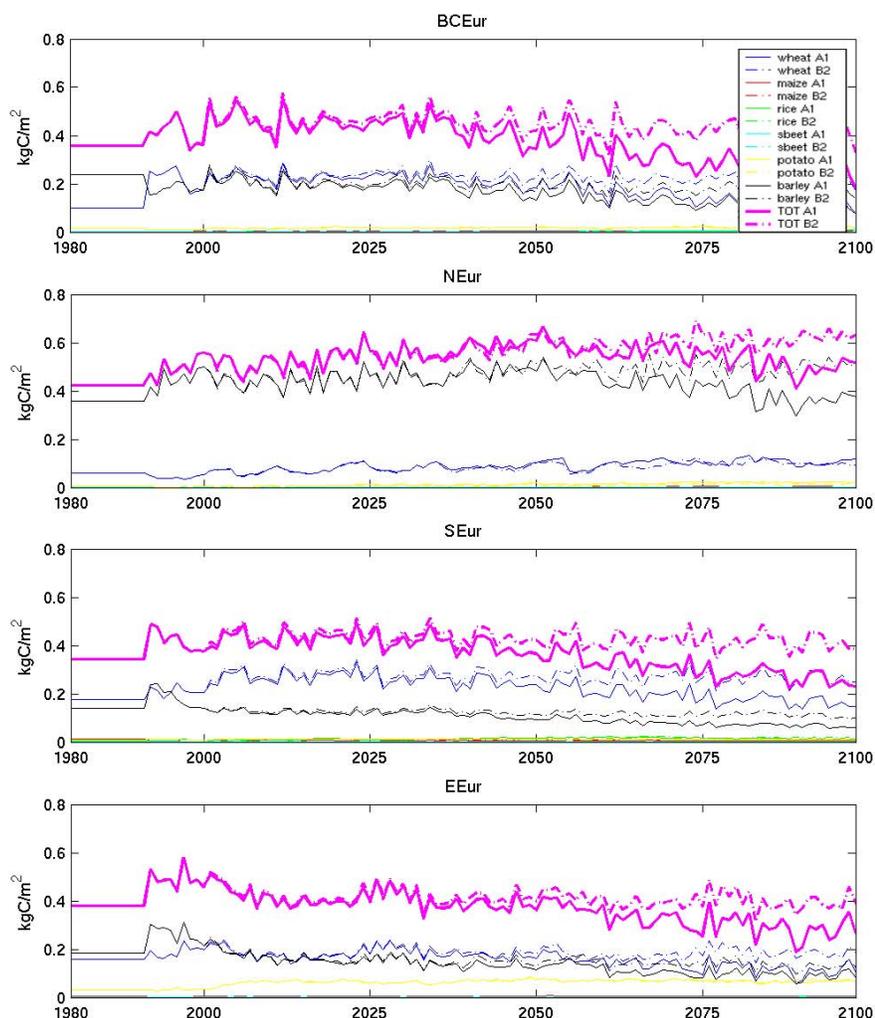
Figura 4-9 Mean PL and PLtot over the selected four regions (see text for the definition of PL).

SO, see definition of PL) increases in the south of Scandinavia, outweighing on average the decrease of PL in the north. Therefore, the resulting PL decreases in the northern part of NEur but increases markedly in the south, leading to an increase of the mean over this region. Hence, an increase in litter occurs only in the southern part of the region. Since SOC pool receives carbon from the litter decomposition only in the south, but respiration occurs everywhere, the mean over the whole region tends to slightly decrease. In this way we observe an increase in average in the PL (and in the litter) but a slight decrease in SOC. When the temperature is high enough to allow a faster decomposition, the flux from the litter to the SOC and from the SOC to the atmosphere increases. Moreover, the fraction of litter that is decomposed and

moved to soil carbon pool is larger than the respired fraction of SOC; hence, SOC has a net increase around 2020, which continues for the next 50 years. It is also interesting to note that the decrease in SOC due to lately and stronger increase of A1 temperature occurs in NEur only after 2075, while already after 2040 in the other regions; this implies a delayed temperature increase only in this region.

Figures 4-10 to 4-12 outline the spatial development of the crop allocation over time. We show rice (Figure 4-10), wheat (Figure 4-11) and maize (Figure 4-12) as characteristic representatives for the overall development. One of the main impacts in the climate change simulations is a northward shift of crop cultivation. Whereas for rice this mainly involves an extension over the grid area, for wheat and maize the maps additionally reveal an increase in the area share in Northern Europe. For most parts of Europe, this implies for both scenarios an increasingly diverse crop pattern. Only, in the south (Spain, Portugal and Italy) we observe a strong increase in wheat shares, up to over 90%, indicating a trend to a more monocultural structure.

In general the intensity and extent of the expansion to the north is much more pronounced for the warmer scenario A1. Comparing the two scenarios we note an interesting pattern for Denmark and Southern Sweden. In our starting year, barley is the dominant crop in terms of area share, being cultivated on around 60% of total agricultural area. For the warmer scenario A1 maize production is not only introduced to these regions, but at the end of the simulation the major part of the total agricultural area (around 60%) is also allocated to maize. In contrast to that, in the colder scenario B2 wheat is becoming the dominant crop in these regions, allocated to some 50-70% of the total agricultural area. This is a direct result of the above described scenario development of the accumulated carbon biomass for wheat and maize. The above-described trend in mean biomass over the simulation time horizon is reflected in the development of the cropping pattern. For instance we observe an increase of the area share for wheat - in particular in Northern Europe - followed by a slight decrease towards the end of the simulation, which is more evident for scenario A1.
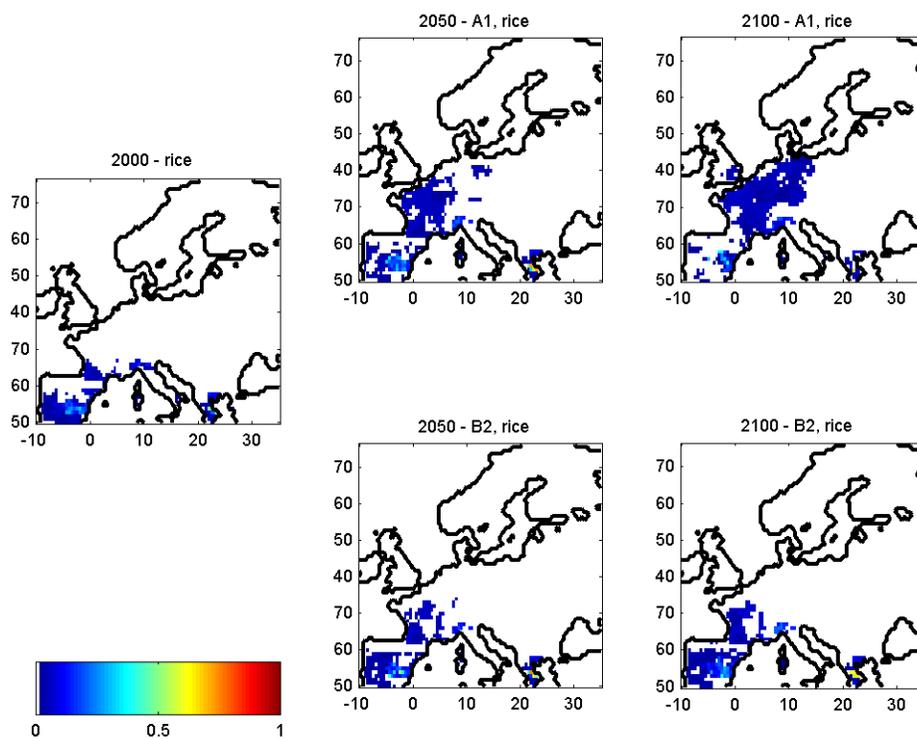
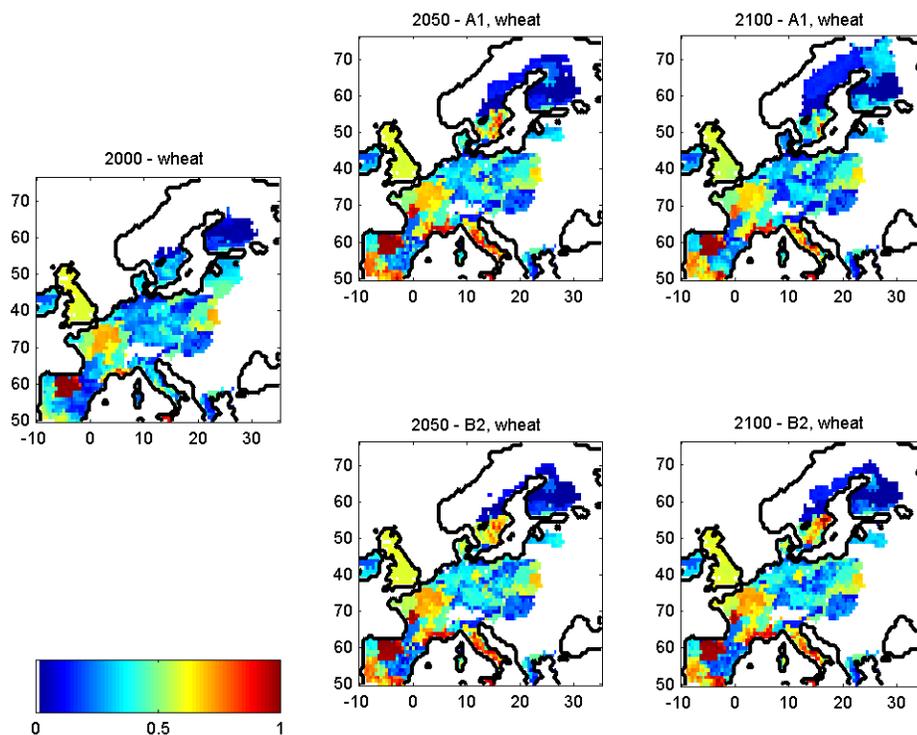**Figure 4-10 Spatial distribution of the allocation coefficients for rice.**

Figure 4-11 Spatial distribution of the allocation coefficients for wheat.
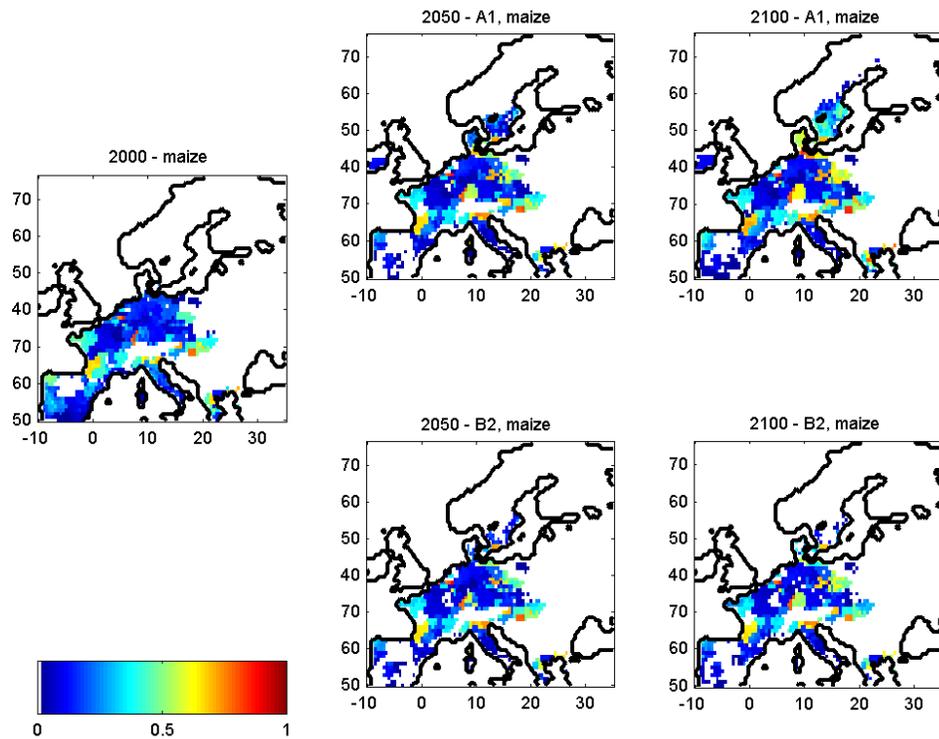
Figure 4-12 Spatial distribution of the allocation coefficients for maize.

In Figure 4-13 we visualize the economic implications of climate change for agricultural production. Figure 4-13-A shows the crop distribution over Europe and plot B depicts the total value of production in constant 1995 US dollars. Ignoring again the spin up phase, we observe an overall nearly constant economic value with small inter-annual variability. Still, for the colder scenario B2 a slight increase in total value and for the warmer scenario A1 a definite decrease in total value is visible. This trend is in accordance with the observed development of the storage organ biomass and the respective area shares of the dominating crops.
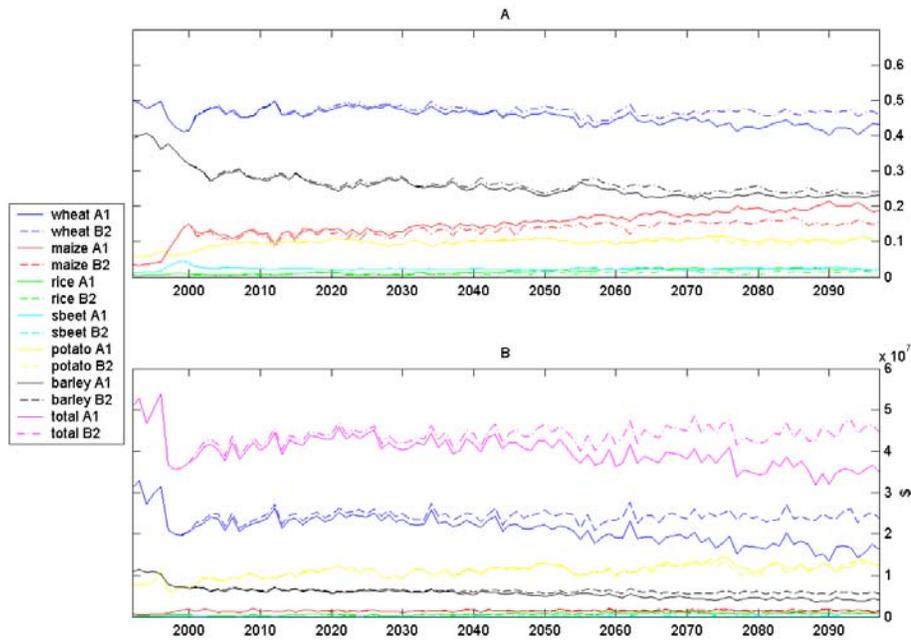
Figure 4-13 The overall economic impact of climate change. In A, the allocation shares of the complete reference grid; in B, the resulting value of production, crop-wise and in total.

In general the production value mainly follows the respective area shares. The greatest part of the production economic value is gained in wheat (around 50%) and barley (around 25%), which also capture an equivalent share of total agricultural area in Europe. Only for maize and potatoes the development of area share and production value differ tremendously. Whereas only around 10% of the area is used for potato cultivation, the corresponding production value makes up around 20% of the total value. For maize production we observe an opposite but even more extreme scenario; cultivated on 15% of the agricultural area, up to even 20% for the end of the simulation horizon, maize production adds only around 4% to the total value of agricultural production. For maize this is mainly a result of the largely underestimated yields, which we already discussed in the previous section. For potatoes, the reason lies in the interplay of price and relative yield. As shown above in Figure 4-7-B, the yield per area of potatoes is around five times larger than the yield of cereals such as wheat and barley. However, as can be seen in Table 1, the price per weight of the dominant cereals and potatoes for the

Western region, which makes up by way the largest part of our reference grid, are nearly equivalent; also in the Eastern regions only a factor close to two is assumed. Consequently, the profitability of potatoes (and also of sugar beets) is much higher than the profitability of cereals. Yet, also the involved costs are usually much higher, leading to the comparably low area share of the tubers. Only in the economic region of the Former Soviet Union the costs of potatoes have been estimated in the calibration to be very low leading to the high area shares of potatoes in EEur, discussed above.

4.4 Discussion and conclusions

In this study we coupled the DVGM LPJ-C to the agricultural land use model KLUM by dynamically exchanging simulated potential productions and the resulting crop patterns. This is a first step to a more comprehensive modelling and understanding of the mutual interaction of vegetation and human activity. The evaluation of the coupled system reveals weaknesses, in particular for the simulation of rice, maize and sugar beets. However, within the limits of the current system the overall performance provides an acceptable basis for future trend estimations.

By forcing the coupled system with future scenarios of climate change we showed the importance of the connection between economic decision, biomass production, and carbon soil pools within the context of a changing climate. Increases in SOC have to be expected following the northward shift of crops, but temperature will play a major role, highly dependent on the increase in time. The differences in SOC between fixed and simulated allocation runs put in evidence that allocation plays a secondary role if compared to the effect of temperature on soil respiration. On the other hand, the dynamics of the soil litter and SOC in a warming climate are currently a source of uncertainties in the biospheric modelling (Knorr *et al.*, 2005). The established theories that prescribe an increase in decomposition rates as a response to the increasing temperature has recently been questioned due to a hypothesized "acclimatization" of micro-organisms to higher temperatures (Giardina and Ryan, 2000; Luo *et al.,* 2001). However, a recent study found that the hypothesis of an increased CO_2 soil flux related to global warming to be fully consistent with evidences (Knorr *et al.*, 2005), without the need to

consider biological adaptation of decomposition rates. LPJ-C includes a direct dependency of respiration rates on temperature and soil humidity according to the formulation by Lloyd and Tayler (1994), which is similar to the Arrhenius equation used by Knorr *et al.* (2005); the description of the SOC decomposition could be, therefore, reviewed following the new proposed theories. Moreover, we describe the crop harvesting with a very simple approach: storage organs are taken out of the field and the rest of the biomass is moved to the agricultural soil. Therefore, we do exclude specific harvesting and agronomic techniques, which can be very relevant in the soil carbon balance. Also the influence of management and technology changes will certainly play a major role in shaping future agricultural land use, influencing soil carbon pools as well as the water cycle. However, these changes and impacts are highly uncertain and hard to predict. Thus, a sound understanding of the independent management trends can build a useful basis for further assessments.

The simulations show for the future a clear impact of land allocation on soil pools, underpinning the importance of dynamic land use modelling for a comprehensive description of the soil carbon pools. The results of biomass production, crop allocation and economic impact show a clear connection. For all crops we observe a shift of potential as well as actual growing area to the north. Rice will be increasingly cultivated also in Central Europe and maize will cover Southern Scandinavia as well. In the simulation of the warmer scenario A1, maize is even becoming the dominant crop in terms of area share for Denmark and Southern Sweden. From the economic side the simulation results suggest a slight gain in a moderately warming climate, and clear losses in the more drastically warming scenario. This is mainly a result of the evident shift from wheat and barley production towards an increasing share of maize production, which, in our simulation is a less profitable crop. For the less warm scenario this trend is less pronounced, as the CO_2 fertilized wheat yields result in a greater share of wheat production.

However, these results are based on the assumption that crop prices as well as the total amount of agricultural area will not change and should be critically assessed within that context. We chose these scenarios because no scenarios based on more realistic assumptions were available. Ronneberger

et al. (2005) showed that the assumption of simple linear extrapolation of past trends leads to highly unrealistic results and suitable dynamic projections of future crop prices are rare. Yet, prices will change along with cultivation habits and according to a changing economy, which will be impacted by climate change from more than just the agricultural side strongly impacting the simulated pattern. Even though a stagnation or decline of total agricultural area is often projected, this aspect has to be judged with care. A changing climate will affect cultivars and management practices, which feed back on the total area used for cultivation. For instance the observed increase of wheat production in the south of Europe is most likely only a result of the model structure, which provokes the use of the complete area for at least one of the simulated crops. Under a warming climate, however, it is more likely that new heat-resistant crops are used in the South, or that a large part of the agricultural area is abandoned due to shortening water supply. On the opposite, Northern Europe might benefit from an increase of total agricultural area as a result of the improved plant growth under a warming climate.

However, even though there is large scope for improvement, our modelling approach is a new baseline on which it is possible to build a high potential integrated tool to assess the carbon cycle. This is a first step to assess the possibility to appropriately represent the trend of future crop patterns under the influence of climate change.

4.5   References

ACCELERATES 2004. Section 6: Final Report. http://www.geo.ucl.ac.be/accelerates

Alcamo J., Kreileman G.J.J., Krol M., Zuidema G. (1994). Modelling the Global Society-Biosphere-Climate System: Part 1: Model Description and Testing. Water, Air, and Soil Pollution, 76, 1–35.

Balkhausen O. and Martin B. (2004). Modelling of Land Use and Land Markets in Partial and General Equilibrium Models: The Current State. Workpackage 9, Deliverable No.3. *The* Impact of decoupling and Modulation in the Enlarged Union: a sectoral and farm level assessment. IDEMA Project, University of Göttingen, Göttingen, Germany.

Beniston M., Tol R.S.J. (1998). Expected Climate Change Impacts in Europe. Energy & Environment, 9, 365-381.

Boons-Prins E. R., de Koning G. H. J., van Diepen C. A., and Penning de Vries F. W. T (1993). Crop-specific parameters for yield forecasting across the European Communtiy. Wageningen, The Netherlands. Simulation Reports CABO-TT.

Caspersen J. P., Pacala S. W., Jenkins J.C., Hurtt G.C., Moorcroft P.R., Birdsey R.A. (2000). Contributions of Land-Use History to Carbon Accumulation in U.S. Forests. Science, 290, 1148-1151.

Chartzoulakis K., Psarras G. (2005) Global change effects on crop photosynthesis and production in Mediterranean: the case of Crete, Greece. Agriculture Ecosystems and Environment, 106 147-157.

Criscuolo L., Knorr W., Ceotto E., Smith B. (2005) An assessment of climate change impacts on potential maize and wheat productivity in Europe using a Dynamic Global Vegetation Model. Submitted: Global Change Biology.

Ewert F., Rounsevell M.D.A., Reginster I., Metzger M.J., Leemans R. (2005) Future scenarios of European agricultural land use: I. Estimating changes in crop productivity. Agriculture, Ecosystems & Environment 107 101-116.

FAOSTAT (2005) http://faostat.fao.org/.

Farquhar G.D., von Caemmerer S. (1982) Modelling of photosynthetic response to environmental conditions. In:Physiological Plant Ecology II:

Water Relations and Carbon Assimilation (eds Nobel PS, Osmond CB, Ziegler H), pp. 549-587. Springer, Berlin.

Farquhar G.D., von Caemmerer S., Berry J.A. (1980) A biochemical model of Photosynthetic CO_2 Assimilation in leaves of C3 Species. Planta 149 78-90.

Foley J.A. (1995). An equilibrium model of the terrestrial carbon budget. Tellus, 47B, 310-319.

Giardina C. P., Ryan M. G. (2000). Evidence that decomposition rates of organic carbon in mineral soil do not vary with temperature. Nature*, 404, 858−861.

Heistermann M., Müller C., Ronneberger K. (2005a) Land in sight? Achievements, deficits and potentials of continental to global scale land-use modeling. Accepted: Agriculture Ecosystems and Environment.

Hertel T. W. (1997). Global trade analysis. Cambridge University Press. Cambridge, UK and New York, NY, USA..

Hurrell J.W., van Loon H. (1997). Decadal variations in climate associated with the North Atlantic oscillation. Climatic Change, 36, 301-326.

IPCC (2001a). Climate Change 2001: Impacts, Adaptation, and Vulnerability. Contribution of the Working Group II to the Third Assessment Report of the Intergovernmental Panel on Climate Change. Cambridge University Press, Cambridge, UK and New York, NY, USA.

IPCC (2001b) Climate Change 2001: The Scientific Basis. Contribution of Working Group I to the Third Assessment Report of the Intergovernmental Panel on Climate Change. Cambridge University Press, Cambridge, UK and New York, NY, USA.

IPCC (2001c) IPCC Special Report on Emissions Scenarios. Cambrigde University Press, Cambridge, UK and New York, NY, USA.

Knorr W., Prentice I. C., House J. I., Holland E. A. (2005). Long-term sensitivity of soil carbon turnover to warming. Nature, 433, 298-301.

Jones R.J.A., Hiederer R., Rusco E., Montanarella L. (2005). Estimating organic carbon in the soils of Europe for policy support. European Journal of Soil Science, 56, 655–671.

Lloyd, J., Taylor J. A (1994). On the temperature dependence of soil respiration. Functional Ecology, 8, 315−323.

Luo Y. Q.,Wan S.Q., Hui D. F., Wallace L. L. (2001). Acclimatization of soil respiration to warming in a tall grass prairie. Nature, 413, 622–625.

McGuire A., Sitch S., Clein J., Dargaville R., Esser G., Foley J., Heimann M., Joos F., Kaplan J., Kicklighter D., Meier R., Melillo J., Moore B., Prentice I., Ramankutty N., Reichenau T., Schloss A., Tian H., Williams L., Wittenberg U. (2001) Carbon balance of the terrestrial biosphere in the twentieth century: Analyses of CO_2, climate and land use effects with four process-based ecosystem models. Global Biogeochemical Cycles, 15, 183-206.

Mitchel T. D., Carter T. R., Jones P. D., Hulme M., New M. (2004). A comprehensive set of high-resolution grids of monthly climate for Europe and the globe: The observed record (1901-2000) and 16 scenarios (2001-2100). Technical report, no. 5. Norwich, UK, Tyndall Centre for Climate Change Research, University of East Anglia.

Olesen J., Bindi M. (2002). Consequences of climate change for European agricultural productivity, land use and policy. European Journal of Agronomy, 16, 239-262.

Rabbinge R., van Diepen C.A. (2000). Changes in agriculture and land use in Europe. European Journal of Agronomy, 13, 85-100.

Ragab R., Prudhomme C. (2002). Climate change and water resources management in arid and semi-arid regions: prospective and challenges for the 21st century. Biosystems Engineering, 81, 3-34.

RIVM (2001). The IMAGE 2.2 model documentation. Technical report, National Institute of Public Health and the Environment, Bilthoven, NL. Electronic version at http://arch.rivm.nl/image/.

Ronneberger K., Tol R. S. J., Schneider U. A. (2005). KLUM: A simple model of global agricultural land use as a coupling tool of economy and vegetation. Hamburg, Germany. FNU Working paper.

Rounsevell M.D.A., Annetts J.E., Audsley E., Mayr T., Reginster I. (2003). Modelling the spatial distribution of agricultural land use at the regional scale. Agriculture, Ecosystems & Environment, 95, 465-479.

Rounsevell M.DA., Ewert F., Reginster I., Leemans R., Carter T.R. (2005). Future scenarios of European agricultural land use: II. Projecting

changes in cropland and grassland. Agriculture, Ecosystems & Environment, 107, 117-135.

Schlesinger M.E., Malyshev S. (2001). Changes in near-surfaces temperature and sea-level for the Post-SRES CO2-stabilization scenarios. Integrated Assessment, 2, 95-110.

Scholze M., Bondeau A., Ewert F., Kucharik C., Priess J., Smith P. (2005). Advances in Large-Scale Crop Modeling. Eos, 86, 26, 28 June 2005.

Sitch S., Smith B., Prentice I., Arneth A., Bondeau A., Cramer W., Kaplan J., Levis S., Lucht W., Sykes M., Thonicke K., Venevsky S. (2003). Evaluation of ecosystem dynamics, plant geography and terrestrial carbon cycling in the LPJ dynamic global vegetation model. Global Change Biology, 9, 161-185.

van Meijl H., van Rheenen T., Tabeau A., and Eickhout B. (2005). The impact of different policy environments on land use in Europe. Submitted to: Agriculture Ecosystems and Environment.

van Tongeren F., van Meijl H., Surry Y. (2001). Global models applied to agricultural and trade policies: a review and assessment. Agricultural Economics, 26, 149-172.

West T. O., Marland G. (2003). Net carbon flux from agriculture: Carbon emissions, carbon sequestration, crop yield, and land-use change. Biogeochemistry, 63, 73–83.

World Development Indicators (2003) CD ROM, World Bank.

5 Conclusions

5.1 Summary

Climate change impacts European agriculture through many aspects of crop production. Not only plant productivity, but also geographical shift of cultivation areas, changes in crop phenology, in land use, and in soil carbon have to be taken into account for assessments of the next future. The modelling framework we provide is a potentially powerful baseline to study the impacts of the changing climate by assessing crop production with a single integrated approach for large-scale studies. LPJ-C enables to describe and quantify the carbon budget at ecosystem scales in natural and agro environments. Yet, LPJ-C provides a description of the crop production process at the interface between detailed crop and general vegetation ecosystem modelling. Not only crops and natural vegetation in a single tool, but also potential and water-limited crop production are included within the same biosphere scheme.

We provide here, for the first time, a grid-based assessment of potential impacts of climate change in Europe using an extended Dynamic Global Vegetation Model (DGVM). Our results show that the increase of CO_2 concentration and the rise of temperature may allow earlier sowing dates, shorten growing seasons, enlarge the potential growing areas and increase the potential crop yield. On the other hand, the climate change could lead to an increase in crop water demand, frequency of extreme loss events and heavily impact the soil carbon budget through the cropland allocation. All those changes may affect the European continent with several distinct regional differences.

Reviewing the work we described in Chapter 2 the model development and parameter optimization of LPJ-C. The model is now able to simulate crops and natural vegetation within a single grid-based modelling framework. The

optimization procedure provides a set of crop parameters, subsequently used in a regional assessment over Europe. Further, we used the resulting modelling framework to study the changes of potential production of maize and wheat together with the shift in their potential growing area. In this modelling context, the results show that wheat yield will suffer from a marked decline through a shorter growing season, but fertilization due to the CO_2 enriched atmosphere will often more than compensate this effect. The net result is an improvement of potential production. The area of potential growth of wheat will largely be unaffected by the future climate regimes that were considered in our simulations. For maize, however, cultivation will clearly expand towards north and east. Since maize, as a C4 plant, is mostly unaffected by the CO_2 fertilization effect, the shorter growing season will lead to a lower NPP, while the mean over the continent will increase according to the large geographical spread.

Furthermore, in Chapter 3, we perform scenario runs to analyse the water-limited production of maize and wheat, and their water requirements. We include an assessment of the change in frequency of extreme yield loss events of wheat, and a study of the water use efficiency (WUE). We show that LPJ-C is able to reproduce the observed relative increase of WUE under water-limited conditions and a CO_2 fertilization effect. The improved WUE of wheat leads to a relatively smaller transpiration per unit of biomass, so that water provided by precipitation will partially satisfy the transpiration demand. On the other hand, wheat will suffer from an increase of yield variability and a higher frequency of extreme crop failures. Maize will suffer from strong losses, unless largely improved irrigation will satisfy the highly increased water demand. Moreover, comparing our reference period (1961-1990) to the climate change period (2071-2100), the potential production of maize for the reference period could be obtained at the end of the century saving a large part of the water demand. Even though this result occurs in the "best scenario combination", this water requirement is likely to be highly unsustainable, so that large potential losses will likely occur. In addition to this, we confirm that the agriculture in the Mediterranean Basin will be a very vulnerable sector due to large water deficit and frequent localized extreme loss events.

As the last part of our assessment, in Chapter 4, we describe and discuss the coupling of LPJ-C with the land-use model KLUM. In this work, we link a profit maximization procedure for land allocation to a process-based description of crop production and soil carbon dynamics. In this way, we provide for the first time a modelling framework to connect economic decision, biomass production, and carbon soil pools within the context of a changing climate in Europe. The coupled system showed that increases in soil carbon have to be expected following the northward shift of crops and their area share changes, but temperature will play a major role in the soil carbon dynamics. Important changes have to be expected for "warm" cereals as rice and maize. Rice will be increasingly cultivated in Central Europe and maize will potentially cover Southern Scandinavia.

5.2 Outlook

The complex nature of the agroenvironmental production system in Europe is the result of the interaction of various natural, human and economic compartments; the predicted impact of climate change is consequently still subject to considerable uncertainties. Agriculture has usually shown a high adaptive capacity to changes in external forcings, and as a result, the actual impacts of the changing climate will depend on the adaptation and mitigation strategies adopted within the coming years and decades.

The inclusion of agronomic aspects of crop production is, therefore, an important step to improve this modelling framework. Even though still poorly understood, nitrogen cycling dynamics and fertilization effect are an aspect of primary importance in agroenvironment. As a next step, hence, it is recommended to include nitrogen in the present context of biosphere modelling. The inclusion of nitrogen fertilization could improve not only the representation of agriculture production, but also the decisions on land use due to relative costs (for fertilizers) and benefits (from yields). Yet, in the present version of the model, the representation photosynthesis is based on a "strong optimality hypothesis"; this hypothesis implicitly considers nitrogen availability as a non-limiting factor by setting photosynthetic capacity to its nitrogen-related optimum as part of LPJ. Even though this hypothesis might be valid for global scale simulation, it is often discussed for smaller scales.

The development of a nitrogen cycling scheme should, therefore, be a high priority, to improve the general representation of the terrestrial vegetation from the basic photosynthetic process.

Moreover, the observed acclimation of photosynthesis rates to increased CO_2 concentration at the leaf level may lead to a smaller degree of CO_2 fertilization, as it is the case in LPJ. However, it remains unknown whether the short-term responses of plants to atmospheric CO_2 increase will be the same as responses over long timescales under either natural selection or continuing breeding techniques for crops. Both can be expected to make maximum use of the advantages of higher CO_2 levels. Finally, the exact degree to which soil and plant respiration rates respond to warming over long timescales still remains a topic of intensive research.

We assume implicitly in the potential production that improvements in technology and cultivars occur constantly to maintain the productivity as near as possible to the potential level. This assumption reflects the idea that competition between seed producers may, over the long-term, result by itself in near-optimal adaptation to the given climatic environment. In this context, we exclude regional differences in cultivars, so that only one parameterization is used to represent each crop over the whole European continent. This simplified modelling strategy could be improved by the inclusion of several cultivar parameterisations per crop. This issue is often discussed as a point of controversy when it comes to the representation of crops within DGVMs. If a parameterisation set should be assigned to each cultivar, the input data to be provided increases. On the other hand, the limited amount of input represents a valuable advantage in large-scale simulation and should be preserved. We provide here a basic modelling framework, which could be expanded and extended in a modular way. At the present time, however, it appears wise to include only a single general parameterisation per crop.

Since LPJ is a well-established DGVM that is widely used in the global research community, this work presents an extension of an important tool in global climate change and carbon cycle assessments to agroecosystem, describing potential and water-limited crop production and coupling to land-use allocation on the basis of economic decision-making. This new system is used to assess several aspects of the agroecosystem in Europe. As such, the

modelling framework presented is a promising new baseline on which it is possible to build a modular tool to quantify the impacts of climate change in large-scale assessments within earth system modelling frameworks.

Appendix I - LPJ-C model description

Here, we describe only the new crop compartment of the LPJ-C, for the general LPJ-GUESS structure please refer to the cited literature (Smith *et al.*, 2001; Sitch *et al.*, 2003). For detailed explanations of the mathematical equations driving the crop development refer to the cited literature of WOFOST (Van Diepen *et al.* 1989, Van Ittersum *et al.* 2003).

Emergence

In the model, the plants immediately emerge as soon as the conditions are satisfied. Thus, no delay between sowing and emergence is simulated. However, the sowing date can be fixed by the user or calculated with a simple procedure: two conditions have to be satisfied to start the growth, the first concerning temperature and the second soil moisture. To satisfy the soil moisture condition, the following FAO general relation has to be verified for ten subsequent days:

$$\frac{ETP}{2} <= P$$

ETP: Potential evapotranspiration [mm]

P: Precipitation [mm]

The temperature condition is represented by a specific mean temperature threshold (*t_eme*). Crop plants emerge only when the mean temperature of the last ten days is above this threshold. Since wheat is a winter cereal, its growth is always fixed on the first day of the year. If the model simulates no water-limited growth, only the temperature requirement has to be satisfied.

Phenology

The crop passes through successive phenological development stages that are described as two phases, the pre-anthesis (vegetative) and the post-

anthesis (grain filling) stage. The length of each stage depends on the development rate that in turn is controlled by temperature. The development rate is expressed on a numerical scale that ranges from 0 to 2, with 0 being emergence, 1 anthesis and 2 maturity. Development rate is then the ratio of an effective daily temperature and temperature sum needed to complete the stage, this assumes proportionality between temperature and development rate. The effective daily temperature is used instead of the normal air temperature because the plant grows differently when the temperature is within certain ranges. The effective daily temperature is specified in a vector (*dtsmtb*) using average air temperature as the independent variable. Development rate can be obtained by:

$$Dr(t) = \frac{T_{eff}(t)}{Tsum_i}$$

Dr(t): Development rate at time step t [d^{-1}]

T$_{eff}$(t): Effective temperature [°C]

Tsum$_i$: Temperature sum required to complete stage *i* [°C d]

The effective temperature, *T$_{eff}$(t)* and the temperature sum required to complete stage *i, Tsum$_i$* are crop dependent and must be specified.

Development stage at time step *t* is the integral of development rate over time:

$$Ds(t) = Ds(t-1) + Dr(t) * \Delta t$$

Ds(t): Development stage at time step *t*

Dr(t): Development rate at time step *t* [d^{-1}]

Δt: Time step [d]

Crop biomass production

APAR

LPJ-C calculates the absorbed photosynthetic active radiation (APAR) in order to compute NPP at a daily time step. Note that in the APAR calculation the α_A parameter is set as 0.90 for crops instead of 0.5 as for the standard model version. This value was changed to take into account a lower light canopy dispersion compared to natural vegetation (C. Prentice personal communication). The APAR depends on the foliar projective cover (FPC) that

represents the proportion of ground area covered by leaves. FPC is calculated using the Lambert-Beer extinction equation using a specific crop canopy extinction coefficient:

$$FPC = 1 - \exp(-Kcrop * LAI)$$

$$APAR = FPC * PAR * \alpha_A$$

FPC: foliar projective cover

Kcrop: crop canopy extinction coefficient

LAI: leaf area index

PAR: photosynthetic active radiation

αA: scaling factor for PAR absorption, set for crop at 0.90

APAR: absorbed PAR

NPP

Comparing to the standard LPJ-GUESS in the photosynthesis/assimilation, only respiration is evaluated in a slightly different way for crops. In the model, the NPP is calculated as the difference between the assimilated carbon and the total respiration costs. The assimilation depends on APAR, and other environmental factors. The sum of the maintenance and growth respiration is the total respiration cost:

$$NPP = Assim - (MResp + GResp)$$

NPP: Net primary productivity [kgC m-2]

Assim: Assimilation [kgC m-2]

MResp: Maintenance respiration [kgC m-2]

GResp: Growth respiration [kgC m-2]

Maintenance respiration

Maintenance metabolic costs may be estimated based on the quantities of biomass components and on crop metabolic activity. Based on this, typical values for the maintenance coefficients for various plant organs are used to calculate the crop maintenance requirements, which are considered proportional to the dry weights of the plant organs to be maintained:

$$MResp = gtemp_{air} * \sum (mr_i * Cmass_i)$$

Mresp: Maintenance respiration rate at reference temperature of 25 °C [kgC d^{-1} m^{-2}]

mr$_i$: Maintenance coefficient of pool *i* [kgC kgC^{-1} d^{-1}]

Cmass$_i$: Carbon biomass in pool i [kgC m^{-2}]

gtemp$_{air}$: respiration air temperature response

The maintenance coefficient of pool i, *mr* (*mrr*, *mrs*, *mro* in the code), is crop dependent. Maintenance respiration in leaf pool is not included in the crop scheme because it is already evaluated directly at the photosynthesis level. The *gtemp$_{air}$* is the response of respiration to air temperature implemented in the standard LPJ. This is an empirical relationship takes into account of temperature acclimation (Lloyd and Taylor, 1994):

$$gtemp_{air} = \exp(308.56 * (\frac{1}{56.02} - \frac{1}{T + 46.02}))$$

This relationship is a modified Arrhenius equation, designed to evaluate the soil respiration process, but in the LPJ context it is used to evaluate also the tissue respiration response depending on the C/N ratio.

Growth respiration

The primary assimilates in excess of the maintenance costs, are converted into structural plant material. In the conversion process of glucose molecules, CO_2 and H_2O are released and this process has a specific efficiency. Each structural compound is formed along a distinct, non crop-specific pathway. The assimilates required to produce a unit weight of a certain plant organ can be calculated. Therefore one conversion coefficient has to be specified for each pool of the plant and the amount of assimilated carbon used in this conversion depends also on specific carbon amount allocated to pools.

$$NPPcorr = NPP * \frac{1}{\sum(\frac{f_i}{cv_i} * (1 - f_r) + \frac{f_r}{cv_r})}$$

NPPcorr: Net primary productivity having into account the conversion costs [kgC d^{-1} m^{-2}]

f$_i$: Allocation coefficient of the pool *i*, with *r* referred to root pool

cv$_i$: Conversion efficiency factor of the pool *i*, with *r* referred to root pool

The conversion efficiency factors, cv_i (*cvf, cvl, cvr, cvs* in the code) and the allocation coefficients f_i (*fstb, frtb, fotb, fltb*), have to be specified for each crop. In this case the growth respiration is also taken into account for the leaf pool because it concerns the conversion from sugars to tissues biomass. We consider growth respiration as the assimilated carbon used for the biomass increase and the *NPPcorr* as the net carbon allocated in the pools:

$$G\operatorname{Re}sp = NPP - NPPcorr$$

Carbon allocation

The distribution over the carbon pools in the plant is strictly related to crop development stage. Once the NPP is completely defined, the allocation can be performed and the carbon is partitioned into roots and the above ground pools as stems, leaves and storage organs using the already mentioned allocation coefficients. During the vegetative phase (DVS<1, pre-anthesis) no carbon is allocated to the storage organs, it is mainly directed to roots and leaves. After the anthesis, mainly storage organs receive a large increase in biomass. The biomass increase is defined:

$$Cmass_{incr,root} = NPPcorr * f_r$$

$$Cmass_{incr,i} = NPPcorr * (1 - f_r) * f_i$$

$Cmass_{incr,root}$: carbon mass increase in roots [kgC m^{-2}]

$Cmass_{incr,i}$: carbon mass increase in the above ground pool *i* [kgC m^{-2}]

The total carbon biomass (*Cmass*) is the integral over time of the carbon biomass increments.

Leaf Area index

The carbon mass is stored in the leaf pool among age classes. The total LAI is therefore expressed as the sum of LAI of all living classes. Classes older then the leaf longevity (*leaflon*, expressed as the fraction of the year) are dropped down and goes to the soil litter carbon pool.

$$LAI = \sum Cmass_{leaf,k} * SLA$$

SLA: pecific Leaf Area [m^2 kgC^{-1}]

$Cmass_{leaf,k}$: Carbon biomass of the leaf pool of age *k* [m^2 kgC^{-1}]

Crop leaf drop factor

Mortality in the leaf pool is considered as the sum of senescence and mutual shading expressed as a reduction coefficients:

$$Mort_{coeff} = (Mort_{sh} + Mort_{age}) * Cmass_{leaf}$$

$Mort_{coeff}$: mortality coefficitent

$Mort_{sh}$: mutual shading mortality rate

$Mort_{age}$: ageing mortality rate

$Cmass_{leaf}$: total carbon biomass in the leaf pool [kgC m^{-2}]

When the LAI exceeds a critic value a drop of leaves is imposed on the crop canopy:

$$LAI_{crit} = \frac{3.2}{Kcrop}$$

$$Mort_{sh} = 0.03 * \frac{LAI - LAI_{crit}}{LAI_{crit}}$$

$Kcrop$: extinction coefficient (Lambert-Beer) of the crop canopy

LAI_{crit}: critical LAI

When a leaf age class overcome the leaf longevity, it is dropped down and a fractional reduction is calculated

$$Mort_{age} = \frac{Cmass_{leaf,k}}{Cmass_{leaf}}$$

All the dead matter is moved to the soil pools as the LPJ-GUESS standard prescribes to close the carbon cycle. After the crop reaches the maturity (DVS=2) the whole canopy dies and all the biomass is transferred to the soil pools. In case the NPP<=0 the crop dies immediately even without reaching maturity.

Table 1 Crop parameters.

Variable name	Description	Maize	Wheat
pathway	Photosinthesis path	C4	C3
leaflon	Leaf longevity	0.5	0.80
Pstemp_min	Min photosynthesis temperature [°C]	6.0	0.0
pstemp_low	Low photosynthesis temperature [°C]	8.0	3.0
pstemp_high	High photosynthesis temperature [°C]	30.0	40.0
pstemp_max	Max photosynthesis temperature [°C]	40.0	50.0
intc	Precipitation interception coefficient	0.01	0.01
dtsmtb	Effective daily temperature table [°C, °C]	See Table 2	See Table 2
tsum1	Required temp sum stage 1 [°C d]	1718.0	1004.0
tsum2	Required temp sum stage 2 [°C d]	1135.0	954.0
fltb	Allocation fract. leaves as function of DVS table	See Table 3	See Table 4
fstb	Allocation fract. stems as function of DVS table	See Table 3	See Table 4
fotb	Allocation fract. storage organs as function of DVS table	See Table 3	See Table 4
frtb	Allocation fract. Roots as function of DVS table	See Table 3	See Table 4
rmo	Maintenance resp. rate storage organs [kgCH2O kg^{-1} d^{-1}]	0.01	0.01
rmr	Maintenance resp. rate roots [kgCH2O kg^{-1} d^{-1}]	0.01	0.01
rms	Maintenance resp. rate stems [kgCH2O kg^{-1} d^{-1}]	0.015	0.015
cvl	Conversion efficiency od leaves	0.68	0.68
cvs	Conversion efficiency od stems	0.66	0.66
cvr	Conversion efficiency od roots	0.69	0.69
cvo	Conversion efficiency od storage organs	0.70	0.70
slatb	Specific leaf area [ha kg^{-1}]	0.0070	0.0032
LAI_eme	LAI at the emergence	0.038	0.099
T_eme	Mean 10 days temp required fo emergence [°C]	13.7	not used
Kcrop	Extinction coefficient	0.81	0.81

Table 2 Effective daily temperature table, *dtsmtb*. Effective daily temperature (*tdsm* in the model, T_{eff} in the text) [°C] depends on air temperature [°C]. As an example, *tdsm* is 30.00 when temperature is 25.00 for maize. Values in between are interpolated, so when temperature is 12.50, *tdsm* is 18.00

Maize		Wheat	
°C	°C	°C	°C
0.00	0.00	0.00	0.00
6.00	0.00	30.00	30.00
30.00	25.00		
35.00	25.00		

Table 3 Maize allocation factors. Variables are expressed as arrays with values depending on DVS, values in between are linearly interpolated (refer to Table 2).

Fltb		fstb		fotb		Frtb	
DVS	Value	DVS	Value	DVS	Value	DVS	Value
0.0	0.55	0.00	0.45	0.00	0.00	0.00	0.40
0.71	0.40	0.71	0.60	0.71	0.00	0.50	0.23
0.99	0.15	0.99	0.85	0.99	0.00	0.60	0.18
1.00	0.00	1.00	0.00	1.00	1.00	0.80	0.10
2.00	0.00	2.00	0.00	2.00	0.00	1.00	0.00
						2.00	0.00

Table 4 Wheat allocation factors. Variables are expressed as arrays with values depending on DVS, values in between are linearly interpolated (refer to Table 2).

Fltb		fstb		fotb		Frtb	
DVS	Value	DVS	Value	DVS	Value	DVS	Value
0.10	0.65	0.10	0.35	0.00	0.00	0.10	0.65
0.25	0.70	0.25	0.30	1.50	1.00	0.20	0.60
0.70	0.60	0.70	0.40	2.00	0.00	0.40	0.30
0.99	0.00	0.99	0.00			0.70	0.07
2.00	0.00	2.00	0.00			1.20	0.00
						2.00	0.00

Appendix II - KLUM's interior

Model description

The allocation algorithm of KLUM is based on the assumption that the most profitable allocation is chosen. Total achievable profit per hectare π of one spatial unit is assumed to be:

$$\pi = \sum_{k=1}^{n} (p_k \alpha_k - c_k \overline{L} l_k) l_k - \gamma \sum_{k=1}^{n} l_k^2 \text{Var}[(p_k \alpha_k - c_k \overline{L} l_k)] \quad \text{(1)}$$

The first part of the equation 1 describes the expected profit, where p_k is the price per product unit, α_k is the productivity per area and l_k denotes the share of total land $\overline{L}$ allocated to crop $k \in \{1 \ldots n\}$ of *n* crops. c_k is the cost parameter for crop *k*. Total costs are assumed to increase in land according to:

$$C = \sum_{k=1}^{n} \tilde{c}_k L_k^2 \quad \text{(2)}$$

where $L_k = l_k \overline{L}$ denotes the total area allocated to crop *k*.

The second term of the equation 1 represents the risk aversion of the representative landowner. Risk perception is quantified by the variance of the expected profit, weighted by a risk aversion factor $0 < \gamma < 1$.

Maximizing π under the constraint that all land shares need to add up to a total not greater than one: $1 \leq \sum_k l_k$, an explicit expression for each land-share l_i allocated to crop $i \in \{1 \ldots n\}$ can be derived:

$$l_i = \frac{\dfrac{1}{2}\sum_{k=1}^{n}\dfrac{\beta_i - \beta_k}{\gamma\sigma_k^2 + \overline{L}c_k} + 1}{\sum_{k=1}^{n}\dfrac{\gamma\sigma_i^2 + \overline{L}c_i}{\gamma\sigma_k^2 + \overline{L}c_k}} \quad \text{(3)}$$

where for simplicity $\beta_k = p_k\alpha_k$ displaces the profitability of crop *k*, $\sigma^2 = \mathrm{Var}[\beta_k]$ displaces the respective variance and $c_k = \tilde{c}_k\overline{L}$. The temporal variability of total costs is assumed to be negligible compared to the variability of prices and productivities.

Adjustment of the cost parameters in KLUM

The assumption of decreasing returns to scale (equation 2) underlying the cost structure of KLUM has consequences for the interpretation and transferability of the calibrated cost parameters. We interpret the increasing cost with increasing area share such that the most suitable land is used first and with further use more and more unsuitable land is applied. This implies that the calibrated cost parameters are depending on the total amount of agricultural area assumed in the calibration and on its relative distribution of quality concerning crop productivity. Thus, the cost parameters calibrated for the sub-national regions cannot simply be adopted in the corresponding gridcell or in other regions. Instead these values need to be adjusted according to the differences in total agricultural area. Assuming that the relative quality distribution does not change, a doubling of the total area would imply a bisection of the cost, since the double amount of suitable area would be available. So, the cost parameter *c* of a sub-national region to its adjusted level $\tilde{c}$ by scaling it according to:

$$\tilde{c} = c\frac{\tilde{L}}{L}$$

where $\tilde{L}$ and L represent the total agricultural area in the adjusted plot and the original region, respectively. For the simple downscaling of the calibrated cost parameters from NUTS2-regional to gridcell level, the fraction of $\tilde{L}$ and L is equal to the total number of gridcells in this region. This procedure assures that under identical conditions, the downscaled model will produce the same results at the large-scale version.

Acknowledgements

The years I spent in Hamburg are much more than a PhD work. My life has changed in both professional and life attitude. Many people, contributed directly or indirectly to make it a unique experience, it would be mostly impossible to thank all of them. I just recall here the closest people who have been with me during this time.

I would like to thank Dr. Wolfgang Knorr for the advices, the work and the understanding he had during his supervision. He has been not only a good supervisor, but also a person who taught me a new attitude in complex problem solving.

Prof. Dr. Richad Tol contributed actively to this thesis as well; I'd like to thank him together with the Volkswagen Stiftung for the financial support given to me through the ECOBICE project. I further include the Max Planck Institute for Biogeochemistry of Jena, the Max Planck Institute for Meteorology of Hamburg and the International Max Planck Research School for Earth System Modeling, especially Dr. Antje Weitz, for providing logistic support.

Here we go now with the list of people who spent work, time, stress and fun with me. The Risk Freaks Gabi, Luis, PatriS, Alvaro, Tomasiccio and Tomas. We spent beautiful non-sense time hanging around in Hamburg and war nights playing strategically Risk, which I won gloriously several times; somehow we shared our time together helping and fighting. I also thank all the friends with whom I spent great time having discussion, sharing feelings and parties: Miren, Tina, Semeena, Beena, Manu, Abhay, Manik, Xhuhua, Patrick, Jana, Swagata, my two patient and excellent office mates Heiko and Tanaka San, Luca, Ingrid, Astrid, Zho, my Argentinean twin sister Nidia, Christine,

Anne, Nophea, Marianne, Melissa, Philipp, the radical Kite Freaks Matze and Sebo, Rona the Sweet Kiwi and Kristina the Radical Russian from Jena. I am very thankful to Sarah, I shared with her a special time, spiced by bitter discussions, sweet conversations and a lot of Franzbroetchen mit Schokolade. And here comes my friend, flatmate, colleague and conational Francesca; we had chat, discussion, thoughts, dinners, schlaf-tot teas together, but I still do not get "What do you mean by PhD?!". I especially thank my parents and my sister Daniela: they always provided help and support with a sweet smile from our crazy Land of the Sun.

Yet, I had the luck to be in the same project of Kerstina. She became immediately not only a (complicated) colleague and a friend, but also the person who introduced me to Chermany, who understood the things happening to me and told me the right thing at the right moment. We worked together on the Chapter 4, so I dedicate it to her.

But the person who gave me the reason and the force to go ahead through the complicated moment is certainly Lisa. Without her I could simply not reach to the end of this PhD. Her sweet help, her courage and her understanding have been constantly my vital reference point. Even thought she was far away, she cared for me when I needed. For this reasons, I dedicate this thesis to her.

Beginn einer neuen Veröffentlichungsreihe des MPIM, welche die vorherigen Reihen "Reports" und "Examensarbeiten" weiterführt:

**„Berichte zur Erdsystemforschung" , *„Reports on Earth System Science*", ISSN 1614-1199
Sie enthält wissenschaftliche und technische Beiträge, inklusive Dissertationen.**